

Modelling of the PACTEL SBL-50 Transient Using RELAP5 Computer Code

Master of Science Thesis within the Nuclear Engineering Program

MD.HASIB UDDIN TALUKDER

MOHAMMED FAZLUR RAHMAN BHUYAN

Department of Nuclear Engineering
CHALMERS UNIVERSITY OF TECHNOLOGY
Göteborg, Sweden 2012
CTH-NT-262

ISSN 1653-4662

Modelling of the PACTEL SBL-50 Transient Using RELAP5 Computer Code

Masters of Science Thesis within the Nuclear Engineering Program

MD.HASIB UDDIN TALUKDER

MOHAMMED FAZLUR RAHMAN BHUYAN

SUPERVISOR

József Bánáti

Researcher, Department of Nuclear Engineering

Chalmers University of Technology

EXAMINER

Anders Nordlund

Associate Professor, Head of the Department

Department of Nuclear Engineering

Chalmers University of Technology

Department of Nuclear Engineering
CHALMERS UNIVERSITY OF TECHNOLOGY

Göteborg, Sweden 2012

Modelling of the PACTEL SBL-50 Transient Using RELAP5 Computer Code

MD.HASIB UDDIN TALUKDER

MOHAMMED FAZLUR RAHMAN BHUYAN

© MD.HASIB UDDIN TALUKDER

MOHAMMED FAZLUR RAHMAN BHUYAN

Thesis Report: CTH-NT-

ISSN Number:

Department of Applied Physics

Chalmers University of Technology

SE-412 96 Göteborg

Sweden

Telephone + 46 (0)31-772 1000

Göteborg, Sweden 2012

MD.HASIB UDDIN TALUKDER

MOHAMMED FAZLUR RAHMAN BHUYAN

Department of Applied Physics

Chalmers University of Technology

Abstract

The main purpose of the current Master of Sciences Thesis was modelling of the PACTEL SBL-50 transient using RELAP5/MOD 3.3 Patch-04 system thermal hydraulic computer code all through the process.

For assessment of performance or evaluation of safety of the nuclear power plants, different kind of thermal-hydraulic experiments are needed. However, experiments are not possible, or rather prohibited to be performed with real nuclear power plants. Therefore, it is essential to accomplish the tests under safe circumstances, and obtain the test data in a small scale before implementation in a large-scale. In small-scale test facilities, computer system codes (such as RELAP5) can simulate most of the postulated transients. Due to the similarity laws in heat and mass transfer, it is assumed that, if a code is capable of predicting the parameters in a scaled-down geometry (i.e. in a test facility) then the features of a similar type of transient can also be predicted in a real reactor. Nevertheless, in order to achieve that, extensive validation and verification efforts are needed.

In most cases, a large amount of effort is necessary for estimation of the possible conditions of a real transient, both in the analytical and experimental fields. The best example for such a coordinated action is an international benchmark project. Different organizations can participate in the international benchmark projects from various countries, which give good opportunities to the code users to construct their own models and to simulate the same transient by a certain computer code. Uncertainties originating from code performance, model parameters, or even user experiences can be revealed by comparison of the results.

It can be seen that a large number of codes, models, model options, users, etc. participating in a benchmark may contribute to underlining a range of factors that are involved in uncertainty evaluation. In a few cases during the last two decades, the PACTEL Facility (Parallel Channel Test Loop), located at Lappeenranta University of Technology (LUT) in Finland, served as a subject for these benchmarks. The PWR PACTEL Benchmark Project was accomplished during a period between 2010 and 2011. The test simulated a small (1.0 mm) break in the cold leg with continuous inventory loss. The project consisted of a “pre-test” (also known as the “blind calculation”) phase and the “post-test” (in other words “open calculation”) phase.

Together with many participants, Chalmers University of Technology took part, both in the pre-test and post-test phases of the benchmark. A simplified single-tube steam generator (SG) model was applied in the pre-test phase and it resulted in a reasonably good agreement with the measured data. Still, there was a margin for improvement, particularly in the temperature measured at the longest heat exchanger tubes of the SGs. Deviations in the initial temperatures were suspected to be originating from a specific phenomenon. Assumption of reverse flow in the longest tube was a realistic explanation of the temperature behaviour. Obviously, the single tube model was not able to reproduce this phenomenon by its one-dimensional nature. However, it was expected that an extension of the model with multiple tubes might confirm or deny existence of this behaviour. In our investigations, we were focusing on proper modelling of reverse flow in the SGs.

According to the simulations, the results obtained with the modified multi-tube SG model showed better agreement with the test results. In particular, the new refined nodalization of the model contributed to a significantly improved temperature variation in the longest tubes of SGs, where flow reversal was experienced.

Keywords : RELAP5, PACTEL, benchmark, simulation, thermal-hydraulics

Acknowledgements

We would like to thank our thesis supervisor József Bánáti, Ph.D., Researcher, Department of Nuclear Engineering, Chalmers University of Technology, Göteborg, Sweden, for guiding us through the preparation of this report. Without his support, this Thesis report would not have been possible.

I am very grateful to Anders Nordlund, Ph.D. Associate Professor, Head of Nuclear Engineering department, Chalmers University of Technology for his comments and suggestions, which were valuable for preparation of the thesis. Thanks and recognition is extended to all those who contributed to this report by presenting their valuable opinions to us.

Last but not the least, special thanks to Alexander Agung, Ph.D., Researcher, Department of Nuclear Engineering. He has supported us in a number of ways and helped us by giving his valuable time and cooperation.

Overall, it was a wonderful experience to work as a team in doing the research and preparing this report on such an important topic.

Nomenclature

Abbreviations

CB:	Control Block
CCFL:	Countercurrent flow limit
CHF:	Critical heat flux
CL:	Cold Leg
ECCS:	Emergency Core Cooling System
EPR:	European/Evolutionary Pressurized Reactor
FDW:	Feedwater
HL:	Hot Leg
HPSI:	High Pressure Safety Injection
IAEA:	International Atomic Energy Agency
ISP:	International Standard Problem
LUT:	Lappeenranta University of Technology
NC:	Natural Circulation
NPP:	Nuclear Power Plant(s)
OECD:	Organisation for Economic Co-operation and Development
PACTEL:	Parallel Channel Test Loop
PWR:	Pressurized Water Reactor
PZR:	Pressurizer
RCP:	Reactor Coolant Pump
RPV:	Reactor Pressure Vessel
RELAP:	Advanced Computational Engine
SBLOCA:	Small-Break Loss of Coolant Accident
SG:	Steam Generator
SL:	Steam Line
SS:	Steady State
SNAP:	Symbolic Nuclear Analysis Package
TH:	Thermal-Hydraulics
U.S.NRC:	United States Nuclear Regulatory Commission
TVO:	Teollisuuden Voima Oy
VVER:	Vodo Vodjanyi Energetitseskij Reaktor

Abstract

Acknowledgements

Nomenclature

Table of Contents

List of Figures

Table of Contents

Chapter 1 Introduction	1
1.1 Thesis background	3
1.1.1 Purpose	3
1.2 PWR PACTEL facility and its scaling concept	3
1.2.1 Facility overview	3
1.3 Steam generators of PWR PACTEL	5
1.4 Features of SBL-50 benchmark transient experiment	8
Chapter 2 Description of the Tools and their Practical Application	10
2.1 Description of RELAP5 computer code	10
2.2 Description of RELAP5/MOD3.3 patch 04 input model	11
2.3 Applicable field of RELAP5	12
2.4 Limitation in RELAP5	12
2.5 SNAP tool	12
2.5.1 Model development with SNAP tool	12
2.5.2 Two way conversion between texts based input and graphics	14
2.5.3 Strategies for achieving steady state	14
2.5.4.1 Procedure to create a new animation model	16
2.6 Other related software	16
2.6.1 MATLAB	16
2.6.2 Corel draw	16
Chapter 3 Theory of nuclear Thermal–Hydraulics	18
3.1 Thermo hydraulics	18
3.1.1 Mass conservation equation	18
3.1.2 Momentum conservation equation	18
3.1.3 Energy conservation equation	19
3.2 Natural circulation flows	19
3.2.1 Flow reversal	20
3.3 Small-break LOCA	21
3.4 Steady state and transient thermal-hydraulics analysis	21
3.4.1 Steady state thermal-hydraulics analysis	21
3.4.2 Transient thermal-hydraulics analysis	22
Chapter 4 Steam Generator Model Development and Description	23
4.1. Description of PWR PACTEL model	23
4.2 Description of PWR PACTEL single tube model	24

4.2.1 SG primary side of single tube model.....	24
4.2.2 SG secondary side.....	24
4.3 Modification of current model by increasing the heat exchanger tubes	25
4.3.1 Modified multitube model with fine nodalization	25
4.3.1.1 SG primary side	25
4.3.1.2 SG secondary side	25
4.3.1 Modified multitube model with rough nodalization.....	26
4.3 Secondary side geometry.....	32
4.4 Primary side geometry.....	35
4.2.1 Geometry calculation of heat exchanger tube.....	38
4.2.2 PACTEL SG tube geometry (Fine nodalization).....	39
4.2.2 PACTEL SG tube geometry (Rough nodalization)	44
4.3 Finer nodalization and elevation change of heat exchanger tube	48
4.3.1 Courant-Friedrichs-Lewy's condition	48
4.3.2 Effects of re-nodalization	50
4.4 Strategies for achieving steady state in our case	50
4.5 Transient calculation	50
4.6 Visualization of the model by using SNAP animation tool	50
Chapter 5 Results Analysis	53
5.1 Steady-state analysis	53
5.2 Transient analysis	53
5.3 Comparison between the single tube model and multi tube model.....	60
Chapter 6 Conclusion and Future Work	63
6.1 Conclusions	63
6.2 Future work.....	63
Reference	65
Appendix A	67
Appendix B	69

List of Figures

Figure 1 : PWR PACTEL test facility	5
Figure 2 : PWR PACTEL steam generator general view	6
Figure 3 : Top view of PWR PACTEL steam generators	6
Figure 4 : Heat exchange tubes of the PWR PACTEL steam generators	7
Figure 5 : Heat exchange tubes of the PWR PACTEL steam generators	8
Figure 6 : Graphical presentation of unheated pipe in SNAP.....	13
Figure 7 : Graphical presentation of heated pipe in SNAP.....	13
Figure 8 : General methods to achieve steady state condition for a part of full system model	14
Figure 9 : Natural circulation in a close loop	19
Figure 10 : PWR PACTEL nodalization scheme of the primary side	27
Figure 11 : The entire primary system model in the SNAP editor.....	28
Figure 12 : The primary side model of steam generator 2 in SNAP	29
Figure 13 : The secondary side model of steam generator 2 in SNAP	30
Figure 14 : The control system view in SNAP	31
Figure 15 : Upper part of the SG	32
Figure 16 : Axial discretization of the SG down comer cold side	32
Figure 17 : Cross section of the steam generator	33
Figure 18 : Lengths of the heat exchanger tubes.....	35
Figure 19 : Radiuses of the U-bendings	37
Figure 20 : Radiuses of the U-bendings	37
Figure 21 : Lower plenum of the SG and its model	47
Figure 22 : Finer nodalization and increasing number of the tube of PACTEL PWR steam generator	49
Figure 23 : Fluid conditions at near the end of the transient	51
Figure 24 : Void distribution at near the end of the transient	52
Figure 25 : Upper plenum pressure	55
Figure 26 : Downcomer mass flow rate	55
Figure 27 : Collapsed level between upper plenum and lower plenum	56
Figure 28 : Integrated break mass flow rate	56
Figure 29 : Hot leg 1 outlet temperature	57
Figure 30 : Cold leg 1 mass flow rate	58
Figure 31 : Diff. pressure in SG2, tube 7, hot side.....	58
Figure 32 : Diff. pressure in SG2 tube cold side	59
Figure 33 : SG1temperature (Tube 50, hot side. 0.7m)	61
Figure 34 : Measured flow rate as a function of the primary mass inventory in the SBL-50 experiment	62

Chapter 1

Introduction

Safety is a matter on which there can be no compromise as the existence of our civilization depends on it. Electricity production today with nuclear energy is a challenging issue around the world due to some severe accidents in nuclear power plants during the 50 years of their operation. Beyond fossil fuels many different source of energy such as solar, hydro, wind and bio-fuels can generate clean electricity without carbon dioxide and greenhouse gas emission. The exception is that nuclear energy is the only option to produce vastly expanded supplies of clean electricity on a global scale. In the wake of the Fukushima nuclear accident in Japan in 2011, researchers and nuclear power experts are thinking once again to review all the safety design for future plants. After the Chernobyl accident, Fukushima is called the second worst nuclear disaster. The former was caused by human errors, while the latter was initiated by an earthquake.

The safety of nuclear power plant is an important issue to produce a vast amount of clean energy. For evaluation of the safety of the nuclear power plants, it is extremely essential to understand the thermal-hydraulic behaviour and phenomena. For assessment of the capabilities and performance of the nuclear power plants, different kind of thermal-hydraulic experiments are needed, but it is not possible or rather prohibited to perform experiments with real nuclear power plants. The safety of nuclear power plant is the main concern. It is essential to accomplish the experiments under safe circumstances, and obtain the test data in a small scale before implementation in a large-scale. In small-scale test facilities, computer system codes (like RELAP5) can simulate most of the transients. It is assumed that, if a code is capable of predicting the parameters in a scaled-down geometry (i.e. in a test facility, such as the PACTEL) then the features of a similar type of transient can also be predicted in a real reactor. However, in order to achieve that, extensive validation and verification efforts are needed.

From the aspect of heat transfer, an electric heat source and a nuclear heat source can behave identically. Therefore, extrapolation from the scaled-down model to the real-size reactor is theoretically possible. A huge amount of efforts was put into estimation of the possible conditions of a real transient, both in the analytical and experimental fields. The best example of such a coordinated action is an international benchmark project. Different organizations can participate in the international benchmark projects from various countries, which gives good opportunities to the code users to create their own models and to simulate the same transient by a certain computer code. Uncertainties originating from code performance, model parameters, or even user experiences can be revealed by comparisons.

Various methods and approaches can be benchmarked against each other. For instance, a code-to-test comparison tells about how well a particular code is able to predict the transient parameters in the experiment. A code-to-code comparison can provide some information about whether a certain code is able to represent a key phenomenon, while some other codes can fail to do so. A user-to-user comparison may highlight the so called “user effects”. In this case, the results of calculations performed by the same code (and preferably the same version) but using different models are judged against each other. Obviously, users with various levels of experiences will create diverging models (i.e. inputs, or nodalizations) for analysing the same problem.

It can be seen that a large number of codes, models, model options, users, etc. participating in a benchmark may contribute to underlining a range of factors that are involved in uncertainty evaluation. With increasing number of code calculations, we are better informed about effects of the contributing factors.

With these objectives in mind, OECD and IAEA organized a number of international benchmark projects. During the last decades, OECD supported the test series of International Standard Problems (ISPs) [1][2] while IAEA coordinated a benchmark in the framework of Standard Problem Exercises (SPEs) for VVER type reactors [1][2].

Lappeenranta University of Technology (LUT) in Finland took part in these benchmarks and once it was the host organization for the 33rd International Standard Problem. The ISP-33 test was performed in the PACTEL Facility operated by LUT. The PACTEL has undergone a reconstruction during the last few years. The name has been changed to PWR PACTEL. This test facility is meant for safety studies related to EPR type pressurized water reactor thermal hydraulics. A series of different kind of experiments carried out by the PWR PACTEL, included the current benchmark test.

The PWR PACTEL benchmark project consisted of a “pre-test” (also known as the “blind calculation”) phase and the “post-test” (in other words “open calculation”) phase.

In the pre-test phase, the participants received only the initial and some boundary conditions of the experiment. Other measured data were unknown for the users. Each participant built a model of facility and simulated the transient with his/her own input. After performing the calculations, the users sent their results to the organizers. This was a pre-condition for further participation in the project.

The post-test phase began when the organizers sent out the entire measured database of the test to the participants upon receiving the blind-calculated data. The exact evolution of the transient parameters became known for the users only at this stage. The analysis may be continued with modification of the model used earlier in the pre-test. In order to achieve better agreement or to correct the possible discrepancies, the users could freely improve their models by re-nodalization, by refinement of the nodes, by increase of components, by modifying some user-given coefficients, or by testing various code options, and so on.

Out of many participants, Chalmers University of Technology took part both in the pre-test and post-test phase of the benchmark. A simplified single-tube SG model was applied in the pre-test phase and it resulted in reasonably good agreement with the measured data [3]. There was a margin for improvement, particularly in the temperature measured at the longest heat exchanger tubes of the SGs. Deviations in the initial temperatures were suspected to be originating from a specific phenomenon. Assumption of reverse flow in the longest tube was a realistic explanation of the temperature behaviour. Obviously, the single tube model was not able to reproduce this phenomenon by its one-dimensional nature. However, an extension of the model with multiple tubes may confirm or deny existence of this particular behaviour. Our investigations were focusing on proper modelling of reverse flow in the SGs. The results of the efforts are documented in the following chapters.

1.1 Thesis background

1.1.1 Purpose

The overall purpose of our project was to modify and renodalize the current single-tube SGs model to multi tube SGs model and simulate the modified model for transient analysis. The focus was on detailed nodalization of vertical EPR type Steam Generators and observation of the effects of the re-nodalization and then compared to the simulation results with the single tube model and test data during small-break LOCA. After that, investigations focused on the modeling of the reverse flow in the longest tube of PWR PACTEL steam generators that was unseen in the single tube model. In addition, investigation was made into natural circulation flow behavior of the thermal hydraulics of pressurized water reactors (PWR) in steam generator during multi tube modelling of PACTEL SBL-50 transient by using RELAP5 computer code

The focus will be on simulation, analysis, comparison and discussion of vertical EPR type Steam Generators during Small-Break LOCA by using RELAP5 MOD 3.3 Patch-04 system thermal hydraulic code all through the process.

1.2 PWR PACTEL facility and its scaling concept

1.2.1 Facility overview

PWR PACTEL facility is designed and conducted by the Lappeenranta University of Technology (LUT) for the research on thermal hydraulics since 1990. A significant change in the original PACTEL facility has been made to construct the PWR PACTEL facility. The main aim of the new design of the PWR PACTEL facility is to simulate the thermal hydraulic behaviour of the Soviet designed VVER-440 pressurized water reactor during the LOCA type accident.

The facility mainly consists of a new vertical steam generator instead of a horizontal steam generator and two primary loops. It consists of primary and secondary systems in the steam generator, emergency core cooling system including a pressure vessel part, and pressurizer. Each loop has 51 full size inverted U-tubes with five different tube heights, a hot leg, and a cold leg in the steam generator. Facility contributes to the validation of different kinds of thermal hydraulics computer codes to simulate the LOCA phenomena in EPR type reactors. This facility has two steam generators but the height of the steam generator is reduced due to the scaling limitation of the laboratory building [3].

Table 1. PWR PACTEL facility characteristics [3]

Reference power plant PWR (EPR)	Reference power plant PWR (EPR)
Volumetric scale	1:405 (pressure vessel) 1:400 (steam generators) 1:562 (pressurizer)
Height scale	1:1 (pressure vessel)
Maximum heating power	1 MW
Maximum primary / secondary pressure	8.0 MPa / 4.65 MPa
Maximum primary / secondary temperature	300 °C / 260 °C
Maximum cladding temperature	800 °C
Number of primary loops	2
Steam generator tube diameter	Ø19.05 x 1.24 mm
Average steam generator tube length	6.5 m
Number of U-tubes in one steam generator	51
Number of instrumented U-tubes SG I / SG II	8 / 14 (51*)
Main material of components	stainless steel (AISI 304)
Insulation material	mineral wool (aluminum cover)

1.2.2 Scaling concept of PWR PACTEL facility

Scaling is a key factor in engineering and in physics for small-scale laboratory experiment. In PWR PACTEL, it was not possible to preserve exact scaling of the EPR type reactor. The height of the PWR PACTEL facility was maximized but is still shorter than EPR plant. The height of the steam generator is $1/4^{\text{th}}$ of the EPR plant [3]

Another important scaling difference of PWR PACTEL is volumetric scaling. The secondary side of PWR PACTEL is almost double of the secondary side of the EPR steam generator. The volumetric scaling and Froude scaling are the key principle of the PWR PACTEL design. Volumetric scaling leads to an overestimation of heat losses to the environment. That is why all parts of the PWR PACTEL facilities are well insulated to minimize the heat losses. Froude scaling gives better simulation results of flow regime in loops for the period of transient. The scaling fetchers process the accident scenario where best estimate computational tools (like RELAP5) are adopted [3]

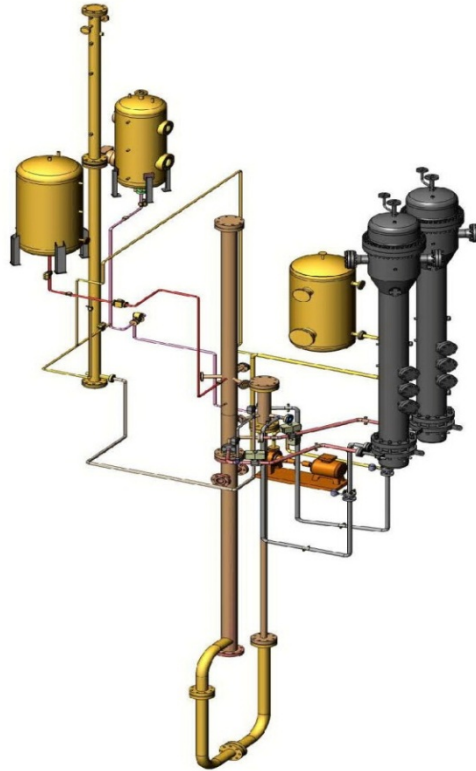


Figure 1 : PWR PACTEL test facility [3] [7]

1.3 Steam generators of PWR PACTEL

Steam generator accuracy and ability are serious concerns in the operation of pressurized water reactors [4]. Even without seeing any extreme accident condition, a reasonable prediction of the steam generator thermal-hydraulic behaviour is a serious task because of the complex flow patterns and geometry of the steam generator [5]. As mentioned above, new vertical steam generators are used in PWR PACTEL to simulate the thermal-hydraulic behaviour similar to EPR steam generators. Two identical vertical steam generators are constructed by scaling down the height. The PWR PACTEL steam generator has two loops, primary and secondary. The heated water is carried out of the reactor core primary side and the heat is transferred to the secondary side.

The primary side of the steam generator contains 51 heat exchanger U-tubes. The average length of the tube is 6.5 m with a triangular grid and 27.4 mm lattice pitch. These 51 tubes are arranged in five categories with different lengths and with each group containing two rows of tubes, as shown in Figure 4 and Figure 5. Compared to the reference steam generator, the heat transfer area and the primary-side volume of PWR PACTEL steam generator is scaled down to a ratio of 1/400[3]

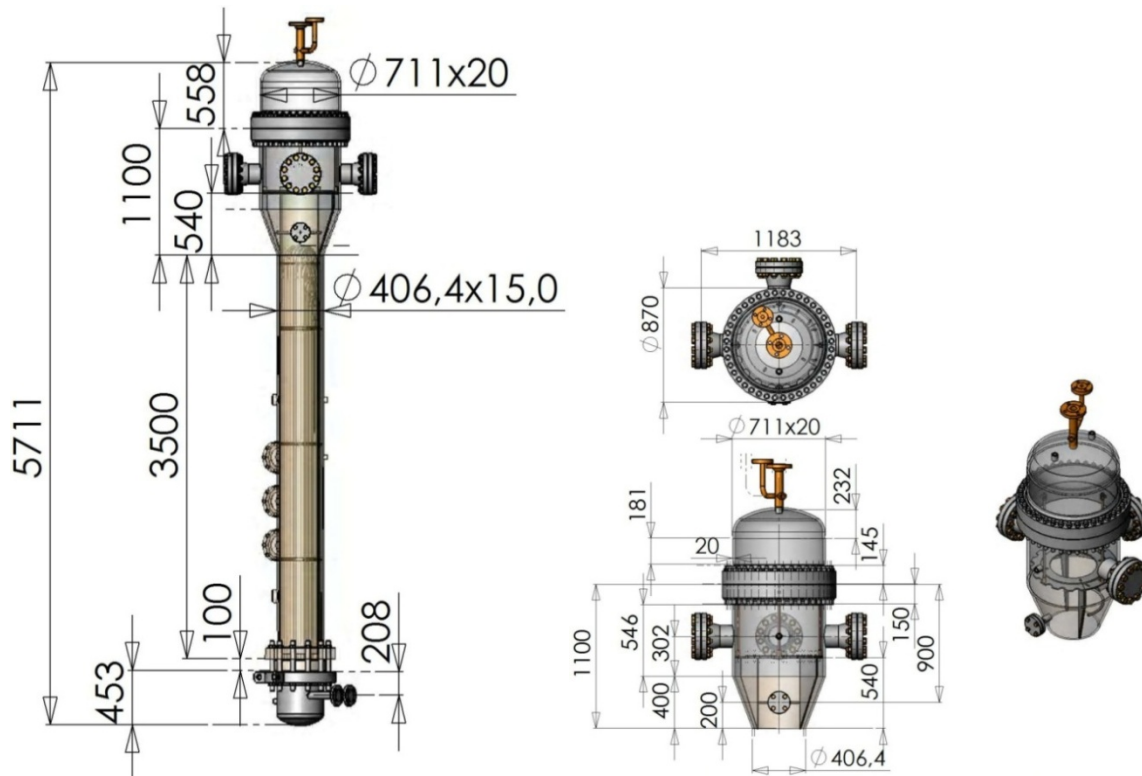


Figure 2 : PWR PACTEL steam generator general view [3]

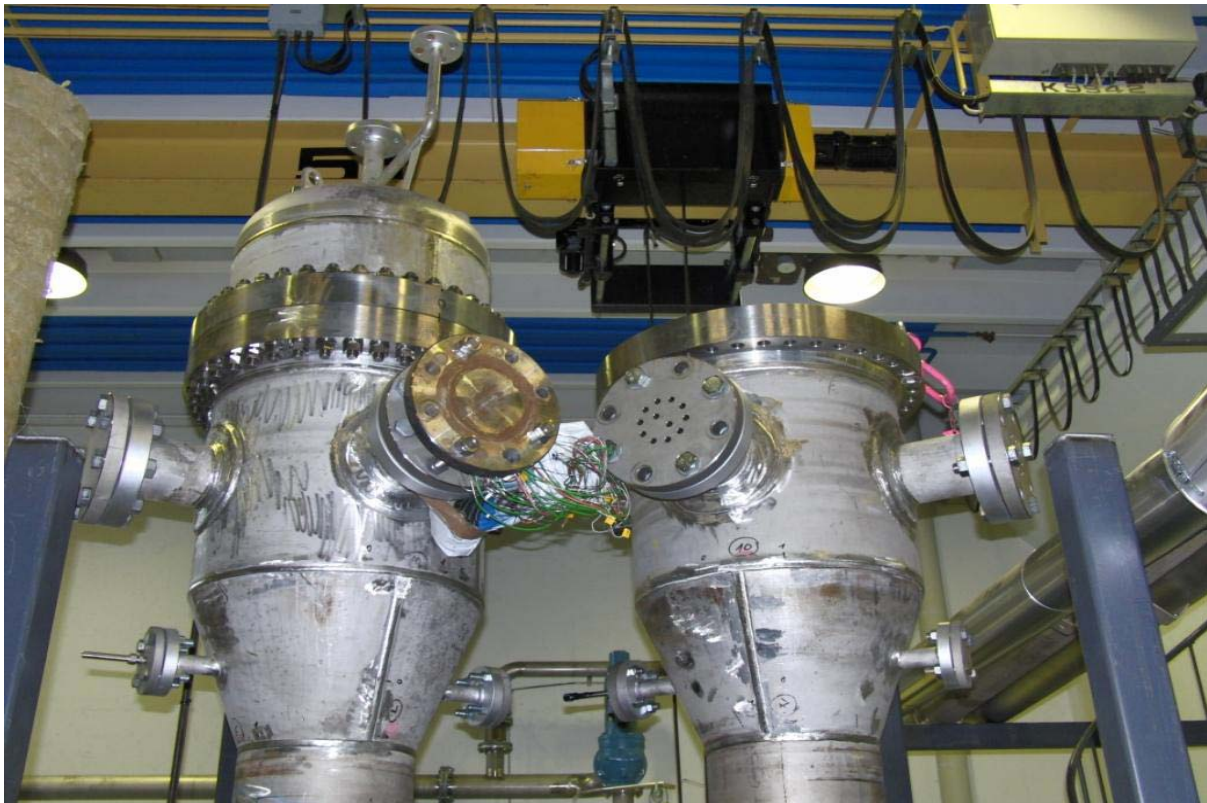


Figure 3 : Top view of the PWR PACTEL steam generators [3]

The secondary side of the steam generators includes hot and cold legs, a down-comer, riser, and steam dome volumes. The hot and cold legs with an inner diameter of 52.5 mm are on

the same elevation, and the cold legs have loop seals. There are no steam separators. Compared to the secondary side of the EPR steam generator, the volume of water is almost double to the secondary side of the PWR PACTEL steam generator and feed water is injected to the secondary side of the steam generator. PWR PACTEL steam generators have no steam separators so 100 mm mineral wool and 0.5 mm aluminum plate are used to cover PWR PACTEL steam generator as an insulator [3][7].

Today, there are no circulation pumps in the loops, but places are reserved for possible pump fitting in PWR PACTEL.

General view of steam generators are shown in Figure 2 and Figure 3

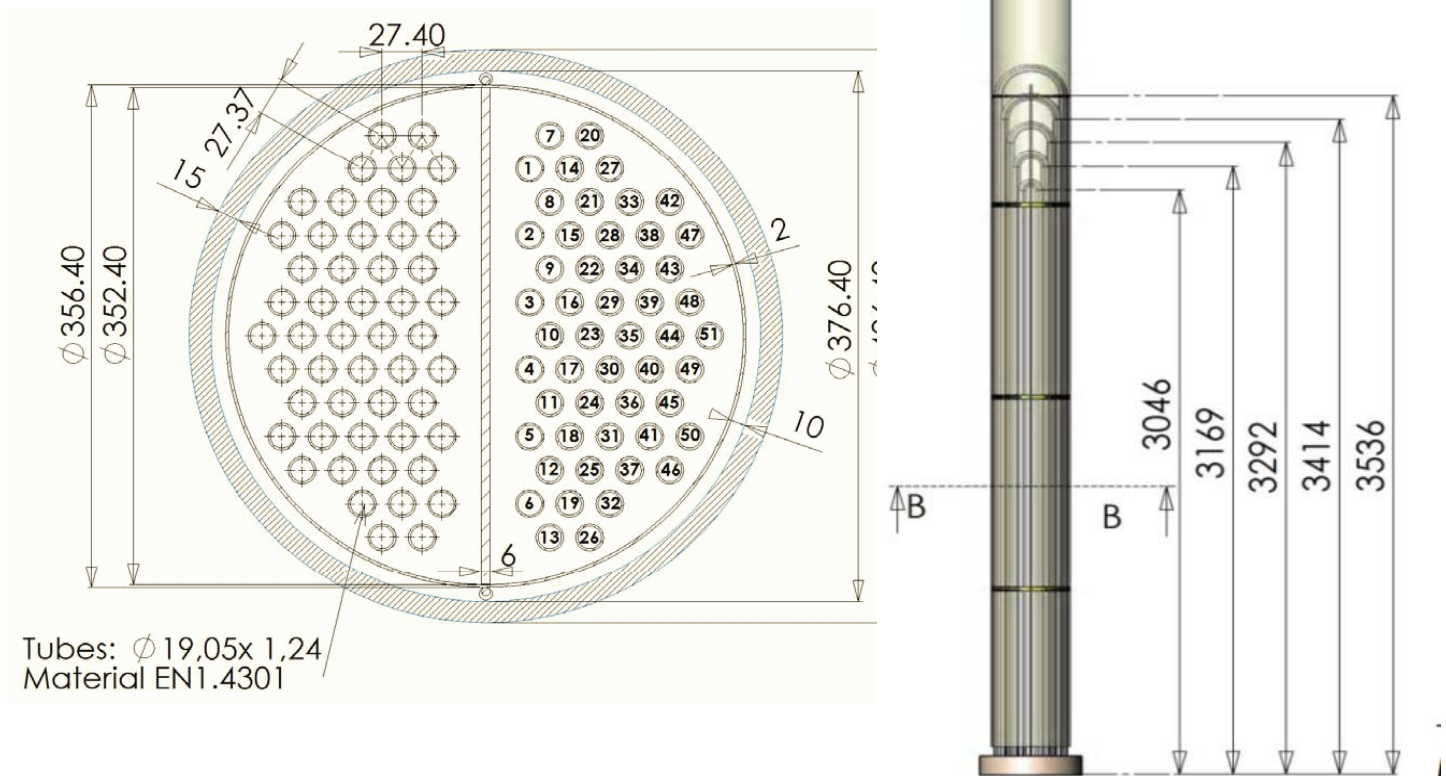


Figure 4 : Heat exchange tubes of the PWR PACTEL steam generators [3].



Figure 5 : Heat exchange tubes of the PWR PACTEL steam generators [3].

1.4 Features of SBL-50 benchmark transient experiment

Benchmark is a standard of estimating the ability of systems by setting one or more test loads on them and then measuring their performance. Within the PWR PACTEL facility, an SBL-50 benchmark experiment was carried out to understand the thermal hydraulic behaviour of EPR type Steam Generators under Small Break Loss of Coolant Accident (SBLOCA) transients. Natural circulation behaviour in the vertical steam generator's primary side is also observed in this experiment during SBLOCA[3]. All this phenomena has been simulated by thermo hydraulic code.

To understand the phenomena during accidents, the following steady state initial condition (Table 2) was carried out in SBL-50 benchmark experiment:

Table 2. Steady state initial condition of SBL-50 benchmark experiment [3]

PARAMETER	VALUE
Primary side pressure	75 bar \pm 1 bar
Secondary side pressures	42.0 bar \pm 0.6 bar
Core power	155 kW \pm 6 kW
Pressurizer collapsed level	5.7 m \pm 0.2 m
Steam generator collapsed levels	3.9 m \pm 0.12 m
Steam generator feedwater temperature	23 °C \pm 1 °C (SG 1) 19 °C \pm 1 °C (SG 2)
Steam generator feed water flow rate	1.5 l/min \pm 0.4 l/min

The transient primarily arises with Steady State operation for a few seconds and then the small break open to create the inventory loss and measurements of parameters were recorded. As a result, change in mass flow rate, difference in temperature and phenomena of real nuclear power plant could be understood.

PWR Benchmark experiment gives unique opportunities to the code users to take part in the exercise, model the facility, and simulate the transient. Seven organizations, from different countries participated in the benchmark exercise and used four different system codes. The first benchmark workshop was held 5th October 2010. In 2010, Takeda and the Finnish power companies TVO and Fortum had provided the financial support for the PWR PACTEL benchmark.

Chapter 2

Description of the Tools and their Practical Application

To understand the behaviour of the nuclear power plant system, many computational tools have been developed. Computational tools describe the real and transient phenomena for the safety of nuclear power plant by simulating the performance of the system. In this chapter, the modelling tools and their application for the thermal-hydraulic system have been discussed.

2.1 Description of RELAP5 computer code

Nuclear power plants may have a potential severe hazard for public health and the environment during accidents. Power plant safety needs to be assessed and demonstrated using safety analysis. In this respect, computer codes play an important role in NPPs design and safety analysis.

RELAP5 is a highly generic one-dimensional code that is used for simulating the behaviour of a nuclear power plant during a transient. It is a rational, systematic and efficient code for nuclear power plant safety analysis. RELAP5 code was originally developed by the US Nuclear Regulatory Commission (NRC) at the Idaho National Engineering Laboratory (INEL) from 1960 to '70s [6]. Till now the development of RELAP5 code is still going on due to the need for a reliable, fast running, well established, two-phase flow transient analysis tool [8].

This one-dimensional RELAP5 thermal-hydraulic code is designed on the basis of six phase equations : two mass conservation equations, two momentum conservation equations and two energy conservation equations [3] [8]. This computational code contains special process models for the deterministic analysis of reactor transient and accidents at nuclear power plant. RELAP5 provides an in-depth knowledge of plant scenario and safety by realistic assumption and best estimated calculations.

The exact applications of the code have included simulations of a large variety of hydraulic and thermal transients in LWR systems such as loss of coolant, anticipated transients without scram, and operational transient, e.g loss of feedwater, loss of offsite power, station blackout, and turbine trip [9] [10].

For computing the behaviour of nuclear power plants, several structural and thermal hydraulics analysis codes have been introduced and developed, but s RELAP5 is still the most used analysis code due to its worldwide use. Many modification have been made for the development of RELAP5 code. Since 1985, when the first RELAP5/MOD2 was introduced,

many changes have been made to make the code more realistic and user friendly, since it is difficult to simulate complex phenomena with the old version of code. Now the code is more complex to use with large range of analytical capability [10]. The latest version of RELAP5/MOD3.3 Patch 04 (release in 2011) is used in the modelling of PACTEL SBL-50 Transient analysis [6] [10].

2.2 Description of RELAP5/MOD3.3 patch 04 input model

Today it can be possible to simulate an extensive number of system transients in light water reactor with RELAP5/MOD3.3 Patch 04. The input model includes; heat structures, control systems and hydrodynamic components like, pipes, single junctions, multiple junctions, valves, time-dependent volumes, time-dependent junctions, flows, branches, cross flow junctions, pumps, accumulators, core neutronics and so on. Normal operations accidents, small break loss of coolant accidents (SBLOCAs), and postulated accident scenarios can be described in terms of input records or cards [9] [10]. This kind of simulation and RELAP5 analysis has become possible due to continuous development and modification of RELAP5 input model [9] [10].

The development of RELAP5 input models were extensively used to extend the experiences in simulations of small break loss of coolant accidents and two-phase natural circulation cooling [10]. Different kind of input models, e.g small, middle, large and common were introduced and developed which contains more volumes, junctions, heat structures and increasing number of nodes of steam generators. For restart calculation, new components were added and another version of RELAP5 was designed without changing any geometry, number of hydraulic component or heat structure. In the input file, RELAP5 user specifies all the component in the system and connect required component by putting the exact geometrical data (such as pipe diameter, cell length, flow area, etc). The control logic of the systems is connected according to the specific card [11]. More detailed view of RELAP5 input model (how its look likes) attached in appendix 1.

Most of the calculation of RELAP5 were performed by SUN SOLARIS operating system. The code version were created on the specific computer and the executable could not be moved to other computers. In 2011, new executable of RELAP5/MOD3.3 patch 4 and was introduced for Microsoft Windows operating system. There was a high demand of the code the user community for minimize the complexity and increase the user friendliness. Therefore, a particular visualization tool, called SNAP was developed. The latest version of RELAP5 are capable of visualization of the model in various views, such as hydrodynamics and control system. It is comfortable to model primary and secondary sides of the steam generators with RELAP5/MOD3.3 input model for single or multi tubes by Model Editor of SNAP [10]. The new versions of RELAP5/MOD3.3 patch3 and

RELAP5/MOD3.3 patch 4 are capable of calculating small time intervals and they are able to show small differences [9] [10].

2.3 Applicable field of RELAP5

RELAP5 is used to simulate a very wide variety of system transients. The core, RCS, secondary systems (including feed water and steam turbines), auxiliary systems, pumps, valves, and all system controls can be simulated by RELAP5 [8] [10]. Most of the applicable field is described in section 2.1

2.4 Limitation in RELAP5

It is generally recognized within the technical community that severe transient behaviour is mostly well characterized by RELAP5. RELAP5 is a one dimensional code, due to that uncertainties associated with current limitations in severe accident condition some behaviour could not be simulated because experimental data for all relevant phenomena are not complete or do not exist. Real transient resources are not always available to develop computer models when data does exist [8] [10]. Consequently, it can be stated that RELAP5 can reliably be used in a transient up to the point of reaching critical heat flux (CHF). Beyond that stage, especially fuel damage is a concern, a dedicated severe accident simulation code should be applied (for instance SCDAP or MELCOR) [8].

2.5 SNAP tool

2.5.1 Model development with SNAP tool

SNAP (Symbolic Nuclear Analysis Package) is a graphical user interface for creating and editing a model for an engineering analysis code. SNAP provides a flexible framework for an analysis by visualization of the code outputs and data. Currently this tool control the runtime job features by keeping track of your input and output files. The present version of SNAP is very handy in visualization of the models or the results of nuclear analysis codes, such as RELAP5, COBRA, FRAPCON-3, MELCOR, PARCS, RADTRAD, CONTAIN and TRACE [12].

The SNAP application frame work contains a Model editor, a Job Status Tool, and a Configuration Tool. The APTPlot utility can be used for plotting the parameter values in curves, regardless of whether they originate from the transient calculation or from recorded experimental data. A group of components can be visualized and edit in a logical way in SNAP model editor. Moreover, The SNAP model editor can import and export models as

ASCII file format. It is also reliable for error checking which gives the user a quick option for error correction. Last but not least, the user can create so called animation masks. With the Animation tool, the calculated results can be visualized in motion pictures, slowing down or speeding up the evolutions of the transient. The Configuration Tool specifies the properties of the job and job status can be displayed. The APTPlot can read and plot the data directly from any SNAP supported code [12] [13].

In the following example, a simple model is shown for simulation of a loss feed water case that has been developed by using SNAP tool :

Case 1 : is an unheated pipe : The Figure 6 below shows an unheated 10m long circular pipe with 10 axial nodes with a flow rate of 1 kg/s and temperature 330K. The diameter of the pipe is 0.1m. There are two boundary conditions: the inlet and the outlet boundaries. Both are at the same pressure and temperature. The inlet boundary is connected with a pipe through a time dependent junction and the outlet boundary is connected with a pipe through a single junction. The transient is simulated for 200s, when the inlet flow rate decreased suddenly from 1kg/s to 0kg/s between 50s and 51s, and it remained zero for the rest of the transient. The calculation was running with a time step 0.1s. The APTPlot utility, was used for plotting the mass flow rate in the middle of the pipe.

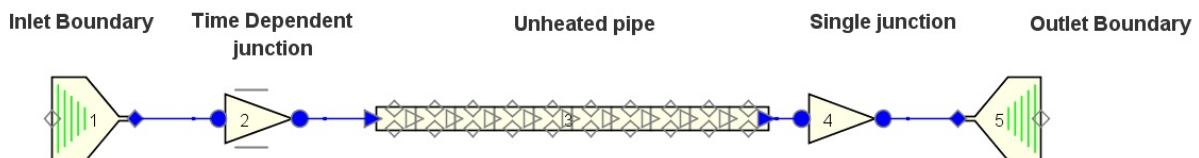


Figure 6 : Graphical presentation of unheated pipe in SNAP

Case2 : In a similar way the developed model can be used for simulating a heated pipe. This is shown in Figure 7 below. In this case, the wall thickness of the pipe is considered to be 3mm, having a 4 radial mesh point. The total heating power is 100kw and the axial power profile is constant and convective heat transfer is considered between the fluid and the wall. The outlet boundary was replaced with saturated steam, with static quality of 1.

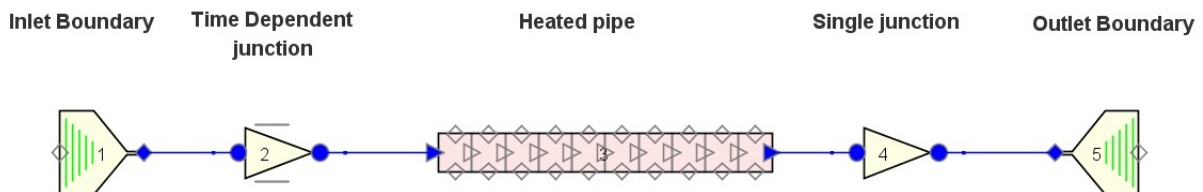


Figure 7 : Graphical presentation of heated pipe in SNAP

The pipe is stainless steel and the properties are built in RELAP5. In a same manner the APTPlot utility was applied to plot the liquid void fraction and the temperature distribution in the pipe.

The SNAP editor is used in this project to modify the current single heat exchanger tube model to multiple (five) heat exchanger tubes for both steam generator 1 and 2. Then the model is re-nodalized with rough and finer nodalization for better result and accuracy. After that by using the model editor checking option, we checked multi tube model. Verification of the model can be done by hydraulic loop check option. This feature is used for detection of possible errors originating from incorrect elevation changes, potentially preventing closer of the loops.

2.5.2 Two way conversion between texts based input and graphics

Figure5 and 6 shows the graphical representation of the simple model. This graphical model can be converted to ASCII code that is shown in appendix section. Moreover, in a similar way, text based ASCII input code cab be convert to graphical representation of the model.

Note: ASCII input is available in appendix A section

2.5.3 Strategies for achieving steady state

To initiate a transient calculation, it is important to achieve a satisfactory steady state condition. The general method for achieving steady state conditions is describes below :

Figure 8 demonstrates a general method to obtain a steady-state achievement for a portion of any model. In previous section figure,5 and 6 showed similar thing for an unheated and a heated pipe, respectively.



Figure 8 : General methods to achieve steady state condition for a part of full system model [13]

The portion of the full system model can be a steam generator, reactor vessel, hot leg, cold leg etc. The inlet boundary consists of a time dependent volume (TDV) and time dependent

junction (TDJ). At the upstream end of the model, and outlet boundary is connected by a single junction (SNGIJUN) and time dependent volume (TDM) to the system model. The inlet boundary condition specifies the inlet flow rate and fluid state e.g. pressure, temperature, internal energy and void fraction or quality as a function of time. The outlet boundary condition specifies the outlet pressure. Reasonably stable conditions may be achieved by this kind of arrangement in the full system model.

Before the transient initiation, it is essential to maintain steady state, both in the experiment and in the simulation. Consequently, the following parameters were controlled in the PWR PACTEL facility in order to obtain satisfactory steady state conditions:

1. SG-1 and SG-2 level
2. SG-1 and SG-2 pressure
3. Primary pressure

Constant SG levels were obtained by a control system connected to feed water injection system. The level controller provided the necessary amount of feed water flow to keep the SG levels constant.

The SG pressure was kept stable by connecting a time dependent volume to the top of the SG. Saturated steam was specified at the outlet boundary volume with a constant pressure.

During the steady state operation, the pressurizer (PRZ) is connected to the facility and the primary pressure is kept constant by control system, with spraying water (if the pressure is high) or by electric heating (if the pressure is under the setpoint).

The mass flow rate is not possible to be controlled in the PWR PACTEL facility because it does not include any pumps. Consequently, the loop flow is always natural circulation, driven by buoyant forces, as consequences of temperature/density differences. Therefore, the resulting mass flow rate of the loop is determined by the buoyant forces and the flow resistances. Differential pressure were measured at some certain points of the facility. However, the pressure losses in every single components or junctions are not generally known. This means that code user can influence the exact value of the mass flow rate only by minor adjustments of the flow resistances (e.g. forward and /or reverse loss coefficients and the wall roughness) in the model.

2.5.4 Application of SNAP animation tool

SNAP animation is a powerful tool to create the animation mask for the transient and animate the entire process by using colour scales for various parameters, such as liquid temperature, void fraction, fluid condition, and pressure distribution.

2.5.4.1 Procedure to create a new animation model

The data in the animation model retrieves from the calculation server and then visualize the model on the screen. The following procedure gives an idea, how to create an animation model by using the animation task.

By pressing the “new” button on the main SNAP toolbar, it shows a new animation model option to create a new animation model. The animation model may contain several components : model options, python data sources, data sources, colour maps, plot definitions and views. These editing components look the same as in SNAP model editor components.

The details application of visualization tool for the PWR PACTEL Benchmark Transient simulation will be described in the animation section 4.6.

2.6 Other related software

2.6.1 MATLAB

MATLAB is one of the leading programming software for numerical computation, algorithm development, data analysis and visualization. Using MATLAB, engineers and scientists in industry and academia can solve technical computing problems faster than with traditional programming languages, such as C, C++, and FORTRAN [14].

The wide range of applications of MATLAB makes it unique .MATLAB including signal and image processing, communications, control design, test and measurement, financial modelling and analysis, and computational biology. For a million engineers and scientists, MATLAB is the language of technical computing [14]. In this report, most of the test result data is plotted by Mathlab.

2.6.2 Corel Draw

Corel Draw is a vector graphics model editor .Corel Draw is developed and marketed by Corel Corporation, Canada. Specially many innovations to vector-based illustration originated with Corel Draw: a node-edit tool that operates differently on different objects, fit text-to-path, stroke-before-fill, quick fill/stroke colour selection palettes, perspective projections, mesh fills and complex gradient fills [15] [16].For graphical view (Figure 21) of multitube model is drawn by Corel Draw editor. Corel Draw differentiates itself from its competitors in a number of ways like,

1. Corel Draw is positioning as a graphics suite, rather than just a vector graphics program.

2. It is capable of handling multiple pages along with multiple master layers.

3. Corel Draw can able to work with all vector-based illustration programs. Corel Draw can open Adobe PDF files : Adobe PageMaker, Microsoft Publisher, Microsoft Word, power point files and other programs .In Coral Draw one can open and edit every aspect of the original layout and design [15] [16].

Chapter 3

Theory of nuclear Thermal-Hydraulics

The purpose of this chapter is to provide a general overview about the theoretical background, which is relevant to the thesis. Theory plays an important role for finding exact analytic solution. Therefore, it is essential to understand the phenomena during transient and the analytical capabilities of the RELAP5 code.

3.1 Thermo hydraulics

Thermal hydraulics may be defined as a complex dicipline, dealig with fluid mechanics and thermal processes. In nuclear power plants, it is in close relationship with basically all the components. The best example is the steam generator in PWRs. It is the component, where water change its liquid state to vapor (or gaseous state) phase and heat energy transferred to the mechanical motion. RELAP5 is mainly based on three balance equations, as follows :

- i. Mass conservation equation
- ii. Momentum conservation equation
- iii. Energy conservation equation

3.1.1 Mass conservation equation

The equation for area integrated mass conservation is as follows [22]

$$\frac{\partial \rho_m}{\partial t}(x, t) + \frac{\partial G_m}{\partial x}(x, t) = 0$$

Where $\rho_m(x, t)$ = area integrated density

$G_m(x, t)$ = area integrated mass flux

3.1.2 Momentum conservation equation

The equation for area integrated momentum conservation is as follows [22]

$$\frac{\partial G_m}{\partial t}(x, t) + \frac{\partial \left(\frac{G_m^2}{\rho_m} \right)}{\partial x}(x, t) = \frac{F_w}{A_x}(x, t) - \frac{\partial \{P\}}{\partial x}(x, t) + \rho_m(x, t)g \cos \theta$$

Where the left hand side of the equation indicates time and spatial dependent momentum

3.1.3 Energy conservation equation

The equation for area integrated energy conservation is as follows [22]

$$\frac{\partial}{\partial t} [\rho_m(z, t) \left(h_m(z, t) + \frac{1}{2}(v^2)_m(z, t) - \{P\} \right)] + \frac{\partial}{\partial z} [G_m(z, t) (h_m^+(z, t) + (v^2)_m(z, t))] = -q_w''(z, t) \frac{P_w}{A_\pi}(z, t) + \{q'''\}(z, t) + \frac{q_w(z, t)}{A_\pi} + G_m(z, t) g \cos \theta$$

Where,

q_w = work frictional force at the wall per unit length

q_w'' = Heat transfer at the walls per unit surface area (negative sign indicates fluid receive energy)

P_w = wetted perimeter

θ = angle between z direction and gravity vector \vec{g}

3.2 Natural circulation flows

Natural circulation flow is based on the principle of the nature flow. This does not require any pump system or external source of energy for fluid circulation. Its operates on differences in density. During natural circulation, it is observed that the flow of the liquid is not fully developed at times or multidimensional otherwise [8].[17]. No external sources of energy for the fluid motion are involved when NC is established.

Natural Circulation Flow Rate : $\nabla P_a = \nabla P_f + \nabla P_L + \nabla P_c$ Where $\nabla P_a = \int \rho dz$

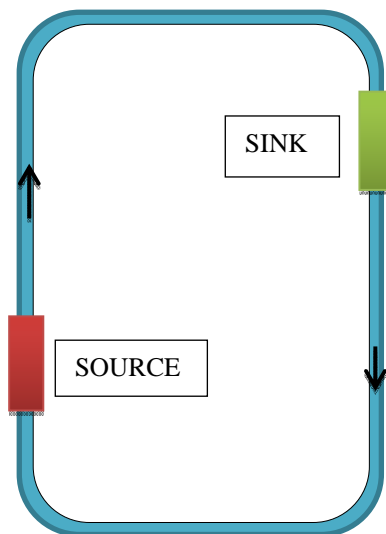


Figure 9: Natural circulation in a close loop [17]

The above expression specifies that the parameters of interest to determine flow rate are [12] :

- a) Single phase and two phase density
- b) Single and two phase pressure loss components

It might be noted that the driving force in a natural circulation loop is small, it is necessary to minimize and determine very accurately the pressure loss components. Balance between the driving and the resisting forces from heat source to heat sink established the circulation. Loop height and density difference is very important for natural circulation. In nuclear power plants, natural circulation flow is known as reliable safety heat transport mechanism for long term cooling of PWR reactor during loss of coolant accident (LOCA).

In the PWR PACTEL, natural circulation flow is used to make the system simple. The elimination of the pump simplified the construction, operation and maintenance of the system. Steam generator has a great application with natural circulation for heat process. In steam generators, thermo-hydrodynamic instability can be minimized by natural circulation. Flow distribution in the U-tubes is uniform in a natural circulation system. Also two-phase flow in fraction of time is good in natural circulation system [8] [18]. A variety of computation methods have been developed to predict thermal hydraulic phenomena associated to natural circulation. Similarly, thermal-hydraulic system codes have been capable of simulating the exact experimental data during transient in the natural circulation process. It is capable of giving the best analytical approaches to predict single-phase and two-phase natural circulation flow because of the lower driving forces [19].

Natural circulation is not always an easy task as it starts up in low pressure and low temperature condition during the pressure and power raising process. In this circumstance, there is a possibility of flow reversal. On the other hand, it is very difficult to predict stability (or instability) in the U tubes, which constitutes a key feature of a natural circulation system.

3.2.1 Flow reversal

Natural circulation systems are not free from instabilities like flow reversal. Sometime instabilities are common in both forced and natural circulation systems. In natural circulation, system instabilities are more than the forced or non-natural circulation system due to the low driving force [18]. Specially this kind of phenomena were observed in a new nodalization model. It means scaling issue is one of the reasons for flow reversal.

To understand the phenomena of reverse flow in U-tubes of a PWR steam generator let us consider a natural circulation flow is moving through the pipes with a common downcomer. Differences in densities cause the flow movement from the inlet to the outlet due to the differences in the heating rates. If any one of these conditions arise, the flow in the pipe can

reverse. This could happen even if heat transfer rate in the boundary condition of the pipe is high or equal [18].

As it is a common behaviour of a natural circulation, flow direction is not determined by the direction of the buoyancy force. Flow can prevail either in the clockwise or in the anticlockwise direction. There are many phenomena, which was observed in SG with asymmetric heating in U-tubes. The flow direction instability that establish in a SG is unpredictable during flow initiation or a seemingly unexplained flow reversal following a transient. Reverse flow also terminated oscillation growth scenario in the steady state condition [18]. The most complicated behaviors observed in SG U-tubes are due to the following reasons: pressure difference in the pipe, temperature difference, flow resistance, and density difference.

The NC flow behavior (stable or instable) has been distinguished by the thermo-hydraulic code RELAP5. The code interpreted the flow characteristic at the time of SBLOCA transient. The flow reversal and the different behavior of parallel groups of U-tubes could also be observed by the help of the code [17] [19].

3.3 Small-break LOCA

Small-break LOCA issue became highlighted in March 1979, after the accident at the Three Mile Island unit 2 (TMI-2) reactors. At that time, most of the attention was on large break LOCA because importance of the small break LOCA was underestimated. When the consequences of a small-break LOCA accident were discovered, it led to a radical change of attention in the detailed safety analyses [20].

The consequences of a small-break LOCA can be characterized by depressurization, loss of reactor coolant, degradation of core cooling, release of reactor coolant in the containment. Generally, any rupture with break size $4.65 \times 10^{-2} \text{ m}^2$ or less in the PWR primary system is known as small-break LOCA (SB-LOCA). The difference between a small break and a large break LOCA is in the rates of coolant discharge and pressure variations with time [20]. The reactor system response to a small break is slower compared to the events after a large break. The duration of the SB-LOCA is longer than the LB-LOCA because the core uncover period is longer. In addition, the core damage may be higher than in a large break LOCA.

3.4 Steady state and transient thermal-hydraulics analysis

3.4.1 Steady state thermal-hydraulics analysis

In order to simulate a transient using RELAP5, a steady-state case must first be run. More about steady-state in section 4.4 and 5.1.

3.4.2 Transient thermal-hydraulics analysis

If we focus on the transients, the initial conditions are usually very sensitive. Many transient parameters or models are derived from steady-state [21]. The transient analysis is a more complex problem than steady-state. Details of the transient calculation are described in sections 4.5 and 5.2.

Chapter 4

Steam Generator Model Development and Description

Steam generator modelling was carried out by the PWR PACTEL project to improve the safety standard of EPR type pressurized water reactor. It is assumed that accident phenomena can be modelled and predicted by the computer code (i.e. in a test facility, such as the PACTEL) similar to the real reactor transient. To achieve the best safety aspect, it is important to design and construct the new model through verification and validation. For this purpose, seven organizations from different countries took part in the experiment with different codes. A list of the participants and used system codes is presented in this table

Table5 : List of Participant [7]

Participant	Code
Chalmers University/Sweden	RELAP5 Mod3.3 Patch-03 ver. "h-h"
Fortum/Finland	APROS 5.09.11
GRS/Germany	ATHLET Mod 2.2 Cycle A
KTH/Sweden	TRACE 5.0 Patch 02
NRI Rez/Czech Republic	RELAP5 Mod3.3
Pisa University/Italy1	RELAP5 Mod3.3
VTT/Finland	APROS 5.10.01

This chapter gives some idea about the different PWR PACTEL models and potential of nodalization for Small Break LOCA (SB-LOCA) accident.

4.1. Description of PWR PACTEL model

PWR PACTEL model was designed in 2009 by some modified parts of original PACTEL facility. The thermal hydraulic behaviour of an EPR type pressurized water reactor is simulated in this model. The model of PWR PACTEL consists of 2 totally new vertical steam generators in 2 loops, a pressurizer and reactor pressure vessel (i.e. U-shape construction with the downcomer, lower plenum, core, and upper plenum) [3]. Especially loops and primary side of the U-tubes in the steam generators were reconstructed for the justification of the steam generator behaviour with more temperature and pressure measurement transducers.

Table 6: Primary side volumes of PWR PACTEL benchmark model[3]

COMPONENT	VOLUME [L]
Lower plenum	102.6
Core	82.6
Upper plenum	147.5
Downcomer	37.0
Hot leg I	5.8
Cold leg I	15.2
Hot leg II	6.8
Cold leg II	15.2
Pressurizer	133.5
Pressurizer line	4.4
Per steam generator U-tubes	74.1
Per Steam generator plenums	44.5
TOTAL	788

4.2 Description of PWR PACTEL single tube model

Modelling of the PWR PACTEL with a single tube has been simulated by the system thermal-hydraulic code RELAP5/MOD 3.3 Patch-03. This version was used throughout the calculation. The primary side of the steam generator consists of 51 vertical U-tubes, which were modelled with a single pipe for both SG [7]. The main input model modifications are as follows :

4.2.1 SG primary side of single tube model

1. The lengths of the steam generators have been replaced by averaging the model of the heat exchange tubes.

4.2.2 SG secondary side

1. Re-nodalization of the hot and cold side (310, 510downcomer and 320, 520 cold riser, 340, 540 hot riser)

2. Re-nodalization of the steam dome (330, 530) and hot side of down comer (350, 550)

All changes made by aiming the same heat exchanger surface geometry as per real SG.

4.3 Modification of current model by increasing the heat exchanger tubes

Previous input decks in RELAP5/mod3.3 have been developed for single tube PWR PACTEL model. This input deck is modified from single tube model to multiple tubes (fine and rough nodalization) (five equivalents pipe) model for both steam generators. The PWR PACTEL facility contains 2 loops in primary side and 2 separate secondary sides.

4.3.1 Modified multitube model with fine nodalization

The primary and secondary sides of the steam generators for the modified multi tube model with fine nodalization are described as follows:.

4.3.1.1 SG primary side

The vertical U-tubes modelled in five individual heat exchanger tubes for both steam generators (221 to 225 and 421 to 425 for SG-1 and SG-2, respectively). The U-tube pipes geometry was determined that way so that the heat exchange of the U-tube surface corresponds with the real steam generators. Heat exchanger tubes (221, 222 and 421, 422 of the SG1 and SG2 respectively) were divided into 29 volumes: 14 ascending, 1 horizontal and 14 descending. Heat exchanger tubes (223, 224 and 423, 424 of the SG1 and SG2 respectively) were divided into 27 volumes: 13 ascending, 1 horizontal and 13 descending. Heat exchanger tubes (225 and 425 of the SG1 and SG2 respectively) were divided into 29 volumes: out of them 12 ascending, 1 horizontal and 12 descending. The heat exchanger U-tubes are connected to the bottom of the inlet plena (210 and 410 of the SG1 and SG2 respectively) and outlet plena (230 and 430 of the SG1 and SG2 respectively) [3] [7].

4.3.1.2 SG secondary side

The feedwater is injected through the time dependent junction 305 of the SG1 and 505 of the SG2 respectively into the cold side riser of the downcomer (15 axial nodes of 310 and 510 of the SG1 and SG2, respectively). The downcomer is connected to the cold side riser (8 axial nodes of 320 and 520 of the SG1 and SG2 respectively) that is marked with blue color (Figure 22). The cold side riser is separated from the hot side of the riser (8 axial nodes in 340 and 540 of the SG1 and SG2 respectively) by the divider plate that is marked with green color (Figure 22). The boiling section and the steam dome are modelled with a pipe (9 axial nodes in 330 and 530 of the SG1 and SG2 respectively) that is marked with yellow color (Figure 22). The hot side of downcomer (350, 550) is connected to the steam dome with a junction (355, 555) [3] [7].

4.3.1 Modified multitube model with rough nodalization

Primary and secondary sides of steam generators for the modified multi tube model with rough nodalization are the same as the fine nodalization. Mainly, the modifications have been made on the cell length of the heat exchanger tube of the primary side of the steam generators. Heat exchanger tubes (221, 222, 223, 224, 225 and 421, 422, 423, 424, 425 of the SG1 and SG2, respectively) were divided to 15 volumes, out of them 7 ascending, 1 horizontal and 7 descending.

The cold side riser of the downcomer was re-nodalized with 8 axial nodes of 310 and 510 of the SG1 and SG2 respectively. Otherwise everything is same as the fine nodalization.

The nodalization scheme of the whole model.(Figure 10) shown below :

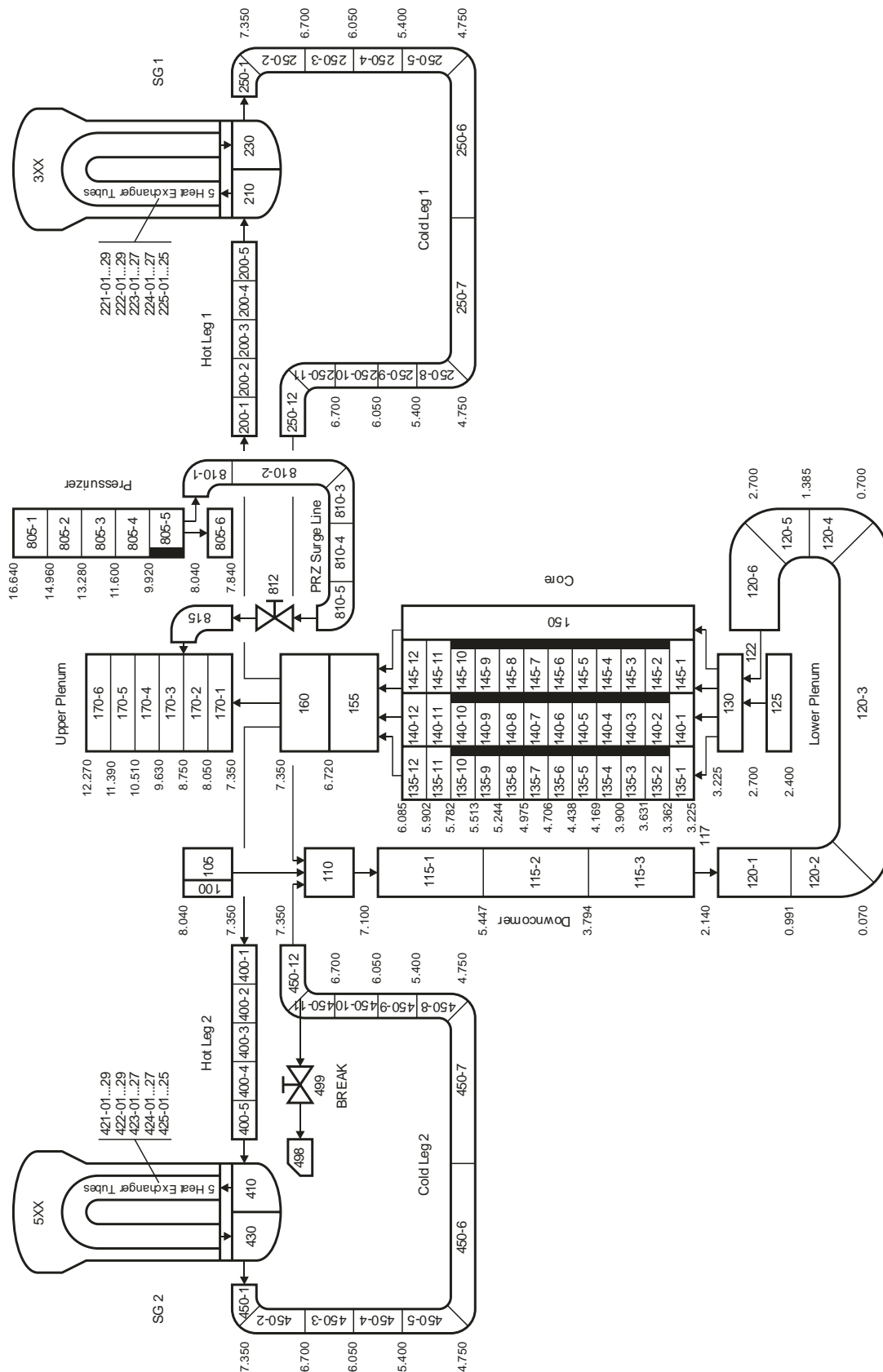


Figure 10 : PWR PACTEL nodalization of the primary side

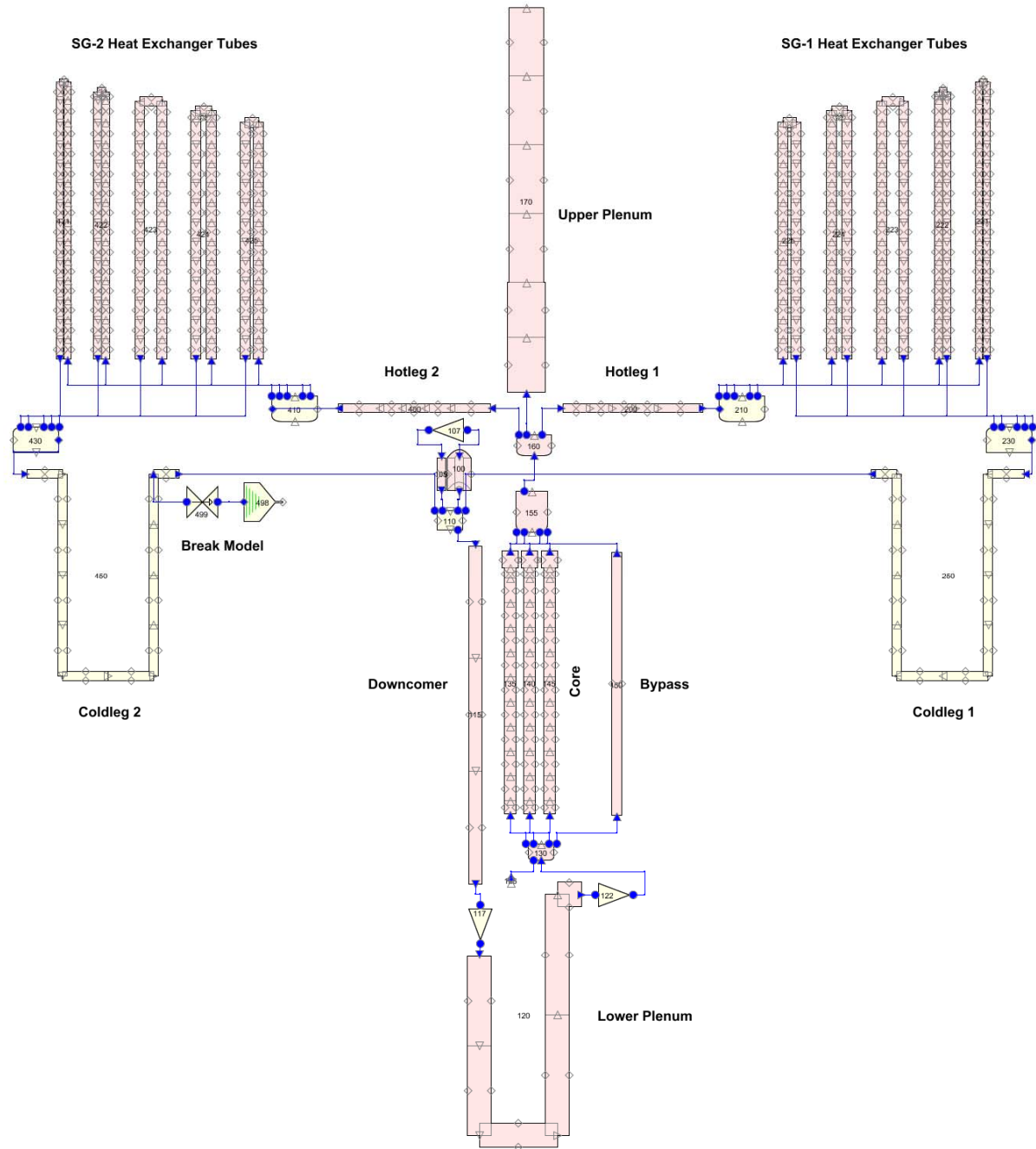


Figure 11 : The entire primary system model in the SNAP editor

SG-2 Primary Side Heat Exchanger Tubes

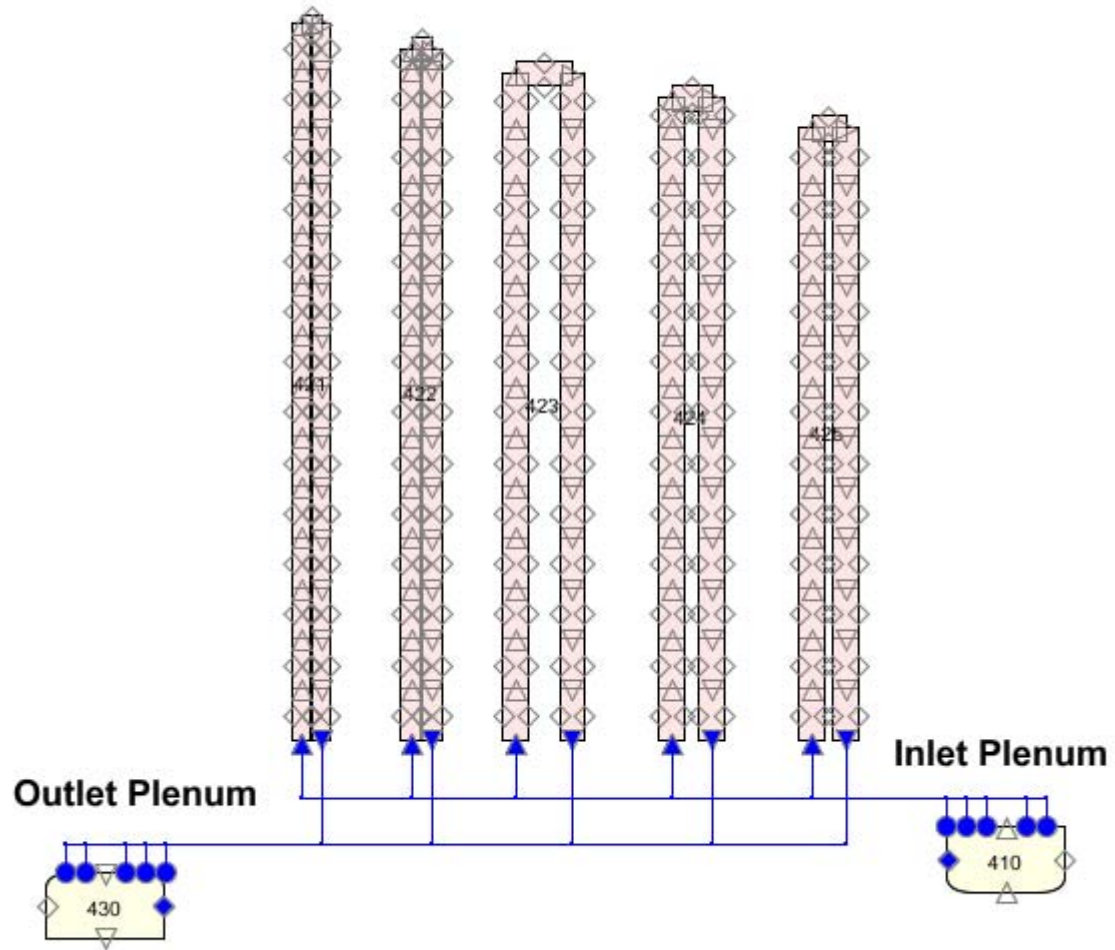


Figure 12 : The primary side model of steam generator 2 in SNAP

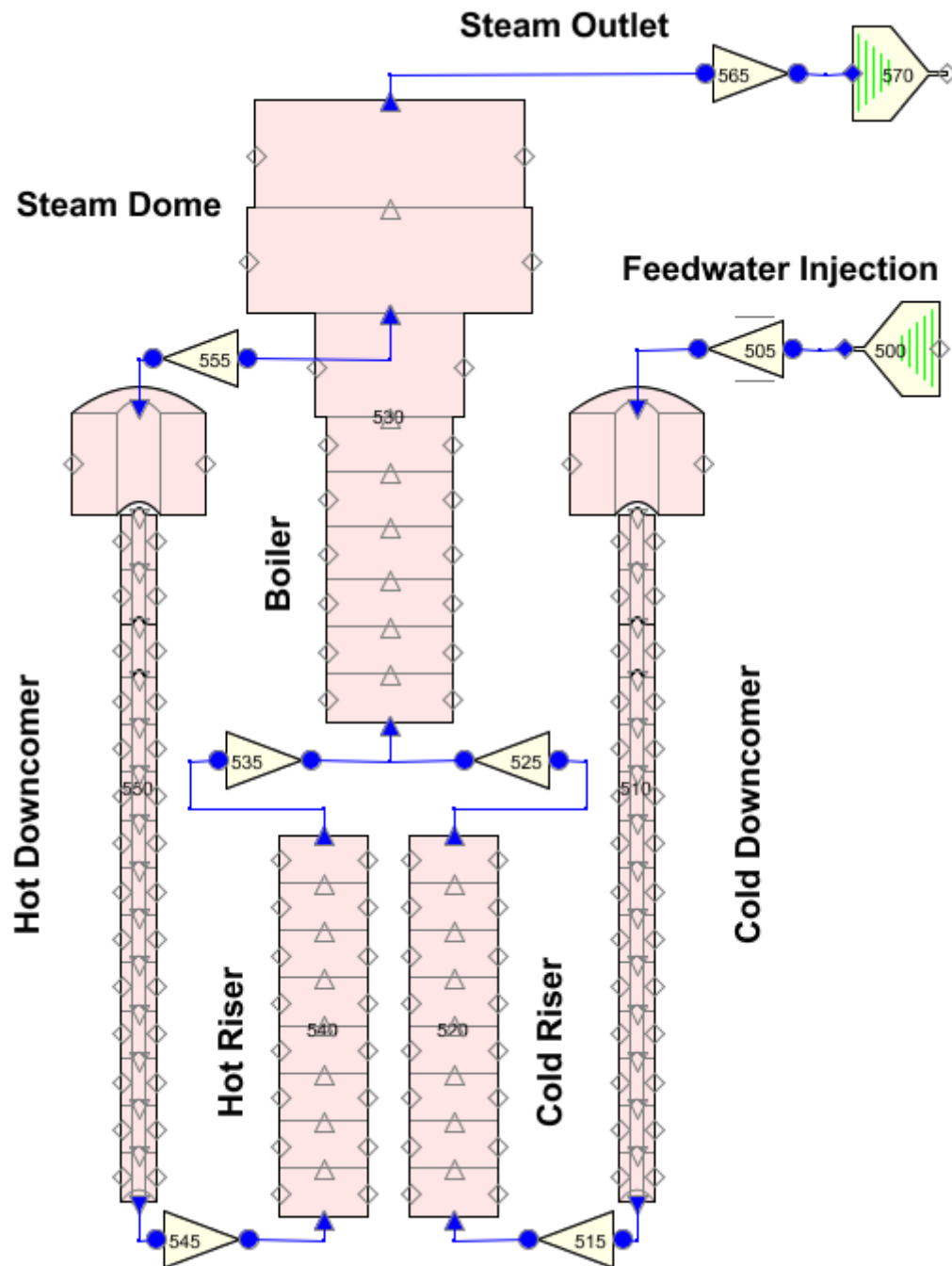


Figure 13 : The secondary side model of steam generator 2 in SNAP

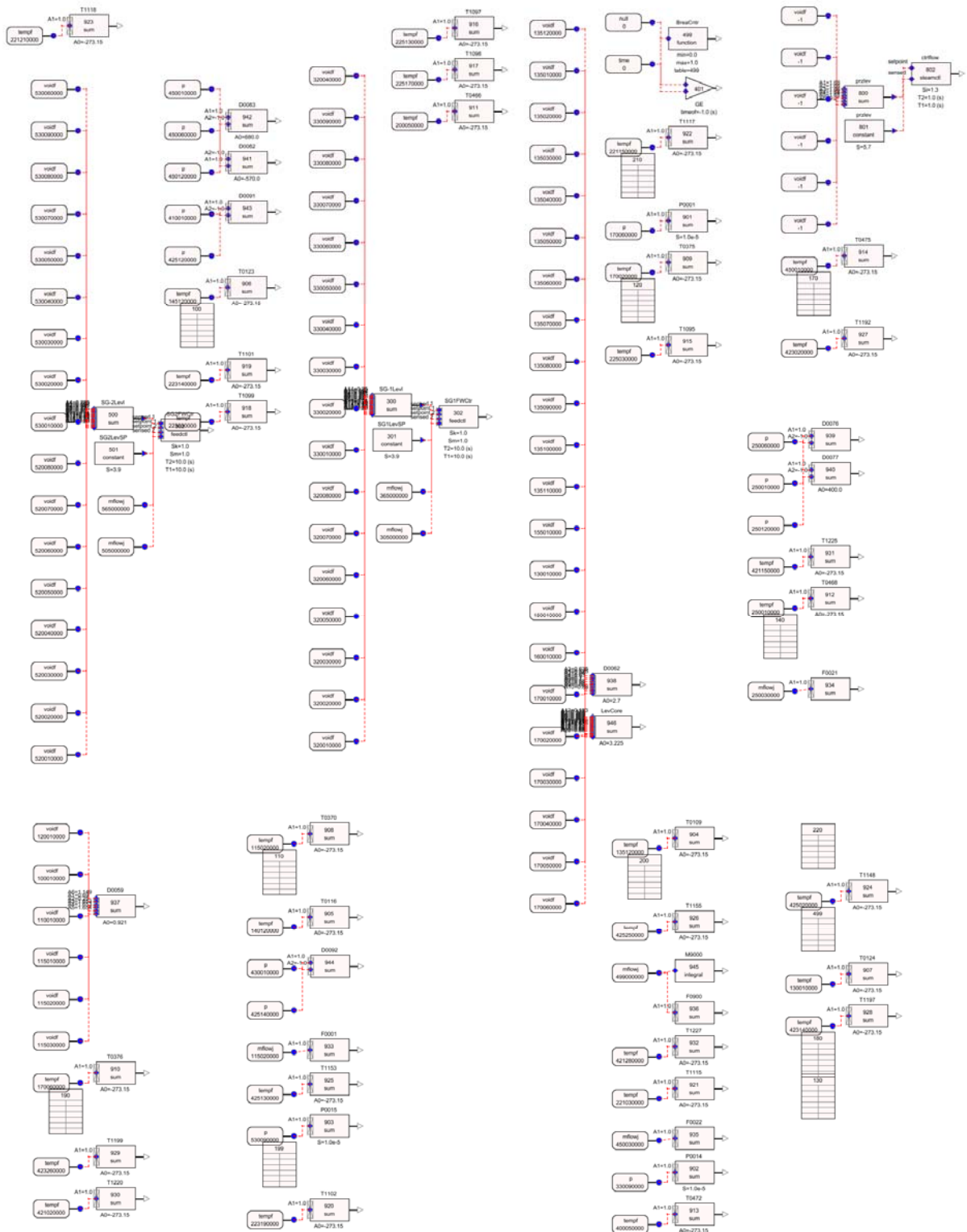


Figure 14 : The control system view in SNAP

4.3 Secondary side geometry

Calculation of the SG downcomer top part

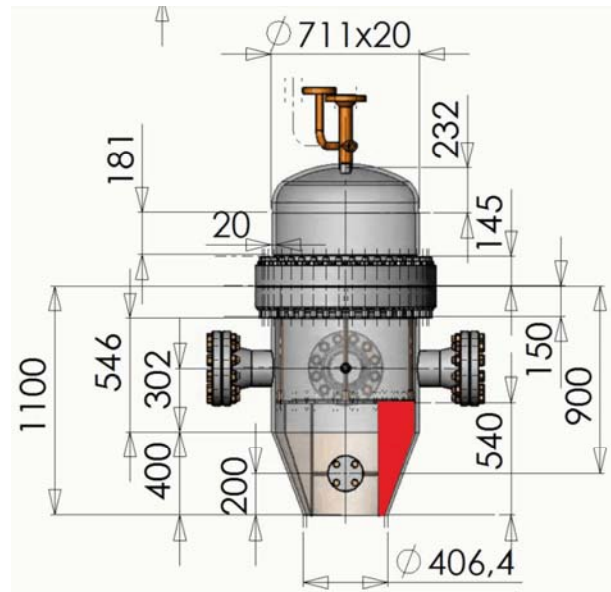


Figure 15 : Upper part of the SG [7]

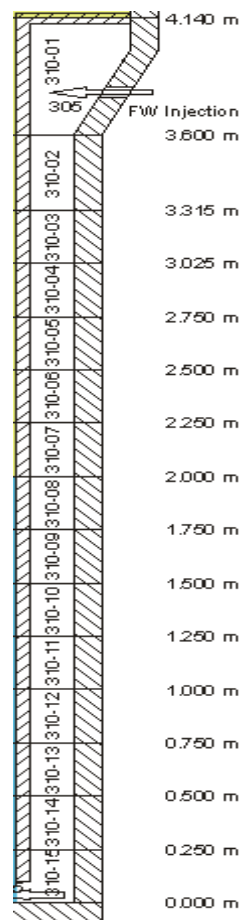


Figure 16 : Axial discretization of the SG downcomer cold side

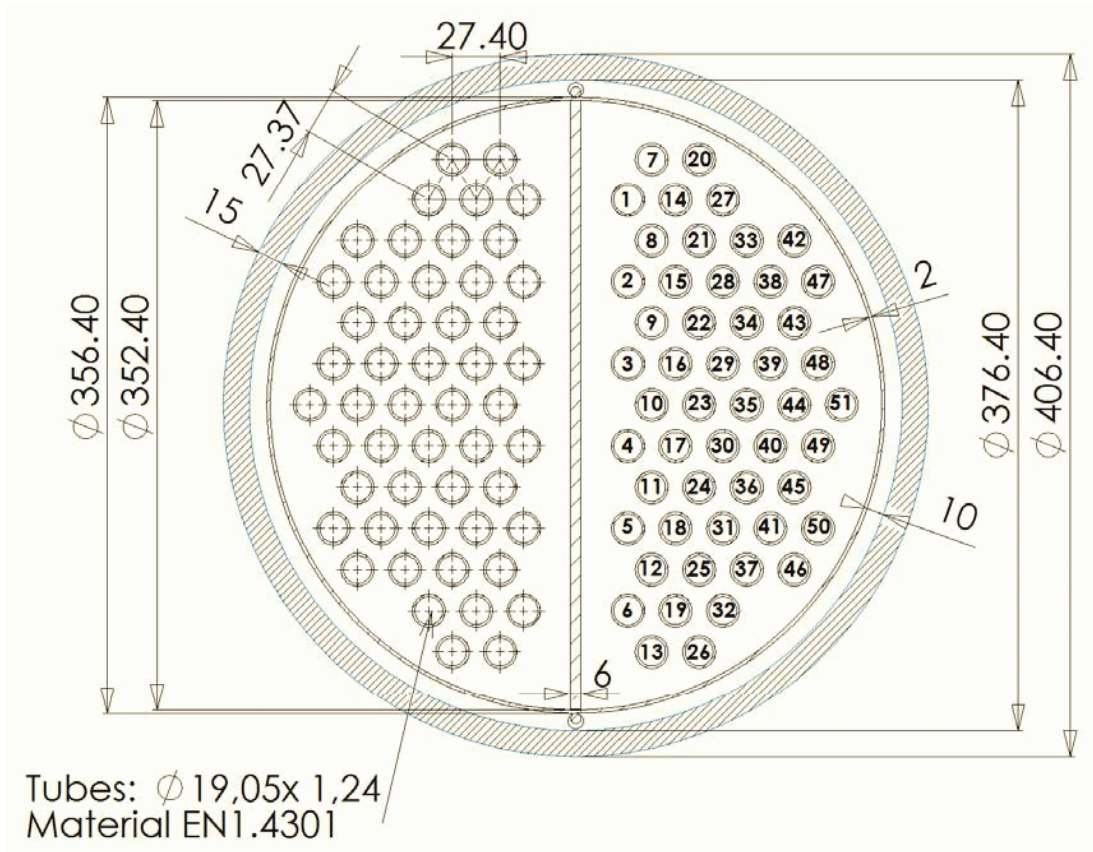


Figure 17 : Cross section of the steam generator

Number of tubes:

$$N_{tube} = 51$$

Inner and outer diameters:

$$D_{DC,i} = 376.4 \text{ mm} \quad D_{DC,o} = 406.4 \text{ mm}$$

$$D_{wrap,i} = 352.4 \text{ mm} \quad D_{wrap,o} = 356.4 \text{ mm}$$

$$D_{tube,i} = 16.57 \text{ mm} \quad D_{tube,o} = 19.05 \text{ mm}$$

Calculation of the free flow areas

Area covered by the tubes:

$$A_{tube} = N_{tube} \cdot 2 \frac{D_{tube,o}^2 \pi}{4} = 51 \cdot 2 \cdot \frac{19.05^2 \pi}{4} = 29072 \text{ mm}^2 = 0.029072 \text{ m}^2$$

Area covered by the divider plate:

$$A_{div} = D_{wrap,i} \cdot b_{div} = 352.4 \cdot 6 = 2124 \text{ mm}^2 = 0.002124 \text{ m}^2$$

Area inside the wrapper:

$$A_{wrap} = \frac{D_{wrap,i}^2 \pi}{4} = \frac{352.4^2 \pi}{4} = 97535 \text{ mm}^2 = 0.097535 \text{ m}^2$$

Total free flow area inside the wrapper:

$$A_{free} = A_{wrap} - A_{tube} - A_{div} = 0.097535 - 0.029072 - 0.002114 = 0.066349 \text{ m}^2$$

Free flow area on the cold side and hot side, symmetrically:

$$A_{free, cold} = A_{free, hot} = 0.033174 \text{ m}^2$$

Calculation of the hydraulic diameter

The wetted perimeter (the sec. side water is in contact with inner surface of the wrapper, with the divider plate, and the outer surface of the tubes) :

$$P_{wet} = P_{wrap} + P_{div} + P_{tube, out}$$

$$P_{wet} = \frac{D_{wrap,i} \pi}{2} + D_{wrap,i} + N_{tube} D_{tube,o} \pi = \frac{352.4 \pi}{2} + 352.4 + 51 \cdot 19.05 \pi = 3958.2 \text{ mm}$$

The hydraulic diameter on the cold side and hot side, symmetrically

$$D_{hyd} = \frac{4A_{free}}{P_{wet}} = \frac{4 \cdot 0.033174}{3958.2} = 34.4 \text{ mm} = 0.0344 \text{ m}$$

Cross section of the downcomer

The total flow area in the downcomer:

$$A_{DC, tot} = \frac{\pi(D_{DC,i}^2 - D_{wrap,o}^2)}{4} = \frac{\pi(376.4^2 - 356.4^2)}{4} = 11510.8 \text{ mm}^2$$

The free flow area in the cold side and the hot side of downcomer, symmetrically :

$$A_{DC, cold} = A_{DC, hot} = \frac{1}{2} A_{DC, tot} = \frac{1}{2} \cdot 11510.8 \text{ mm}^2 = 5755.4 \text{ mm}^2 = 0.0057555 \text{ m}^2$$

4.4 Primary side geometry

Calculation of the average tube length

The length of one tube :

$$L = 2L_{straight} + R_{U-bend}\pi$$

The average tube length can be determined by summing up the lengths divided by the total number :

$$\bar{L} = \frac{1}{N_{tube}} \sum_{i=1}^n L_i = \frac{1}{51} \sum_{i=1}^{51} L_i = \frac{1}{51} \cdot 343.7672 \text{ m} = 6.7405 \text{ m}$$

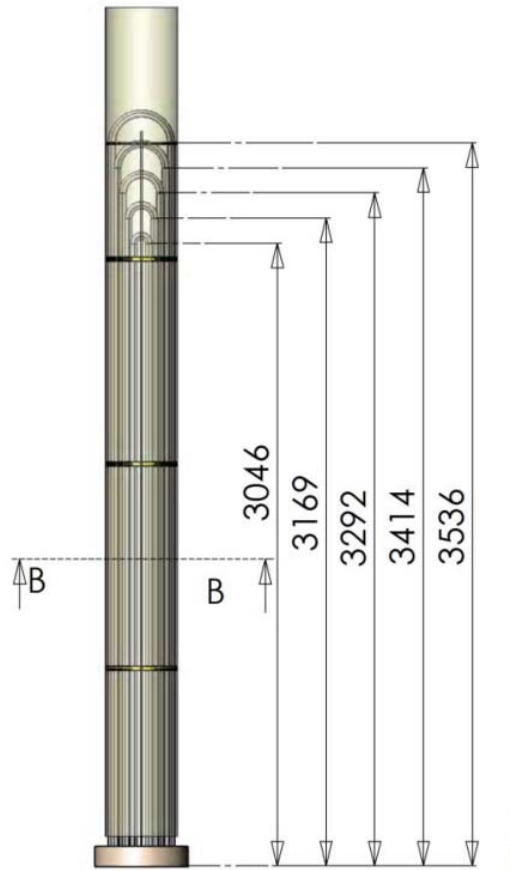


Figure 18: Lengths of the heat exchanger tubes [3][7]

Calculation of the primary side flow area

Flow area in the cold side and hot side, symmetrically : (Flow Area calculation of heat exchanger tube)

(1) First Heat exchanger tube (uppermost tube)

Length L=7.52 m

$$\text{Flow area} = N_{\text{tube}} \frac{D_{\text{tube}}^2 \pi}{4} = 0.0010782 \text{ m}^2$$

Here, $N_{\text{tube}} = 5$, $D_{\text{tube}} = 16.57 \text{ mm}$

(2) Second Heat exchanger tube (uppermost tube)

Length L=7.20 m

$$\text{Flow area} = N_{\text{tube}} \frac{D_{\text{tube}}^2 \pi}{4} = 0.001940784 \text{ m}^2$$

Here, $N_{\text{tube}} = 9$, $D_{\text{tube}} = 16.57 \text{ mm}$

(3) Third Heat exchanger tube (uppermost tube)

Length L=6.87 m

$$\text{Flow area} = N_{\text{tube}} \frac{D_{\text{tube}}^2 \pi}{4} = 0.00237207 \text{ m}^2$$

Here, $N_{\text{tube}} = 11$, $D_{\text{tube}} = 16.57 \text{ mm}$

(4) Fourth Heat exchanger tube (uppermost tube)

Length L=6.54 m

$$\text{Flow area} = N_{\text{tube}} \frac{D_{\text{tube}}^2 \pi}{4} = 0.0028033 \text{ m}^2$$

Here, $N_{\text{tube}} = 13$, $D_{\text{tube}} = 16.57 \text{ mm}$

(5) Fifth Heat exchanger tube (uppermost tube)

Length L=6.21 m

$$\text{Flow area} = N_{\text{tube}} \frac{D_{\text{tube}}^2 \pi}{4} = 0.0020033 \text{ m}^2$$

Here $N_{\text{tube}} = 13$, $D_{\text{tube}} = 16.57 \text{ mm}$

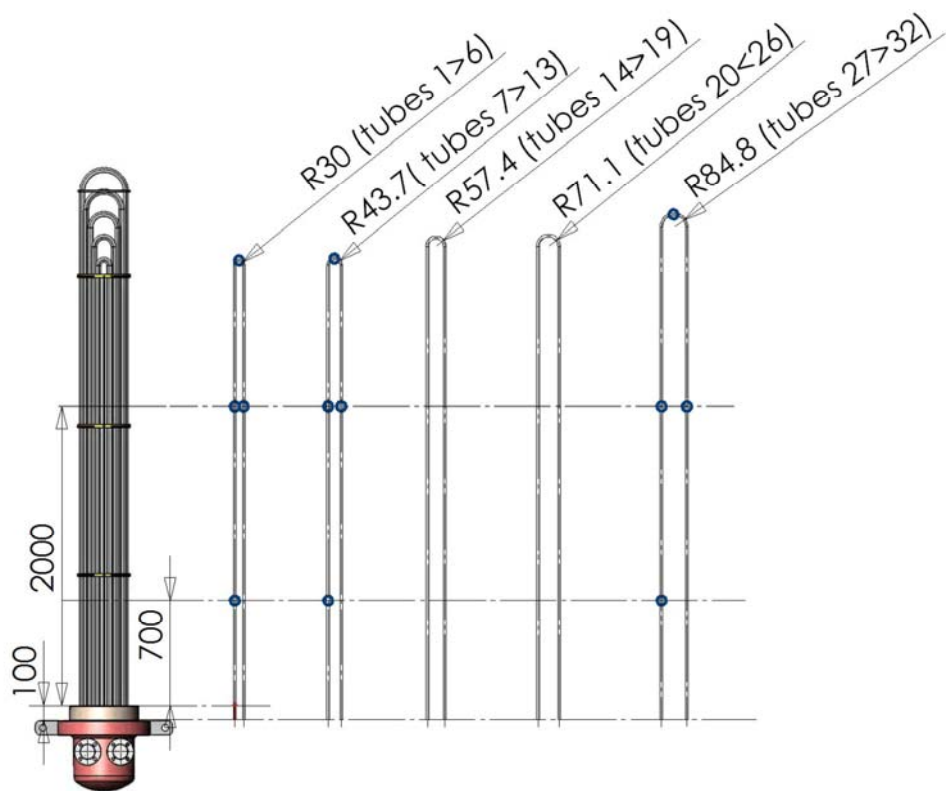


Figure 19: Radiuses of the U-bendings [7]

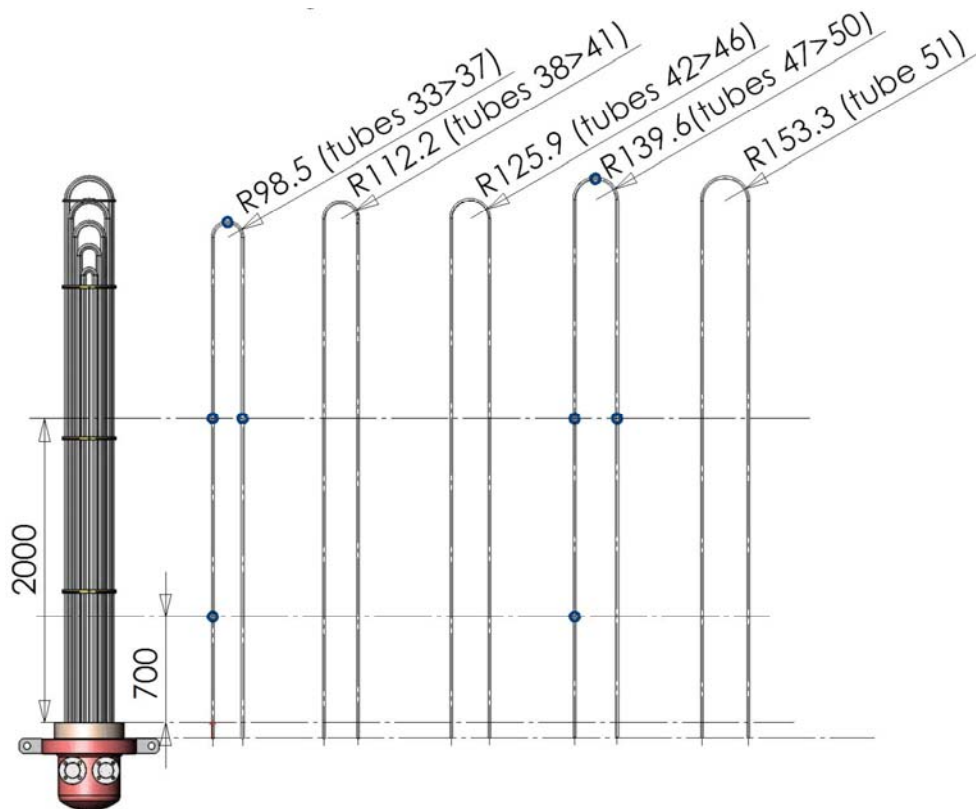


Figure 20: Radiuses of the U-bendings [7]

4.2.1 Geometry calculation of heat exchanger tube

Geometry of the SG tubes(SG-1 and SG-2, respectively) is summarized in the table below :

Table 7 Geometry of the SG heat exchanger tubes

Tube no.	Row no.	Straight Length	U-Bend Radius	U-Bend Length	Total Length	Top Elevation	Horizontal Part in the Model	Vertical Part in the Model
		[m]	[m]	[m]	[m]	[m]	[m]	[m]
1	1	3,0460	0,0300	0,0942	6,1862	3,0760	0,170	3,020
2	1	3,0460	0,0300	0,0942	6,1862	3,0760	0,170	3,020
3	1	3,0460	0,0300	0,0942	6,1862	3,0760	0,170	3,020
4	1	3,0460	0,0300	0,0942	6,1862	3,0760	0,170	3,020
5	1	3,0460	0,0300	0,0942	6,1862	3,0760	0,170	3,020
6	1	3,0460	0,0300	0,0942	6,1862	3,0760	0,170	3,020
7	2	3,0460	0,0437	0,1373	6,2293	3,0897	0,170	3,020
8	2	3,0460	0,0437	0,1373	6,2293	3,0897	0,170	3,020
9	2	3,0460	0,0437	0,1373	6,2293	3,0897	0,170	3,020
10	2	3,0460	0,0437	0,1373	6,2293	3,0897	0,170	3,020
11	2	3,0460	0,0437	0,1373	6,2293	3,0897	0,170	3,020
12	2	3,0460	0,0437	0,1373	6,2293	3,0897	0,170	3,020
13	2	3,0460	0,0437	0,1373	6,2293	3,0897	0,170	3,020
14	3	3,1690	0,0574	0,1803	6,5183	3,2264	0,200	3,171
15	3	3,1690	0,0574	0,1803	6,5183	3,2264	0,200	3,171
16	3	3,1690	0,0574	0,1803	6,5183	3,2264	0,200	3,171
17	3	3,1690	0,0574	0,1803	6,5183	3,2264	0,200	3,171
18	3	3,1690	0,0574	0,1803	6,5183	3,2264	0,200	3,171
19	3	3,1690	0,0574	0,1803	6,5183	3,2264	0,200	3,171
20	4	3,1690	0,0711	0,2234	6,5614	3,2401	0,200	3,171
21	4	3,1690	0,0711	0,2234	6,5614	3,2401	0,200	3,171
22	4	3,1690	0,0711	0,2234	6,5614	3,2401	0,200	3,171
23	4	3,1690	0,0711	0,2234	6,5614	3,2401	0,200	3,171
24	4	3,1690	0,0711	0,2234	6,5614	3,2401	0,200	3,171
25	4	3,1690	0,0711	0,2234	6,5614	3,2401	0,200	3,171
26	4	3,1690	0,0711	0,2234	6,5614	3,2401	0,200	3,171
27	5	3,2920	0,0848	0,2664	6,8504	3,3768	0,280	3,295
28	5	3,2920	0,0848	0,2664	6,8504	3,3768	0,280	3,295
29	5	3,2920	0,0848	0,2664	6,8504	3,3768	0,280	3,295
30	5	3,2920	0,0848	0,2664	6,8504	3,3768	0,280	3,295
31	5	3,2920	0,0848	0,2664	6,8504	3,3768	0,280	3,295
32	5	3,2920	0,0848	0,2664	6,8504	3,3768	0,280	3,295
33	6	3,2920	0,0985	0,3094	6,8934	3,3905	0,280	3,295
34	6	3,2920	0,0985	0,3094	6,8934	3,3905	0,280	3,295
35	6	3,2920	0,0985	0,3094	6,8934	3,3905	0,280	3,295
36	6	3,2920	0,0985	0,3094	6,8934	3,3905	0,280	3,295
37	6	3,2920	0,0985	0,3094	6,8934	3,3905	0,280	3,295
38	7	3,4140	0,1122	0,3525	7,1805	3,5262	0,370	3,417
39	7	3,4140	0,1122	0,3525	7,1805	3,5262	0,370	3,417
40	7	3,4140	0,1122	0,3525	7,1805	3,5262	0,370	3,417
41	7	3,4140	0,1122	0,3525	7,1805	3,5262	0,370	3,417
42	8	3,4140	0,1259	0,3955	7,2235	3,5399	0,370	3,417
43	8	3,4140	0,1259	0,3955	7,2235	3,5399	0,370	3,417
44	8	3,4140	0,1259	0,3955	7,2235	3,5399	0,370	3,417
45	8	3,4140	0,1259	0,3955	7,2235	3,5399	0,370	3,417
46	8	3,4140	0,1259	0,3955	7,2235	3,5399	0,370	3,417
47	9	3,5360	0,1396	0,4386	7,5106	3,6756	0,450	3,535
48	9	3,5360	0,1396	0,4386	7,5106	3,6756	0,450	3,535
49	9	3,5360	0,1396	0,4386	7,5106	3,6756	0,450	3,535
50	9	3,5360	0,1396	0,4386	7,5106	3,6756	0,450	3,535
51	10	3,5360	0,1533	0,4816	7,5536	3,6893	0,450	3,535

4.2.2 PACTEL SG tube geometry (Fine nodalization)

Geometries of the SG-1 and SG-2 heat exchanger tubes are identical. In the multitube model, the following geometry is used for the heat exchanger tubes of both SG. The following five tables describe in detailed geometry the tubes for SG 1 multitube (fine nodalization) model (Figure 22).

Table 8: SG 1 tube 221 geometry (Finer nodalization)

Node	Elevation change	Inlet elevation	Outlet elevation	Lenght	No. of tubes in this bundle	Flow area	Thermal conn. with sec. side volume	Heat structure multipl. factor
	m	m	m	m		m ²		
221-01	0,250	0,000	0,250	0,250	5	0,0010782	340-01	1,250
221-02	0,250	0,250	0,500	0,250	5	0,0010782	340-02	1,250
221-03	0,250	0,500	0,750	0,250	5	0,0010782	340-03	1,250
221-04	0,250	0,750	1,000	0,250	5	0,0010782	340-04	1,250
221-05	0,250	1,000	1,250	0,250	5	0,0010782	340-05	1,250
221-06	0,250	1,250	1,500	0,250	5	0,0010782	340-06	1,250
221-07	0,250	1,500	1,750	0,250	5	0,0010782	340-07	1,250
221-08	0,250	1,750	2,000	0,250	5	0,0010782	340-08	1,250
221-09	0,250	2,000	2,250	0,250	5	0,0010782	330-01	1,250
221-10	0,250	2,250	2,500	0,250	5	0,0010782	330-02	1,250
221-11	0,250	2,500	2,750	0,250	5	0,0010782	330-03	1,250
221-12	0,275	2,750	3,025	0,275	5	0,0010782	330-04	1,375
221-13	0,290	3,025	3,315	0,290	5	0,0010782	330-05	1,450
221-14	0,220	3,315	3,535	0,220	5	0,0010782	330-06	1,100
221-15	0,000	3,535	3,535	0,450	5	0,0010782	330-06	2,250
221-16	-0,220	3,535	3,315	0,220	5	0,0010782	330-06	1,100
221-17	-0,290	3,315	3,025	0,290	5	0,0010782	330-05	1,450
221-18	-0,275	3,025	2,750	0,275	5	0,0010782	330-04	1,375
221-19	-0,250	2,750	2,500	0,250	5	0,0010782	330-03	1,250
221-20	-0,250	2,500	2,250	0,250	5	0,0010782	330-02	1,250
221-21	-0,250	2,250	2,000	0,250	5	0,0010782	330-01	1,250
221-22	-0,250	2,000	1,750	0,250	5	0,0010782	320-08	1,250
221-23	-0,250	1,750	1,500	0,250	5	0,0010782	320-07	1,250
221-24	-0,250	1,500	1,250	0,250	5	0,0010782	320-06	1,250
221-25	-0,250	1,250	1,000	0,250	5	0,0010782	320-05	1,250
221-26	-0,250	1,000	0,750	0,250	5	0,0010782	320-04	1,250
221-27	-0,250	0,750	0,500	0,250	5	0,0010782	320-03	1,250
221-28	-0,250	0,500	0,250	0,250	5	0,0010782	320-02	1,250
221-29	-0,250	0,250	0,000	0,250	5	0,0010782	320-01	1,250

Table 9 :SG 1 tube 222 geometry (Finer nodalization)

Node	Elevation change	Inlet elevation	Outlet elevation	Lenght	No. of tubes in this bundle	Flow area	Thermal connectio n with sec. side	Heat structure multipl. factor
	m	m	m	m		m ²		
222-01	0,250	0,000	0,250	0,250	9	0,0019408	340-01	2,250
222-02	0,250	0,250	0,500	0,250	9	0,0019408	340-02	2,250
222-03	0,250	0,500	0,750	0,250	9	0,0019408	340-03	2,250
222-04	0,250	0,750	1,000	0,250	9	0,0019408	340-04	2,250
222-05	0,250	1,000	1,250	0,250	9	0,0019408	340-05	2,250
222-06	0,250	1,250	1,500	0,250	9	0,0019408	340-06	2,250
222-07	0,250	1,500	1,750	0,250	9	0,0019408	340-07	2,250
222-08	0,250	1,750	2,000	0,250	9	0,0019408	340-08	2,250
222-09	0,250	2,000	2,250	0,250	9	0,0019408	330-01	2,250
222-10	0,250	2,250	2,500	0,250	9	0,0019408	330-02	2,250
222-11	0,250	2,500	2,750	0,250	9	0,0019408	330-03	2,250
222-12	0,275	2,750	3,025	0,275	9	0,0019408	330-04	2,475
222-13	0,290	3,025	3,315	0,290	9	0,0019408	330-05	2,610
222-14	0,100	3,315	3,415	0,100	9	0,0019408	330-06	0,900
222-15	0,000	3,415	3,415	0,370	9	0,0019408	330-06	3,330
222-16	-0,100	3,415	3,315	0,100	9	0,0019408	330-06	0,900
222-17	-0,290	3,315	3,025	0,290	9	0,0019408	330-05	2,610
222-18	-0,275	3,025	2,750	0,275	9	0,0019408	330-04	2,475
222-19	-0,250	2,750	2,500	0,250	9	0,0019408	330-03	2,250
222-20	-0,250	2,500	2,250	0,250	9	0,0019408	330-02	2,250
222-21	-0,250	2,250	2,000	0,250	9	0,0019408	330-01	2,250
222-22	-0,250	2,000	1,750	0,250	9	0,0019408	320-08	2,250
222-23	-0,250	1,750	1,500	0,250	9	0,0019408	320-07	2,250
222-24	-0,250	1,500	1,250	0,250	9	0,0019408	320-06	2,250
222-25	-0,250	1,250	1,000	0,250	9	0,0019408	320-05	2,250
222-26	-0,250	1,000	0,750	0,250	9	0,0019408	320-04	2,250
222-27	-0,250	0,750	0,500	0,250	9	0,0019408	320-03	2,250
222-28	-0,250	0,500	0,250	0,250	9	0,0019408	320-02	2,250
222-29	-0,250	0,250	0,000	0,250	9	0,0019408	320-01	2,250

Table 10 :SG 1 tube 223 geometry (Finer nodalization)

Node	Elevation change	Inlet elevation	Outlet elevation	Lenght	No. of tubes in this bundle	Flow area	Thermal connection with sec. side	Heat structure multipl. factor
	m	m	m	m		m ²		
223-01	0,250	0,000	0,250	0,250	11	0,0023721	340-01	2,750
223-02	0,250	0,250	0,500	0,250	11	0,0023721	340-02	2,750
223-03	0,250	0,500	0,750	0,250	11	0,0023721	340-03	2,750
223-04	0,250	0,750	1,000	0,250	11	0,0023721	340-04	2,750
223-05	0,250	1,000	1,250	0,250	11	0,0023721	340-05	2,750
223-06	0,250	1,250	1,500	0,250	11	0,0023721	340-06	2,750
223-07	0,250	1,500	1,750	0,250	11	0,0023721	340-07	2,750
223-08	0,250	1,750	2,000	0,250	11	0,0023721	340-08	2,750
223-09	0,250	2,000	2,250	0,250	11	0,0023721	330-01	2,750
223-10	0,250	2,250	2,500	0,250	11	0,0023721	330-02	2,750
223-11	0,250	2,500	2,750	0,250	11	0,0023721	330-03	2,750
223-12	0,275	2,750	3,025	0,275	11	0,0023721	330-04	3,025
223-13	0,270	3,025	3,295	0,270	11	0,0023721	330-05	2,970
223-14	0,000	3,295	3,295	0,280	11	0,0023721	330-05	3,080
223-15	-0,270	3,295	3,025	0,270	11	0,0023721	330-05	2,970
223-16	-0,275	3,025	2,750	0,275	11	0,0023721	330-04	3,025
223-17	-0,250	2,750	2,500	0,250	11	0,0023721	330-03	2,750
223-18	-0,250	2,500	2,250	0,250	11	0,0023721	330-02	2,750
223-19	-0,250	2,250	2,000	0,250	11	0,0023721	330-01	2,750
223-20	-0,250	2,000	1,750	0,250	11	0,0023721	320-08	2,750
223-21	-0,250	1,750	1,500	0,250	11	0,0023721	320-07	2,750
223-22	-0,250	1,500	1,250	0,250	11	0,0023721	320-06	2,750
223-23	-0,250	1,250	1,000	0,250	11	0,0023721	320-05	2,750
223-24	-0,250	1,000	0,750	0,250	11	0,0023721	320-04	2,750
223-25	-0,250	0,750	0,500	0,250	11	0,0023721	320-03	2,750
223-26	-0,250	0,500	0,250	0,250	11	0,0023721	320-02	2,750
223-27	-0,250	0,250	0,000	0,250	11	0,0023721	320-01	2,750

Table 11 :SG 1 tube 224 geometry (Finer nodalization)

Node	Elevation change	Inlet elevation	Outlet elevation	Lenght	No. of tubes in this bundle	Flow area	Thermal connectio n with sec. side	Heat structure multipl. factor
	m	m	m	m		m ²		
224-01	0,250	0,000	0,250	0,250	13	0,0028034	340-01	3,250
224-02	0,250	0,250	0,500	0,250	13	0,0028034	340-02	3,250
224-03	0,250	0,500	0,750	0,250	13	0,0028034	340-03	3,250
224-04	0,250	0,750	1,000	0,250	13	0,0028034	340-04	3,250
224-05	0,250	1,000	1,250	0,250	13	0,0028034	340-05	3,250
224-06	0,250	1,250	1,500	0,250	13	0,0028034	340-06	3,250
224-07	0,250	1,500	1,750	0,250	13	0,0028034	340-07	3,250
224-08	0,250	1,750	2,000	0,250	13	0,0028034	340-08	3,250
224-09	0,250	2,000	2,250	0,250	13	0,0028034	330-01	3,250
224-10	0,250	2,250	2,500	0,250	13	0,0028034	330-02	3,250
224-11	0,250	2,500	2,750	0,250	13	0,0028034	330-03	3,250
224-12	0,275	2,750	3,025	0,275	13	0,0028034	330-04	3,575
224-13	0,145	3,025	3,170	0,145	13	0,0028034	330-05	1,885
224-14	0,000	3,170	3,170	0,200	13	0,0028034	330-05	2,600
224-15	-0,145	3,170	3,025	0,145	13	0,0028034	330-05	1,885
224-16	-0,275	3,025	2,750	0,275	13	0,0028034	330-04	3,575
224-17	-0,250	2,750	2,500	0,250	13	0,0028034	330-03	3,250
224-18	-0,250	2,500	2,250	0,250	13	0,0028034	330-02	3,250
224-19	-0,250	2,250	2,000	0,250	13	0,0028034	330-01	3,250
224-20	-0,250	2,000	1,750	0,250	13	0,0028034	320-08	3,250
224-21	-0,250	1,750	1,500	0,250	13	0,0028034	320-07	3,250
224-22	-0,250	1,500	1,250	0,250	13	0,0028034	320-06	3,250
224-23	-0,250	1,250	1,000	0,250	13	0,0028034	320-05	3,250
224-24	-0,250	1,000	0,750	0,250	13	0,0028034	320-04	3,250
224-25	-0,250	0,750	0,500	0,250	13	0,0028034	320-03	3,250
224-26	-0,250	0,500	0,250	0,250	13	0,0028034	320-02	3,250
224-27	-0,250	0,250	0,000	0,250	13	0,0028034	320-01	3,250

Table 12 :SG 1 tube 225 geometry (Finer nodalization)

Node	Elevation change	Inlet elevation	Outlet elevation	Lenght	No. of tubes in this bundle	Flow area	Thermal connection with sec. side	Heat structure multipl. factor
	m	m	m	m		m ²		
225-01	0,250	0,000	0,250	0,250	13	0,0028034	340-01	3,250
225-02	0,250	0,250	0,500	0,250	13	0,0028034	340-02	3,250
225-03	0,250	0,500	0,750	0,250	13	0,0028034	340-03	3,250
225-04	0,250	0,750	1,000	0,250	13	0,0028034	340-04	3,250
225-05	0,250	1,000	1,250	0,250	13	0,0028034	340-05	3,250
225-06	0,250	1,250	1,500	0,250	13	0,0028034	340-06	3,250
225-07	0,250	1,500	1,750	0,250	13	0,0028034	340-07	3,250
225-08	0,250	1,750	2,000	0,250	13	0,0028034	340-08	3,250
225-09	0,250	2,000	2,250	0,250	13	0,0028034	330-01	3,250
225-10	0,250	2,250	2,500	0,250	13	0,0028034	330-02	3,250
225-11	0,250	2,500	2,750	0,250	13	0,0028034	330-03	3,250
225-12	0,270	2,750	3,020	0,270	13	0,0028034	330-04	3,510
225-13	0,000	3,020	3,020	0,170	13	0,0028034	330-04	2,210
225-14	-0,270	3,020	2,750	0,270	13	0,0028034	330-04	3,510
225-15	-0,250	2,750	2,500	0,250	13	0,0028034	330-03	3,250
225-16	-0,250	2,500	2,250	0,250	13	0,0028034	330-02	3,250
225-17	-0,250	2,250	2,000	0,250	13	0,0028034	330-01	3,250
225-18	-0,250	2,000	1,750	0,250	13	0,0028034	320-08	3,250
225-19	-0,250	1,750	1,500	0,250	13	0,0028034	320-07	3,250
225-20	-0,250	1,500	1,250	0,250	13	0,0028034	320-06	3,250
225-21	-0,250	1,250	1,000	0,250	13	0,0028034	320-05	3,250
225-22	-0,250	1,000	0,750	0,250	13	0,0028034	320-04	3,250
225-23	-0,250	0,750	0,500	0,250	13	0,0028034	320-03	3,250
225-24	-0,250	0,500	0,250	0,250	13	0,0028034	320-02	3,250
225-25	-0,250	0,250	0,000	0,250	13	0,0028034	320-01	3,250

4.2.2 PACTEL SG tube geometry (Rough nodalization)

The following five tables describe the geometry of the tubes for SG 1 multitube (Rough nodalization) model. Geometry of the SG-1 and SG-2 heat exchanger tubes is identical.

Table 13 : SG 1 tube 221 geometry (Rough nodalization)

Node	Elevation change	Inlet elevation	Outlet elevation	Lenght	No. of tubes in this bundle	Flow area	Thermal conn. with sec. side volume	Heat structure multipl. factor
221-01	0,5	0	0,5	0,5	5	0,0010782	340-01	2,5
221-02	0,5	0,5	1	0,5	5	0,0010782	340-02	2,5
221-03	0,5	1	1,5	0,5	5	0,0010782	340-03	2,5
221-04	0,5	1,5	2	0,5	5	0,0010782	340-04	2,5
221-05	0,45	2	2,45	0,45	5	0,0010782	330-01	2,25
221-06	0,45	2,45	2,9	0,45	5	0,0010782	330-02	2,25
221-07	0,635	2,9	3,535	0,635	5	0,0010782	330-03	3,175
221-08	0	3,535	3,535	0,45	5	0,0010782	330-03	2,25
221-09	-0,635	3,535	2,9	0,635	5	0,0010782	330-03	3,175
221-10	-0,45	2,9	2,45	0,45	5	0,0010782	330-02	2,25
221-11	-0,45	2,45	2	0,45	5	0,0010782	330-01	2,25
221-12	-0,5	2	1,5	0,5	5	0,0010782	320-04	2,5
221-13	-0,5	1,5	1	0,5	5	0,0010782	320-03	2,5
221-14	-0,5	1	0,5	0,5	5	0,0010782	320-02	2,5
221-15	-0,5	0,5	0	0,5	5	0,0010782	320-01	2,5

Table 14 : SG 1 tube 222 geometry (Rough nodalization)

Node	Elevation change	Inlet elevation	Outlet elevation	Lenght	No. of tubes in this bundle	Flow area	Thermal conn. with sec. side volume	Heat structure multipl. factor
222-01	0,5	0	0,5	0,5	9	0,0019408	340-01	4,5
222-02	0,5	0,5	1	0,5	9	0,0019408	340-02	4,5
222-03	0,5	1	1,5	0,5	9	0,0019408	340-03	4,5
222-04	0,5	1,5	2	0,5	9	0,0019408	340-04	4,5
222-05	0,45	2	2,45	0,45	9	0,0019408	330-01	4,05
222-06	0,45	2,45	2,9	0,45	9	0,0019408	330-02	4,05
222-07	0,515	2,9	3,415	0,515	9	0,0019408	330-03	4,635
222-08	0	3,415	3,415	0,37	9	0,0019408	330-03	3,33
222-09	-0,515	3,415	2,9	0,515	9	0,0019408	330-03	4,635
222-10	-0,45	2,9	2,45	0,45	9	0,0019408	330-02	4,05
222-11	-0,45	2,45	2	0,45	9	0,0019408	330-01	4,05
222-12	-0,5	2	1,5	0,5	9	0,0019408	320-04	4,5
222-13	-0,5	1,5	1	0,5	9	0,0019408	320-03	4,5
222-14	-0,5	1	0,5	0,5	9	0,0019408	320-02	4,5
222-15	-0,5	0,5	0	0,5	9	0,0019408	320-01	4,5

Table 15 : SG 1 tube 223 geometry (Rough nodalization)

Node	Elevation change	Inlet elevation	Outlet elevation	Lenght	No. of tubes in this bundle	Flow area	Thermal conn. with sec. side volume	Heat structure multipl. factor
223-01	0,5	0	0,5	0,5	11	0,0023721	340-01	5,5
223-02	0,5	0,5	1	0,5	11	0,0023721	340-02	5,5
223-03	0,5	1	1,5	0,5	11	0,0023721	340-03	5,5
223-04	0,5	1,5	2	0,5	11	0,0023721	340-04	5,5
223-05	0,45	2	2,45	0,45	11	0,0023721	330-01	4,95
223-06	0,45	2,45	2,9	0,45	11	0,0023721	330-02	4,95
223-07	0,395	2,9	3,295	0,395	11	0,0023721	330-03	4,345
223-08	0	3,295	3,295	0,28	11	0,0023721	330-03	3,08
223-09	-0,395	3,295	2,9	0,395	11	0,0023721	330-03	4,345
223-10	-0,45	2,9	2,45	0,45	11	0,0023721	330-02	4,95
223-11	-0,45	2,45	2	0,45	11	0,0023721	330-01	4,95
223-12	-0,5	2	1,5	0,5	11	0,0023721	320-04	5,5
223-13	-0,5	1,5	1	0,5	11	0,0023721	320-03	5,5
223-14	-0,5	1	0,5	0,5	11	0,0023721	320-02	5,5
223-15	-0,5	0,5	0	0,5	11	0,0023721	320-01	5,5

Table 16 : SG 1 tube 224 geometry (Rough nodalization)

Node	Elevation change	Inlet elevation	Outlet elevation	Lenght	No. of tubes in this bundle	Flow area	Thermal conn. with sec. side volume	Heat structure multipl. factor
224-01	0,5	0	0,5	0,5	13	0,0028034	340-01	6,5
224-02	0,5	0,5	1	0,5	13	0,0028034	340-02	6,5
224-03	0,5	1	1,5	0,5	13	0,0028034	340-03	6,5
224-04	0,5	1,5	2	0,5	13	0,0028034	340-04	6,5
224-05	0,45	2	2,45	0,45	13	0,0028034	330-01	5,85
224-06	0,45	2,45	2,9	0,45	13	0,0028034	330-02	5,85
224-07	0,27	2,9	3,17	0,27	13	0,0028034	330-03	3,51
224-08	0	3,17	3,17	0,2	13	0,0028034	330-03	2,6
224-09	-0,27	3,17	2,9	0,27	13	0,0028034	330-03	3,51
224-10	-0,45	2,9	2,45	0,45	13	0,0028034	330-02	5,85
224-11	-0,45	2,45	2	0,45	13	0,0028034	330-01	5,85
224-12	-0,5	2	1,5	0,5	13	0,0028034	320-04	6,5
224-13	-0,5	1,5	1	0,5	13	0,0028034	320-03	6,5
224-14	-0,5	1	0,5	0,5	13	0,0028034	320-02	6,5
224-15	-0,5	0,5	0	0,5	13	0,0028034	320-01	6,5

Table 17 : SG 1 tube 225 geometry (Rough nodalization)

Node	Elevation change	Inlet elevation	Outlet elevation	Lenght(m)	No. of tubes in this bundle	Flow area	Thermal conn. with sec. side volume	Heat structure multipl. factor
225-01	0,5	0	0,5	0,5	13	0,0028034	340-01	6,5
225-02	0,5	0,5	1	0,5	13	0,0028034	340-02	6,5
225-03	0,5	1	1,5	0,5	13	0,0028034	340-03	6,5
225-04	0,5	1,5	2	0,5	13	0,0028034	340-04	6,5
225-05	0,45	2	2,45	0,45	13	0,0028034	330-01	5,85
225-06	0,45	2,45	2,9	0,45	13	0,0028034	330-02	5,85
225-07	0,12	2,9	3,02	0,12	13	0,0028034	330-03	1,56
225-08	0	3,02	3,02	0,17	13	0,0028034	330-03	2,21
225-09	-0,12	3,02	2,9	0,12	13	0,0028034	330-03	1,56
225-10	-0,45	2,9	2,45	0,45	13	0,0028034	330-02	5,85
225-11	-0,45	2,45	2	0,45	13	0,0028034	330-01	5,85
225-12	-0,5	2	1,5	0,5	13	0,0028034	320-04	6,5
225-13	-0,5	1,5	1	0,5	13	0,0028034	320-03	6,5
225-14	-0,5	1	0,5	0,5	13	0,0028034	320-02	6,5
225-15	-0,5	0,5	0	0,5	13	0,0028034	320-01	6,5

Calculation of the volumes of the hot side and cold side plenums:

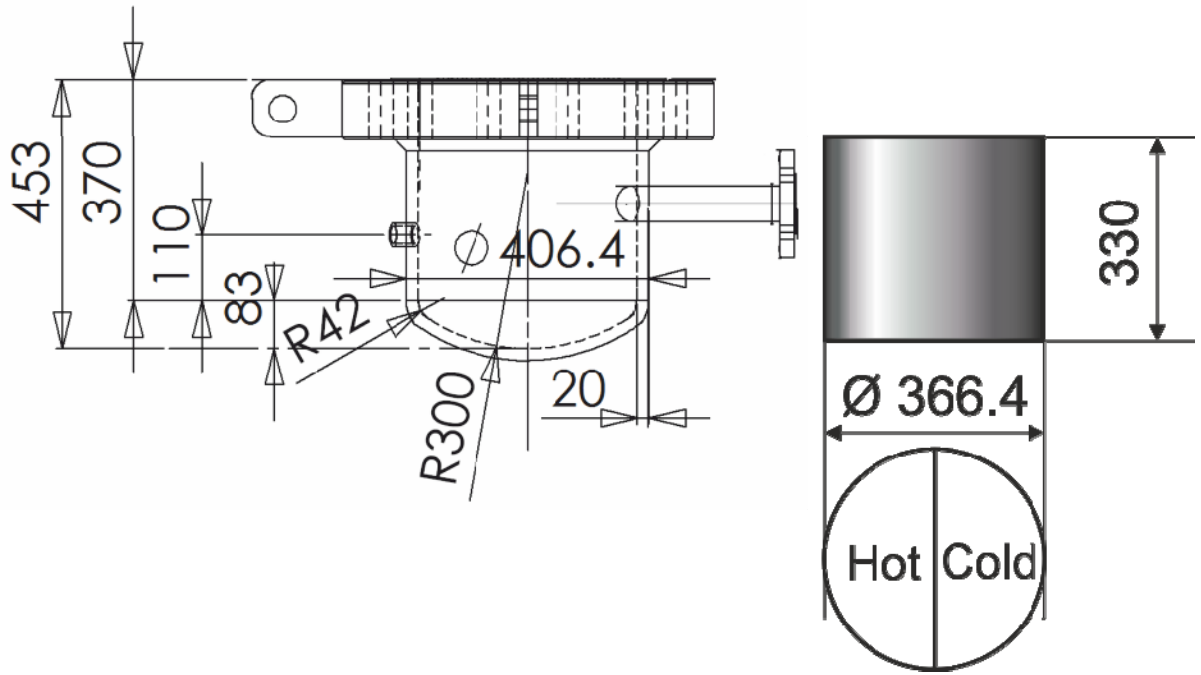


Figure 21: Lower plenum of the SG and its model [7]

Inner diameter of the plenum: $D_{plenum,i} = 366.4 \text{ mm}$

Estimated height of the plenum: $H_{plenum} = 330 \text{ mm}$

Total volume of the plenum:

$$V_{plenum,total} = \frac{D_{plenum}^2 \pi}{4} H_{plenum} = \frac{366.4^2 \pi}{4} \cdot 330 = 34794832 \text{ mm}^3 = 0.034795 \text{ m}^3$$

Volume of the hot side and cold side of the plenum, symmetrically:

$$V_{plenum,hot} = V_{plenum,cold} = \frac{1}{2} V_{plenum,total} = \frac{1}{2} \cdot 0.034795 \text{ m}^3 = 0.017397 \text{ m}^3$$

Hydraulic diameter of the hot side and cold side of the plenum, symmetrically:

$$D_{hyd} = \frac{4A}{P_{wet}} = \frac{4D^2 \pi}{4(D + \frac{D\pi}{2})} = \frac{0.3664\pi}{1 + \frac{\pi}{2}} = 0.1425 \text{ m}$$

4.3 Finer nodalization and elevation change of heat exchanger tube

Figure 22 below shows the re-nodalization and the elevation changes of the PACTEL PWR steam generator multi tube model. The previous model was designed for single tube model. Now this model is modified by increasing the number of heat exchanger tubes. The number of nodes increased nearly to double in the SG heat transfer region and in the SG downcomers. In the previous model, the cell length was set to almost 0.5 m while in the modified model it is 0.25 m. The simulation with the finer nodalization takes longer than with rough nodalization but more accurate result are can be expected. In the case of finer nodalization, the results are dependent on a number of factors , such as the so-called Courant time limit. If the length of time-step exceeds the Courant time limit, it gives an unreliable result or an error. In our model, the Courant-Friedrich-Lewy condition is used to verify the stability of the calculation. Determination of the relationship between the applicable time-step and the node length is described below.

4.3.1 Courant-Friedrichs-Lewy's condition [23]

The Courant-Friedrich-Lewy's condition has been given in the following for a one dimension case

$$\frac{u \Delta t}{\Delta x} \leq C \quad 1$$

Where, u =velocity (m/s), Δt = time step(s), Δx = length interval and C = Constant

The equation can also be written in following way

$$\theta = \frac{u \Delta t}{\Delta x} \quad 2$$

Where θ = Dimension less courant number

So the courant time step can be written in the following way

$$\Delta t_{\text{courant}} = \frac{\Delta x \theta}{u} \quad 3$$

From this equation it can be seen that time step Δt is directly influenced by length interval Δx . If the length interval is increased, the time step also increases.

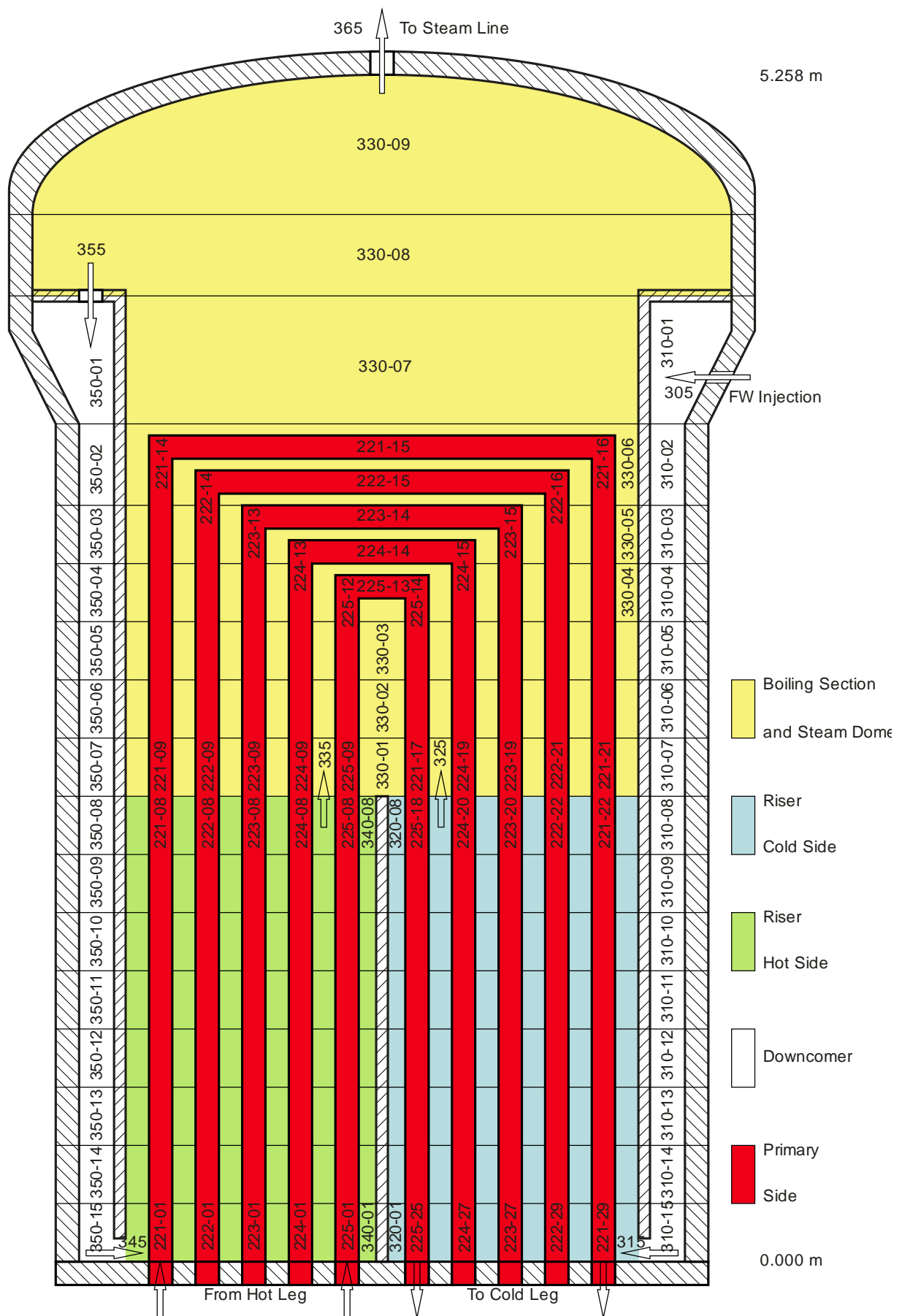


Figure 22 : Finer nodalization and increased number of tubes in PWR PACTEL steam generator

4.3.2 Effects of re-nodalization

To simulate a model by using RELAP5 a larger time step is always allowed for so that no information is missed due to same.. The time step is directly related to the length interval. If the length interval is decreased, the time interval also decreases as can be seen from the Courant –Friedrich –Lewy condition. However, the problem is that simulation will take more time when using smaller time steps.

During the simulation of our model, it was clearly seen that application of smaller node lengths required smaller time steps, which took more time for computation.

4.4 Strategies for achieving steady state in our case

In steady state conditions, three parameters, such as mass flow rate, pressure and temperature must be kept constant during operation. To achieve steady state in our case, the pressurizer was connected in the model and the water level was kept constant in both steam generators.

4.5 Transient calculation

Before starting the transient calculation, the pressurizer was isolated from the model, in the same way as in the experiment. The water level was kept constant in both steam generators by using a feed water controller in RELAP5. The transient was terminated when the top of the core dried out and the core temperature exceeded 350°C.

4.6 Visualization of the model by SNAP animation tool

Visualization of the multi tube model by SNAP animation tool is seen below. In Figure 23 Fluid conditions at near the end of the transient and Figure 24 Void distribution at near the end of the transient.

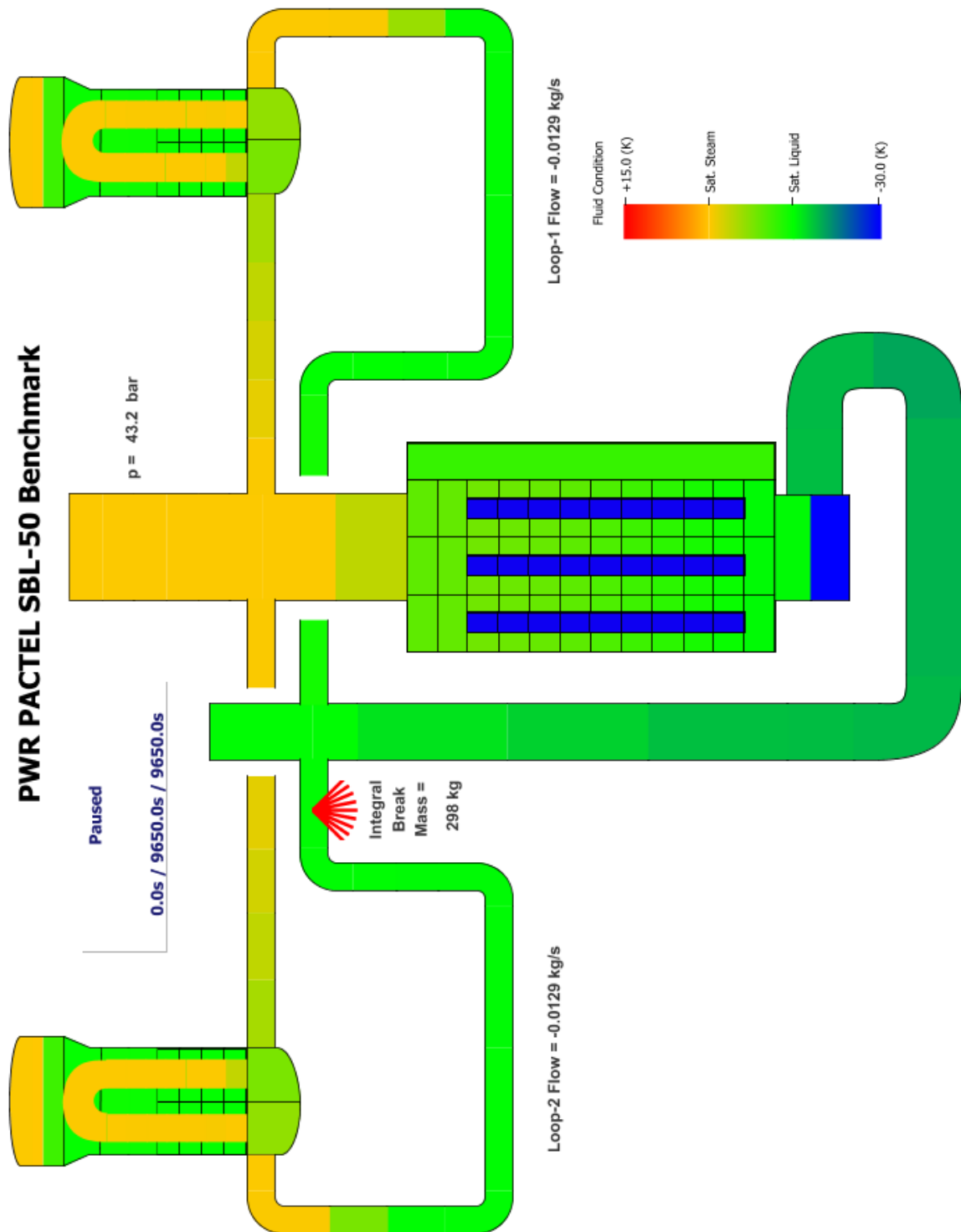


Figure 23 : Fluid conditions near the end of the transient

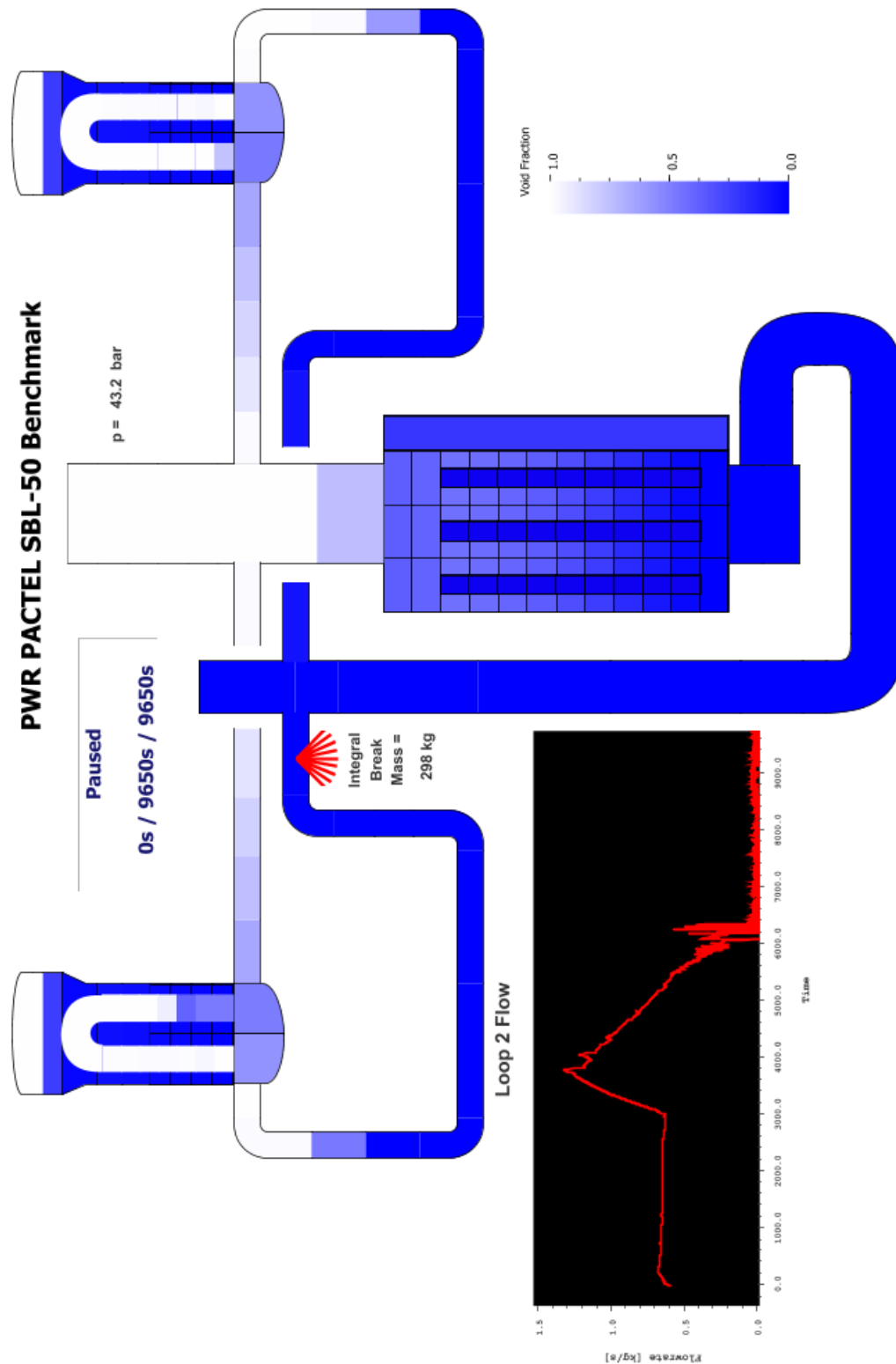


Figure 24 : Void distribution near the end of the transient

Chapter 5

Analysis of the Results

In this thesis, we obtained new results from the multi-tube model. The results performed by the same code but using different models are judged against each other. Obviously, input and output data of the multi-tube model (fine & rough nodalizations) have been used to compare with the single tube model and test data for analysing the same problem. It also reflects the reliability and validity of the new multi-tube model.

5.1 Steady-state analysis

A long initialization period is needed for achieving the proper steady-state conditions and to reach the correct initial conditions. The steady-state period was run for 1000 s in case of our modified model. The following initiative was taken during the steady-state run:

A primary side pressure boundary volume was connected to the pressurizer with a defined pressure of 75 bar and saturated steam. A secondary side pressure boundary was connected to the head of the steam generator with a defined pressure of 42 bar and using saturated steam.

5.2 Transient analysis

Transient calculations are usually performed in two steps. First convergence of the steady state must be achieved and then proper transient calculation can be run from the steady state. The following initiative was taken during the transient run:

- I. Restart the input file from the last block of steady-state run and resetting the time to zero in the restart
- II. Pressurizer was isolated from the system by deleting all necessary components connected to the pressurizer
- III. Opening the break valve.
- IV. Transient period was considered 0s to 10 000s

Boundary conditions:

- I. Heat losses simulation according to ambient temperature
- II. Unintentional break valve closure simulation (6700s to 7960s)

During the transient period (for finer multi-tube) time step had been controlled in three steps that are shown in the following table:

Table 18 : Transient period (Fine multi- tube)

Transient period	End time	MIN.DT(s)	MAX.DT(ms)
0s to 2800 s	2800s	1e-7	150
2801s to 4000 s	4000s	1e-7	10
4001s to 10000 s	10000s	1e-7	20

Until transient period 2800, MAX.DT was 150ms after MAX.DT was reduced to 10ms until 4000s and then MAX.DT was slightly increased to 20ms. MAX.DT was reduced due to finer nodalization as already discussed in previous section in re-nodalization effect.

Table 19 : The table below describes the break valve opening as a function of a time

Time (s)	Break valve conditions
0 s	just open the break
6700 s	Still open
6701 to 7960 s	Break valve closed (unintentional quasi steady-state)
7960 s	Open the valve
10000 s	Keep open for the rest of the transient

For better agreement of the transient result with the test data, the discharge coefficient was varied during transient. The discharge coefficient was considered to be 0.82 in the new model.

Figure 25 and Figure 26 show upper plenum pressure and downcomer mass flow rate respectively during transient. The figures show the comparison of the transient results (fine multi-tube, rough multitube, and single tube model) with the test data. The transient results agree well with the test data, as can be seen in the figures. In the beginning of the transient (when the break valve opens), the pressure dropped (Figure 25), the downcomer mass flow rate was constant up to 2790 s and single phase flow was observed during this time. After 2790s, two-phase flow was observed when the primary mass inventory was less than 75 % (collapsed levels reached the hot leg elevation). The upper plenum pressure dropped (Figure 25) again and stabilized after 4600 s. The downcomer mass flow rate suddenly increased and reached its maximum value, but decreased again later in this period. When primary inventory was less than 50%, the upper plenum pressure was stabilizing and the mass flow rate became nearly zero in the end of the transient due to flow stagnation.

Upper Plenum Pressure

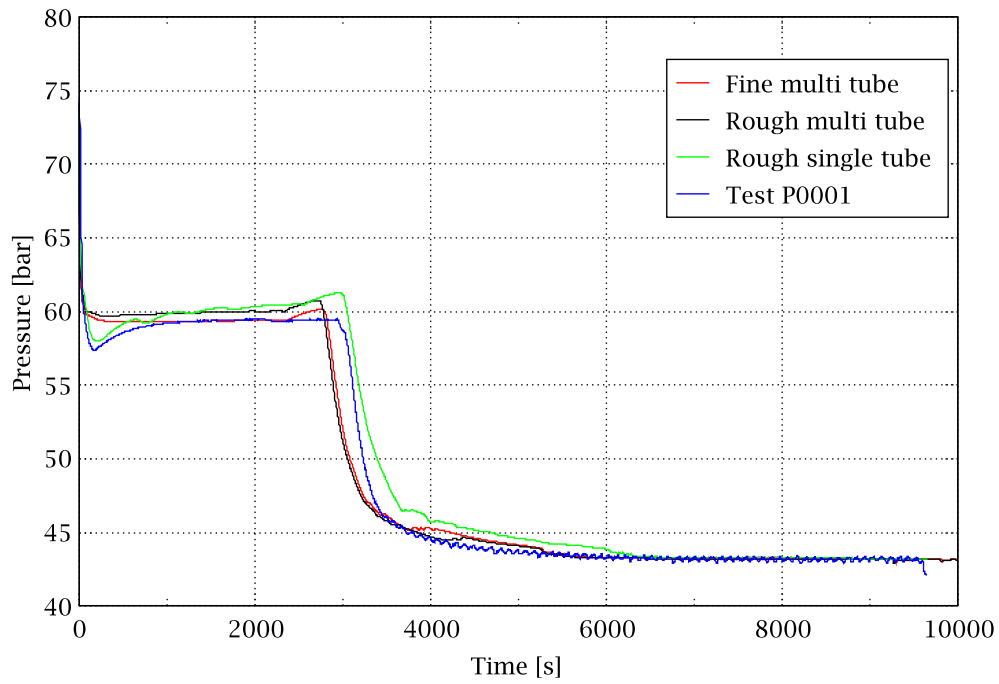


Figure 25 : Upper plenum pressure

Downcomer Mass Flowrate

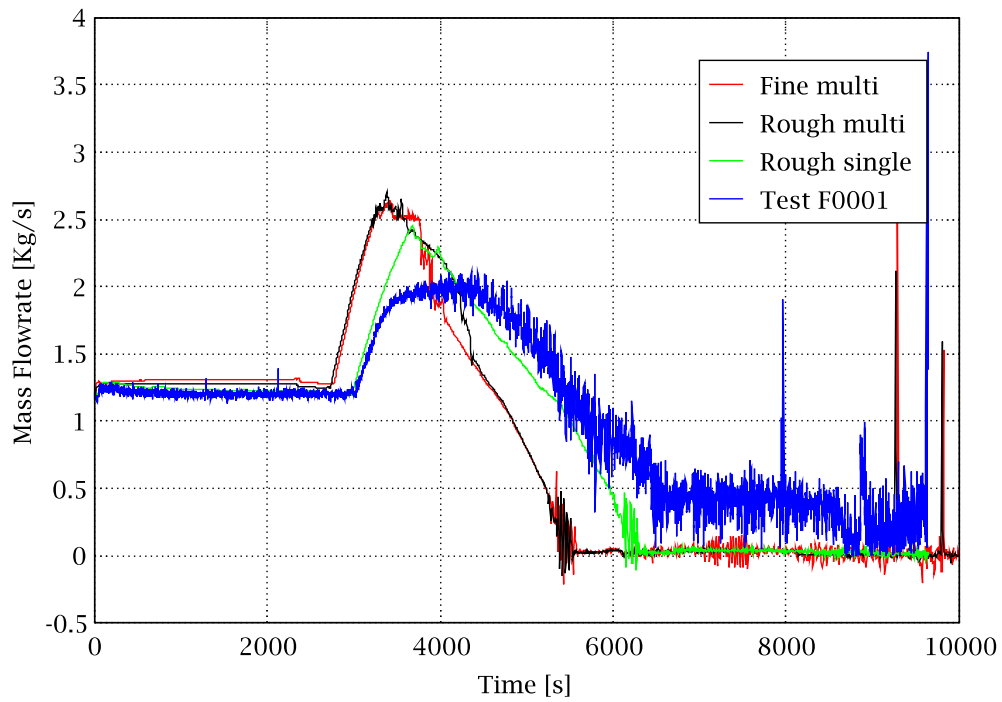


Figure 26 : Downcomer mass flow rate

Collapsed Level Between LP and UP

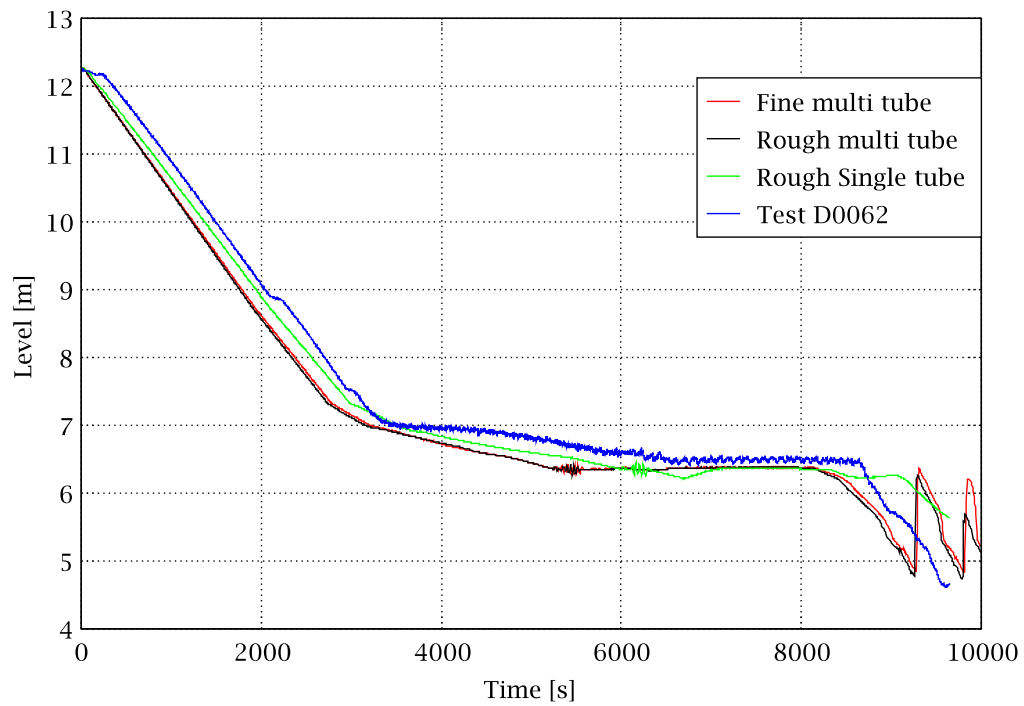


Figure 27 : Collapsed level between upper plenum and lower plenum

Integrated Break Mass Flowrate

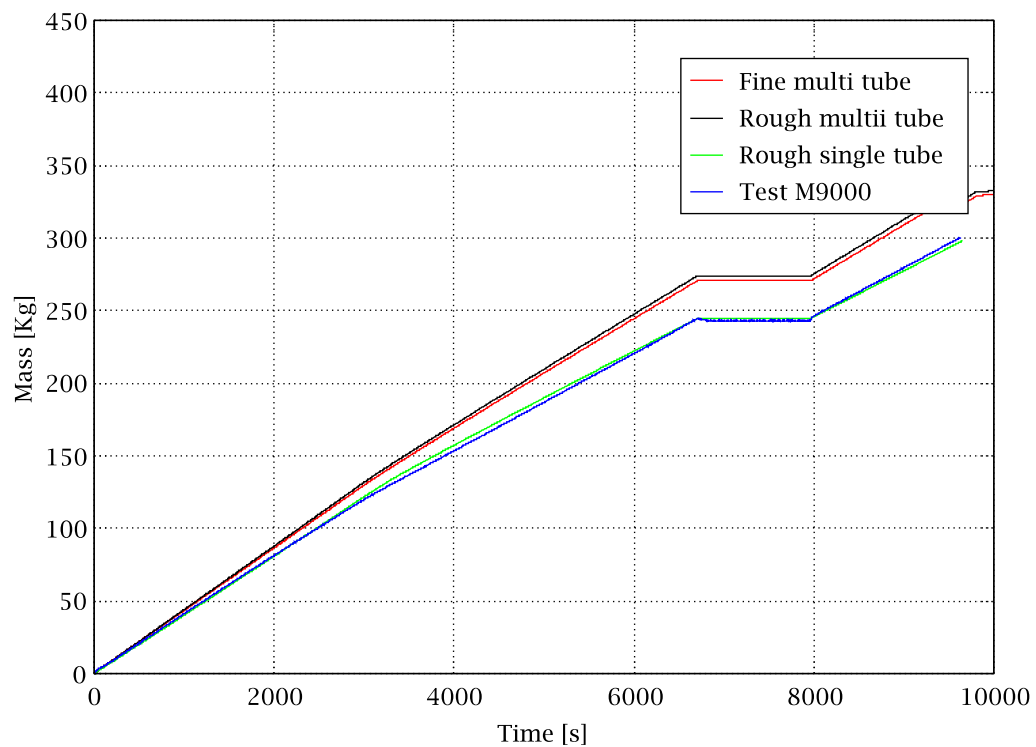


Figure 28 : Integrated break mass flow rate

Figure 27 shows the collapsed level between LP and UP. From Figure 27 it can be seen that transient results (for fine multi tube, rough multi tube and single tube) agree well with test results, but for fine and rough multi-tube some variation is observed after 8500 s at the end of transient because integrated mass leaked out 300kg of the facility before the end of the transient as seen in the figure.

Figure 28 shows integrated break mass flow rate. The single tube results agree well with test results but the multitube fine and rough models overestimated the test results.

Hot Leg 1 Outlet Temperature

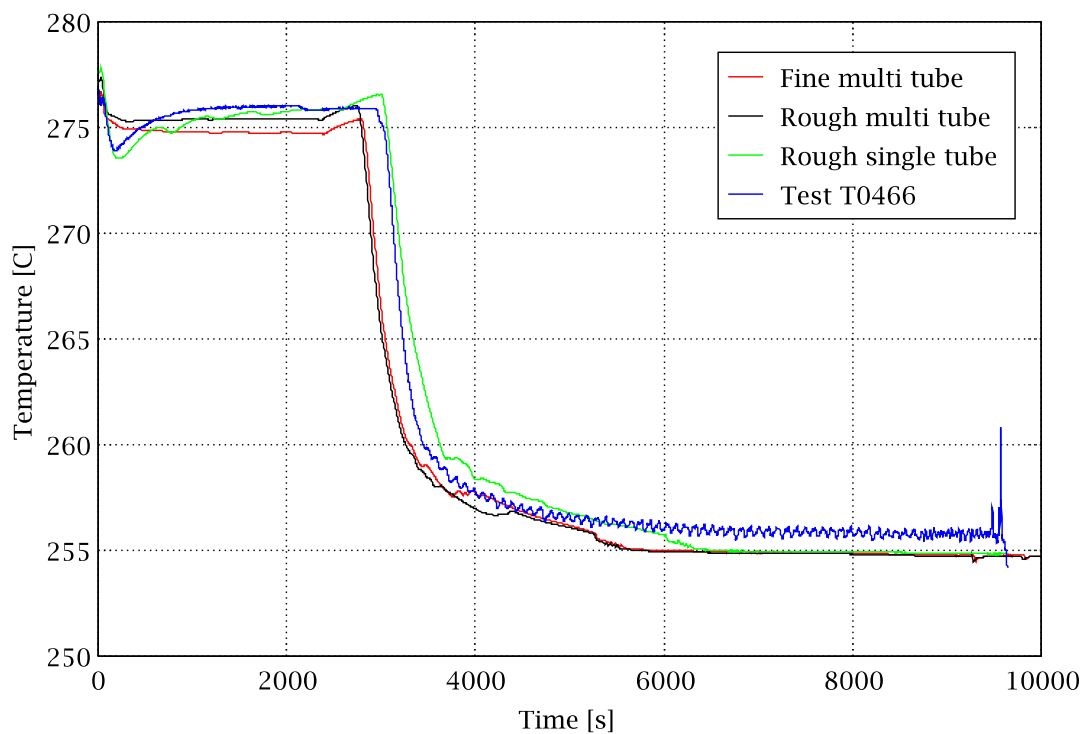


Figure 29 : Hot leg 1 outlet temperature

Figure 29 shows hot leg 1 outlet temperature. The transient result agrees well with the measurement data.

Cold Leg 1 Mass Flowrate

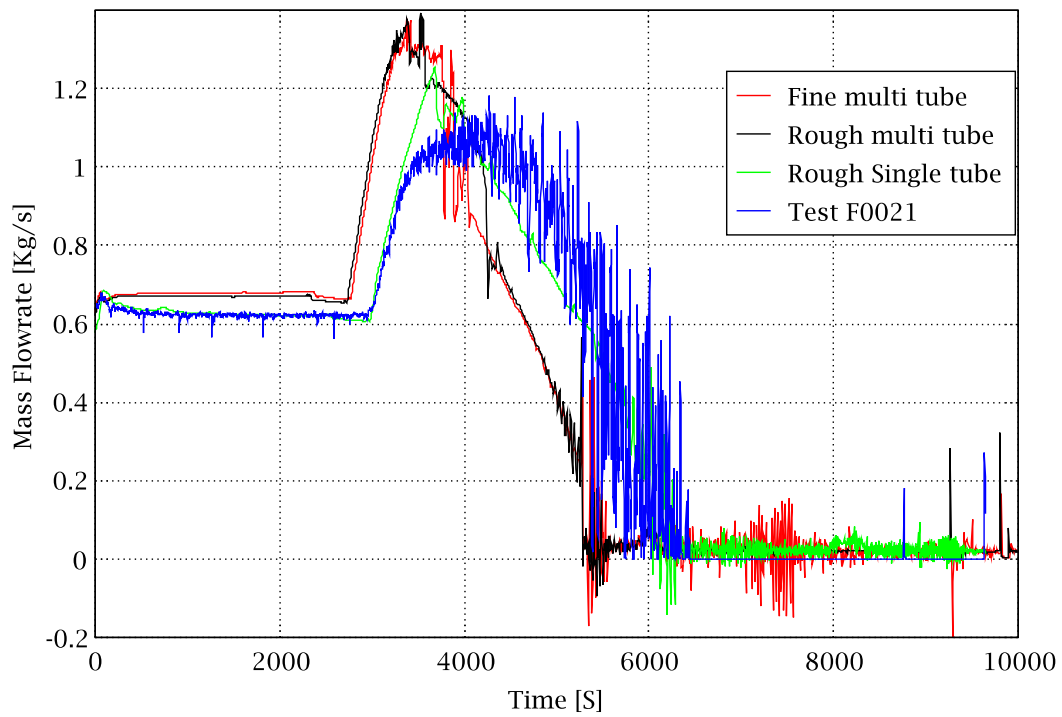


Figure 30 : Cold leg 1 mass flow rate

Diff.Pressure in SG 2 Tube 7 Hot Side

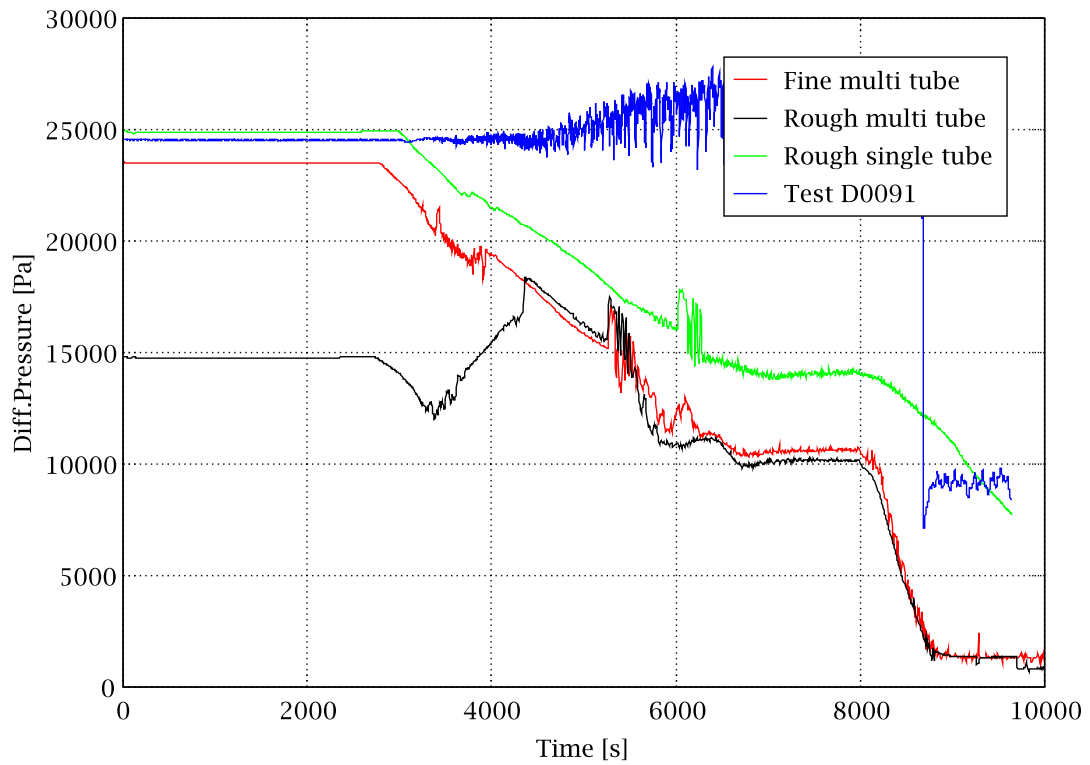


Figure 31 : Diff. pressure in SG2, tube 7, hot side

Figure 30 shows cold leg 1 mass flow rate. Mass flow rate variations are similar to downcomer flow rate variations during transient as already discussed in Figure 26. Fine and rough multi- tube model transient results are slightly overestimated compared to the test results, but the single tube model agrees well with test data.

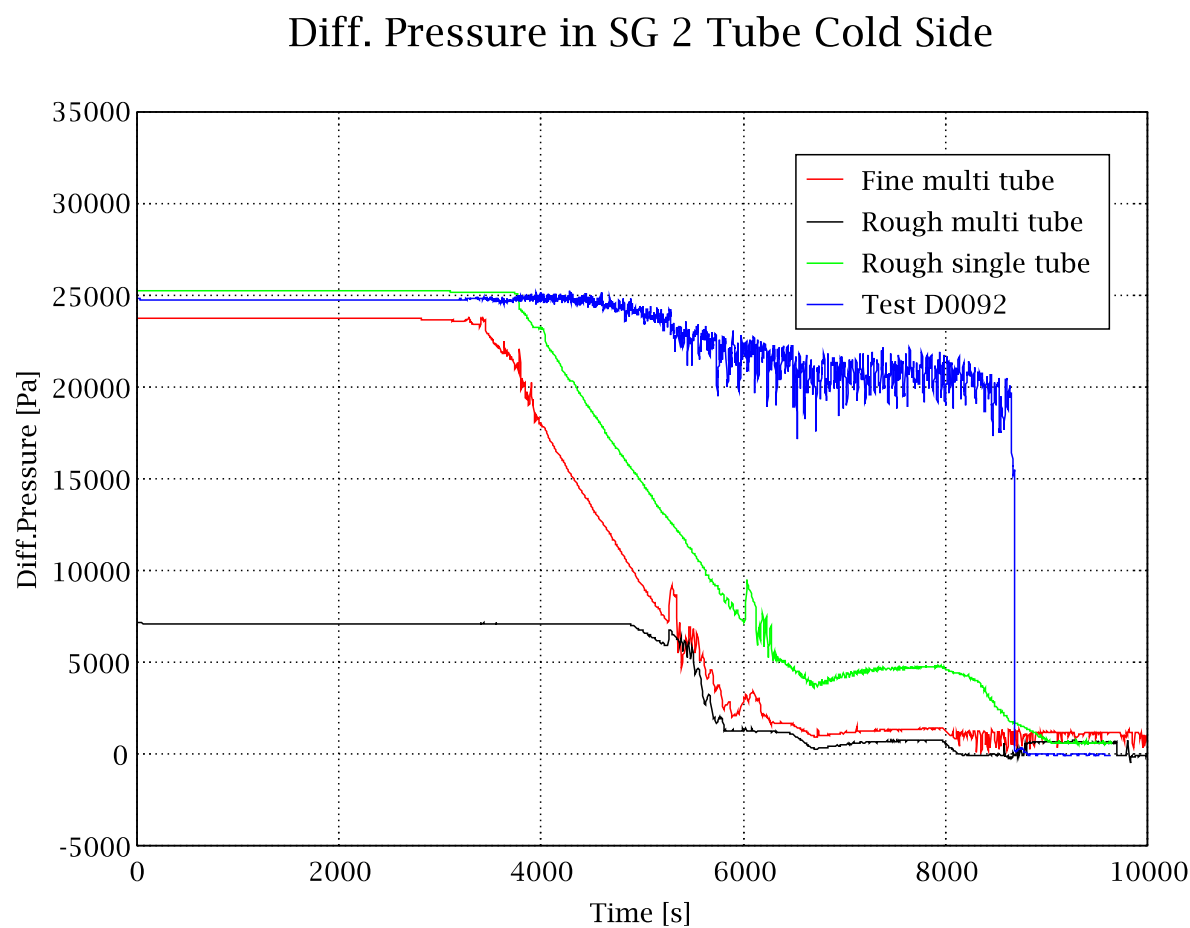


Figure 32 : Diff. pressure in SG2 tube cold side

The following table describes the key events during transient :

Table 20 : key events during transient

Time intervals (s)	Characteristics events
0-200 s	Break valve opening, rapid pressure decrease and reaching saturation condition Reverse flow has been observed for the longest tube of the SGs
201-2790 s	Slow re-pressurization of the primary system with increase of temperature. Upper plenum voiding and collapsed level reaches the hot leg elevation. Reverse flow has been observed for the longest tube of the SGs
2791 to 3570 s	Natural circulation is intensified and reaching the maximum down comer flow of 2.6 Kg/s
3571 to 6700 s	Primary flow decreasing gradually Two phase mixture in the hot legs Steam accumulated at the top of the steam generator tubes in the primary side
6701 to 7960 s	Break valve close Unintentional quasi steady-state
7961 to 9000 s	Re-opens the break valve Void penetration in the core Reflux condensation mode in the SGs tube Cold leg loop seal beginning to form
9200 s	Loop seal cleared at the SG side
9200 to 9500 s	Strong void oscillation in the core
9800 s	Integrated mass leaked out 300kg
1000 s	Terminate the simulation

5.3 Comparison between the single tube model and multi tube model

The most important phenomenon that has been observed in our new model is the reverse flow in the longest tube of the steam generators, which was unseen in the single tube model because of its one dimensional nature (i.e. the same flow rates at the inlet and at the outlet). Figure 33 shows the fluid temperature of the SG1 in the longest tube (tube 50, hot side, at elevation 0.7 m). It can be seen in the figure, that there is a deviation of the temperatures in the beginning of the transient with the single tube model, but there is better agreement with the multi-tube model. It can be concluded that the multi-tube model has revealed the existence of reverse flow in the longest tube of the SGs during the initial phase. In Figure 33 it can be clearly seen that after 4000 s of transient time, there is no reverse flow in the longest tube. This has been repeated in every model (both in the multi-tube and the single tube) and these agree well with test data after 4000s.

There are a number of possible explanations for the reverse flow during the initial period of the transients. These are related to the temperature and density variations at the upper heat exchanging regions of the steam generators. Distribution of flow resistances is also an important factor for generation of reverse flow at the first phase of the transient.

SG 1 Temperature (Tube 50, Hot Side, 0.700 m)

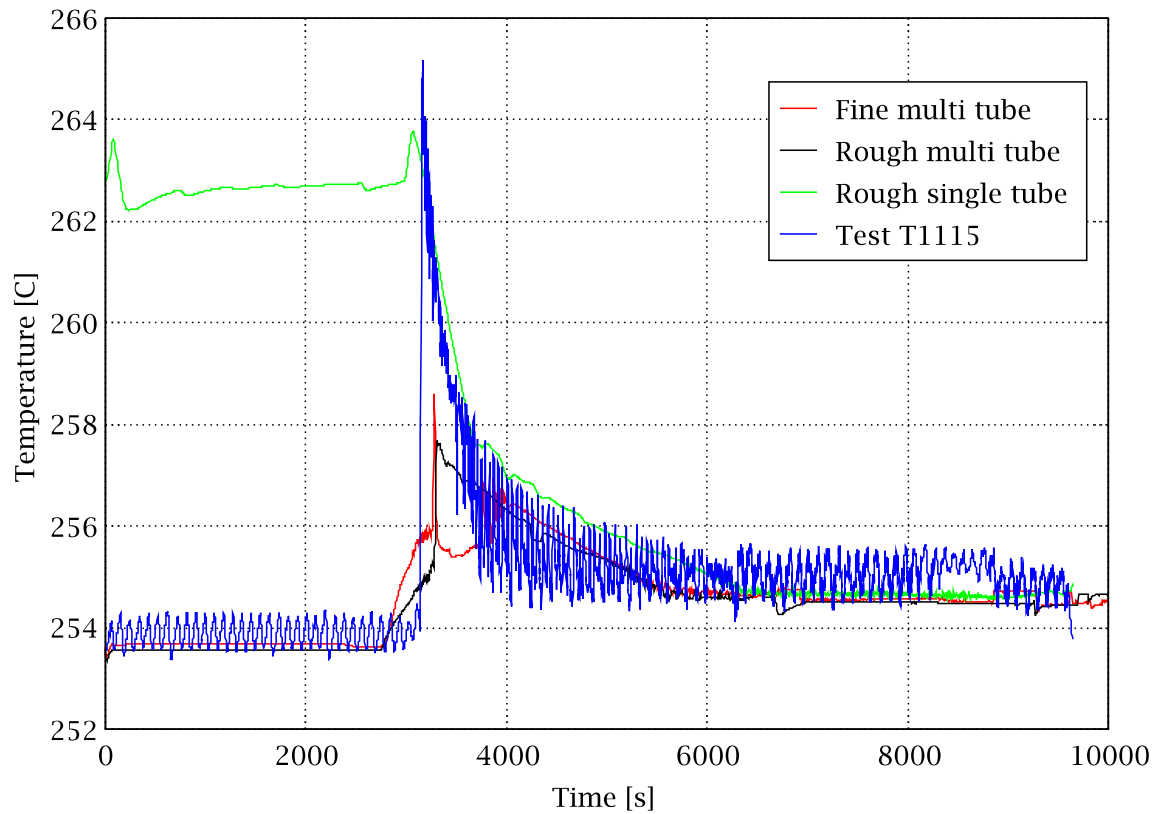


Figure 33 : SG1 temperature (Tube 50, hot side. 0.7m)

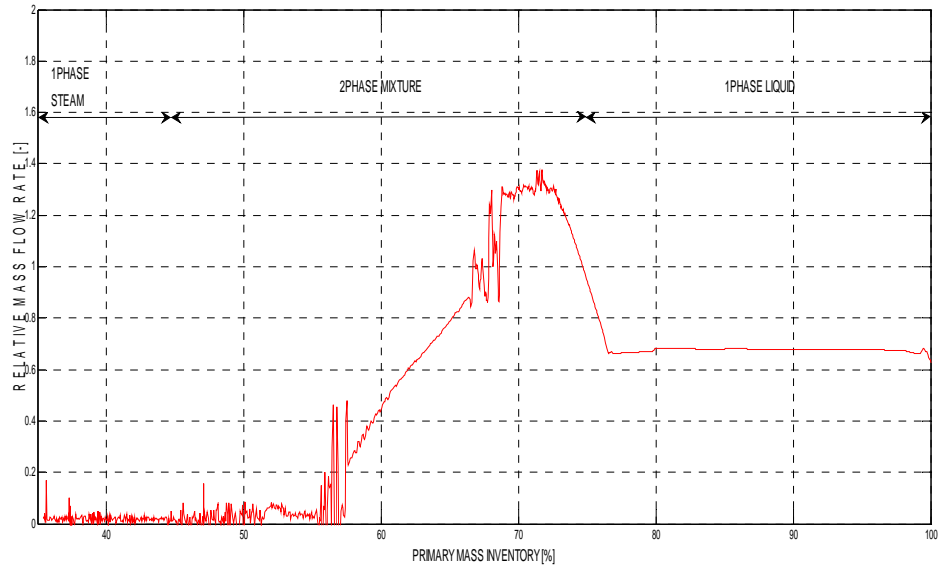


Figure 34 : Measured flow rate as a function of the primary mass inventory in the SBL-50 experiment

In Figure 34 the measured natural circulation mass flow rate in the fine multi-tube model is plotted as a function of the primary system mass inventory. In the beginning of the transient the downcomer mass flow rate was constant up to 74% -100% and single phase flow was observed during this time. When the mass inventory was less than 74%, the maximum flow rate was observed with the two phase flow. The downcomer mass flow rate suddenly increased and reached its maximum value, but after that it decreased again from the peak value. When primary inventory was less than 50%, the core was dry (dried?) out and the mass flow rate almost zero in the end of the transient due to flow stagnation.

Chapter 6

Conclusion and Future Work

6.1 Conclusions

According to the calculations, the simulation of the PACTEL SBL-50 experiment has been successful, although the modelling of transient was quite challenging, even if the test was relatively simple. The main goal of this project was achieved by a more detailed nodalization of vertical EPR-type steam generators during a small break LOCA.

The PWR PACTEL Benchmark Project consisted of a “pre-test” and the “post-test” phase. In the post test phase the single tube model (rough nodalization) and test data agrees well with the pre-test results but was not capable of prediction of flow reversal. This phenomenon occurred in the longest tubes, which was characterized by a large temperature difference between the neighbouring tubes. With refinement and extension of the SG models multiple tubes and smaller node sizes, reverse of the flow has become well predicted, which was unseen in single tube model.

Moreover, the PWR PACTEL Benchmark Project provided unique opportunities and challenges for all participants to build, analyze, and compare their own models and calculations with achievements by others, within the frame of this international activity.

6.2 Future work

In future, the current RELAP5 model of the PACTEL can be used for making an attempt to convert to a TRACE model. The conversion is not a straightforward process. For the time being, it can easily happen that the user has to re-build his/her model from scratch, particularly if a model is as sophisticated as the PACTEL's. Obviously, such a case would exceed the time-frame available for this thesis project. Therefore conversion of the model was not attempted.

However, it should be mentioned that the TRACE code is supposed to gradually take over all features of RELAP5, TRAC-B, TRAC-P, and other NRC codes during its developmental phase. In the long run, NRC will not support the parallel development of multiple codes, but they will focus on supporting one single code, and it will be TRACE.

Another possible direction of continuation of this work is the consideration of non-condensable gases. It is a proven fact that non-condensable gases can influence the heat transfer in a transient. It was also a fact that dissolved gases (mainly air) remained

within the coolant in the primary system of the PACTEL at the beginning of the Benchmark Test. (By pure natural circulation, without pumps, it is nearly impossible to remove the gases entirely from the system). The exact amount of gases was not measured, just estimated and documented in the description of the test. Consequently, a new model, which takes into account the presence of the non-condensable gases, may improve the agreement even further between the simulated and measured data. It might also be helpful for explanation of certain behaviour of transient. For instance, the dissolved air accumulated in the bending at the top of the SG U-tubes. Degradation of the heat transfer can be modelled in a new input, considering all the effects of the gases released from water and trapped in the SG heat exchanger tubes.

References

- [1] Nuclear Energy Agency, Organisation for Economic Co-operation and Development, "Nuclear Safety Research in OECD Countries, Summary Report of Major Facilities and Programmes at Risk," www.oecd-neo.org/nsd/reports/nea3144-research.pdf.
- [2] Nuclear Energy Agency, "International Reactor Physics Benchmark Experiments Project," <http://www.oecd-neo.org/science/wprs/irphe/>, 19 December, 2011.
- [3] Vesa Riikonen, Virpi Kouhia, Antti Räsänen, Harri Partanen, "General Description of the PWR PACTEL Test Facility," Research Report Lappeenranta University of Technology, Nuclear Safety Research Unit, vol. YTY 1/2009, 2009-06-17.
- [4] Dr. J. JOKINIEMI, "Steam Generator Tube Rupture Scenarios," VTT PROCESSES, Aerosol Technology Group. <http://cordis.europa.eu/documents/documentlibrary/66628891EN6.pdf>.
- [5] K. S. Chung, P. B. Abramson, M. F. Kennedy, and J. S. Kim, "Performance of Large LWR System Codes in Calculating," Reactor Analysis & Safety Division, Argonne National Laboratory, pp. <http://www.osti.gov/bridge/servlets/purl/6487927-Mea4Lk/6487927.pdf>, 1982-08-10.
- [6] United States Nuclear Regulatory Commission(NRC), "Computer Codes," <http://www.nrc.gov/about-nrc/regulatory/research/comp-codes.html>, 2011-03-21.
- [7] Vesa Riikonen, Virpi Kouhia, "Summary Report of PWR PACTEL Benchmark Experiment Blind Calculations," Research Report Lappeenranta University of Technology, Nuclear Safety Research Unit, Vol: PAX 1/2011, 2011-05-02.
- [8] D.L.Knudson, L.S.Ghan, C.A.Dobbe, "SCDAP/RELAP5 Evaluation Of The Potential For Steam Generator Tube Ruptures As A Result Of Severe Accidents In Operating Pressurized Water," Idaho National Engineering and Environmental Laboratory, Vol. 1 NEEL/EXT-98-00286 , <http://www.inl.gov/technicalpublications/Documents/3156830.pdf>, September, 1998.
- [9] Paul Scherrer Institut, "RELAP5," Laboratory for Thermal Hydraulics, <http://lth.web.psi.ch/codes/RELAP5.htm>, June, 2009.
- [10] United States Nuclear Regulatory Commission (NRC), "RELAP5/MOD3.3 Code Manual Volume V Users Guidelines," October, 2010.
- [11] United States Nuclear Regulatory Commission (NRC), "RELAP5/MOD3.3 Code Manual Volume II Users Guidelines," October, 2010.

- [12] United States Nuclear Regulatory Commission (NRC), "Symbolic Nuclear Analysis Package (SNAP) User's Manual,," February,2011.
- [13] Chester Gingrich, "Symbolic Nuclear Analysis Package - SNAP version 1.0: Features and Applications," December 2009.
- [14] Math Work, "MATLAB (The Language of Technical Computing)"
<http://www.mathworks.se/products/matlab/>.
- [15] Corel Corporation, "Corel,A Short History of CorelDraw,"
<http://www.corel.com/corel/pages/index.jsp?pgid=2100019>, 2012.
- [16] Wikipedia, "CorelDRAW," <http://en.wikipedia.org/wiki/CorelDRAW>.
- [17] Dilip Saha, "Local Phenomena Associated with natural Circulation," vol. Annex_05, nr
www.iaea.org/OurWork/ST/NE/NENP/NPTDS/Annex_05.doc.
- [18] P.K. Vijayan , A.K. Nayak, "Introduction to Instabilittes in Natural Circulation Systems,"
Reactor Engineering Division, Bhabha Atomic Research Centre.India, nr
www.iaea.org/OurWork/ST/NE/NENP/NPTDS/Annex_07.doc.
- [19] "Natural Circulation, Section 3.6,"
www.iaea.org/NaturalCirculation/SOAR_Phenomena6_Draft...
- [20] N. Aksan, "International Standard Problems and Small Break Loss-of-Coolant Accident (SBLOCA)," Paul Scherrer Institut (PSI), 13 December 2007. .
- [21] CEA Saclay, "Multiphysics and LWR Transient Analysis, Reactor analysis: Advances and new needs," PHYSOR 2008, Interlaken, Sept. 14-19,2008.
- [22] Christophe Demaziere, Physics of Nuclear Reactors, Chalmers University of Technology ,
Gothenburg, Sweden, 2009.
- [23] Wikipedia, "Courant–Friedrichs–Lewy condition," http://en.wikipedia.org/wiki/Courant_Friedrichs_Lewy_condition.

Appendix A

Part of multi-tube ASCII input file given below,

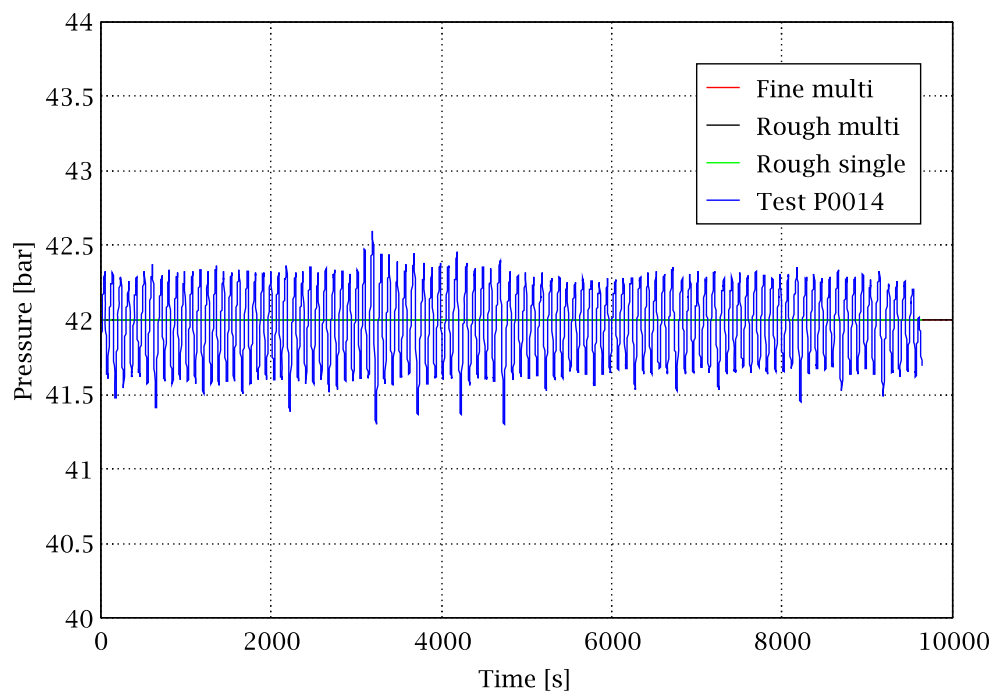
```
*-----+-----+-----+-----+-----+-----+
+-----+
*      #221      SG-1 Heat exchanger tube 1
*              Simulating 5 tubes
*              3.535 m up, 0.450 m horiz, 3.535 m down
*-----+-----+-----+-----+-----+-----+
*      NAME      TYPE
2210000  SG1Utub1 pipe
*      NO.VOLS
2210001  29
*      FLOWAREA  VOL.NO
2210101  0.0010782 29
*      FLOWAREA  JUN.NO
2210201  0.0        28
*      LENGTH    VOL.NO
2210301  0.250      11
2210302  0.275      12
2210303  0.290      13
2210304  0.220      14
*2210305  0.450      15      * Horizontal
2210305  0.1        15      * Horizontal
2210306  0.220      16
2210307  0.290      17
2210308  0.275      18
2210309  0.250      29
*      VOLUME    VOL.NO
2210401  0.0        29
*      AZIM.ANG  VOL.NO
2210501  0.0        29
*      INCL.ANG  VOL.NO
2210601  90.0       14
2210602  0.0        15
2210603  -90.0      29
*      ELEV.CHG  VOL.NO
2210701  0.250      11
2210702  0.275      12
2210703  0.290      13
2210704  0.220      14
2210705  0.000      15      * Horizontal
2210706  -0.220     16
2210707  -0.290     17
2210708  -0.275     18
2210709  -0.250     29
*      WALLROUGH HYDR.DIA  VOL.NO
2210801  2.0e-6     0.01657 29
*      FLOSS      RLOSS    JUN.NO
2210901  0.0        0.0     13
2210902  0.0        0.0     15      * 2 elbows
2210903  0.0        0.0     28
*      TLPVBFE    VOL.NO
2211001  0000000    29
*      EFVCAHS    JUN.NO
```

2211101	0101000	28	* CCFL on				
*	EBT	PRESSURE	TEMP/QUAL	-----	-----	-----	
VOL.NO							
*							
*2211201	003	75.0e5	550.0	0.0	0.0	0.0	29
*2211201	003	75.0e5	547.028	0.0	0.0	0.0	1
*2211202	003	75.0e5	544.663	0.0	0.0	0.0	2
*2211203	003	75.0e5	542.581	0.0	0.0	0.0	3
*2211204	003	75.0e5	540.747	0.0	0.0	0.0	4
*2211205	003	75.0e5	539.133	0.0	0.0	0.0	5
*2211206	003	75.0e5	537.712	0.0	0.0	0.0	6
*2211207	003	75.0e5	536.461	0.0	0.0	0.0	7
*2211208	003	75.0e5	535.360	0.0	0.0	0.0	8
*2211209	003	75.0e5	534.387	0.0	0.0	0.0	9
*2211210	003	75.0e5	533.529	0.0	0.0	0.0	10
*2211211	003	75.0e5	532.770	0.0	0.0	0.0	11
*2211212	003	75.0e5	532.040	0.0	0.0	0.0	12
*2211213	003	75.0e5	531.369	0.0	0.0	0.0	13
*2211214	003	75.0e5	530.905	0.0	0.0	0.0	14
*2211215	003	75.0e5	529.522	0.0	0.0	0.0	15
*2211216	003	75.0e5	529.248	0.0	0.0	0.0	16
*2211217	003	75.0e5	528.945	0.0	0.0	0.0	17
*2211218	003	75.0e5	528.697	0.0	0.0	0.0	18
*2211219	003	75.0e5	528.500	0.0	0.0	0.0	19
*2211220	003	75.0e5	528.327	0.0	0.0	0.0	20
*2211221	003	75.0e5	528.176	0.0	0.0	0.0	21
*2211222	003	75.0e5	528.043	0.0	0.0	0.0	22
*2211223	003	75.0e5	527.928	0.0	0.0	0.0	23
*2211224	003	75.0e5	527.827	0.0	0.0	0.0	24
*2211225	003	75.0e5	527.739	0.0	0.0	0.0	25
*2211226	003	75.0e5	527.662	0.0	0.0	0.0	26
*2211227	003	75.0e5	527.595	0.0	0.0	0.0	27
*2211228	003	75.0e5	527.538	0.0	0.0	0.0	28
*2211229	003	75.0e5	527.488	0.0	0.0	0.0	29
* VOL/FLOW							
2211300	1						
*	FLOWF	FLOWG	VELJ	JUN.NO			
2211301	0.0	0.0	0.0	28			
*	HYDR.DIA	FORM	GAS_INT	SLOPE	JUN.NO		
2211401	0.01657	0.0	0.8	1.0	13		
2211402	0.01657	0.0	0.35	1.0	15		
2211403	0.01657	0.0	0.8	1.0	28		

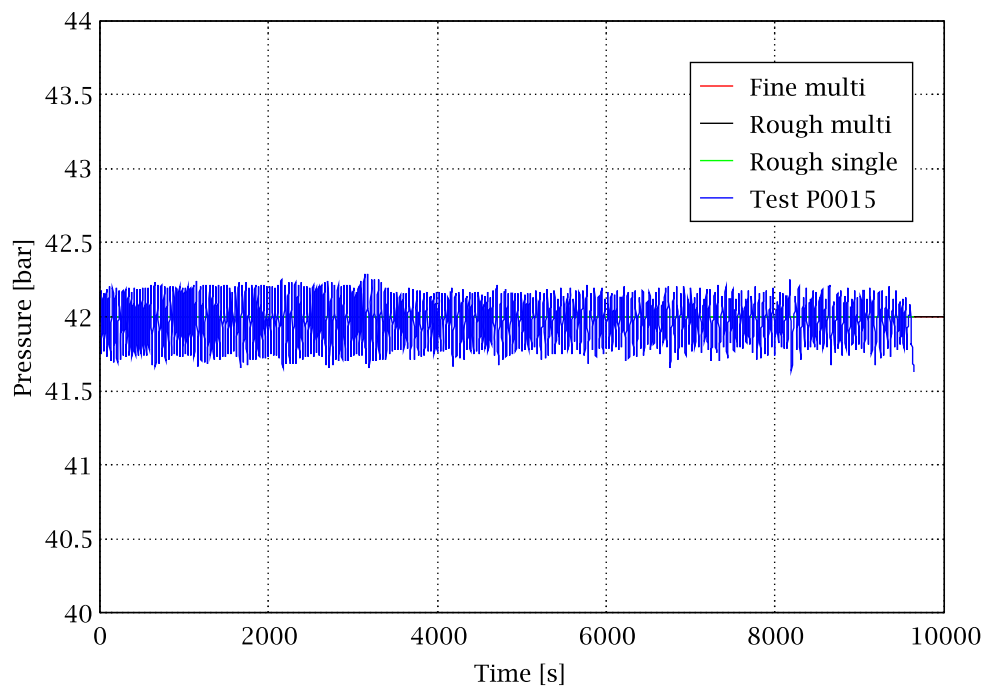
Appendix B

The rest of the test result comparison figure is given below,

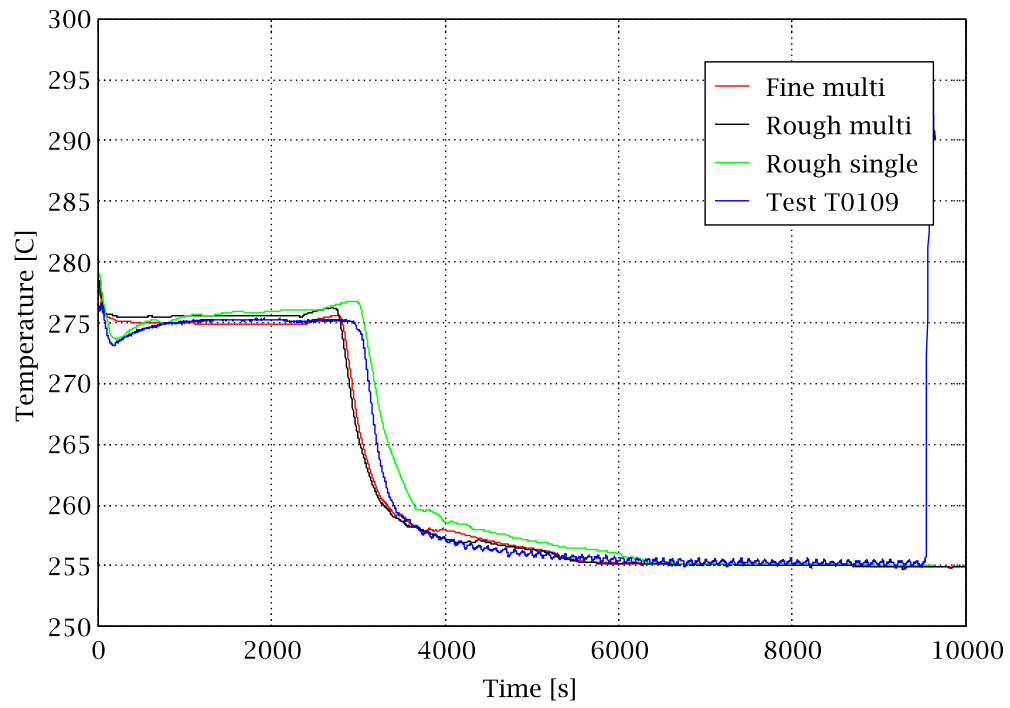
SG 1 Pressure



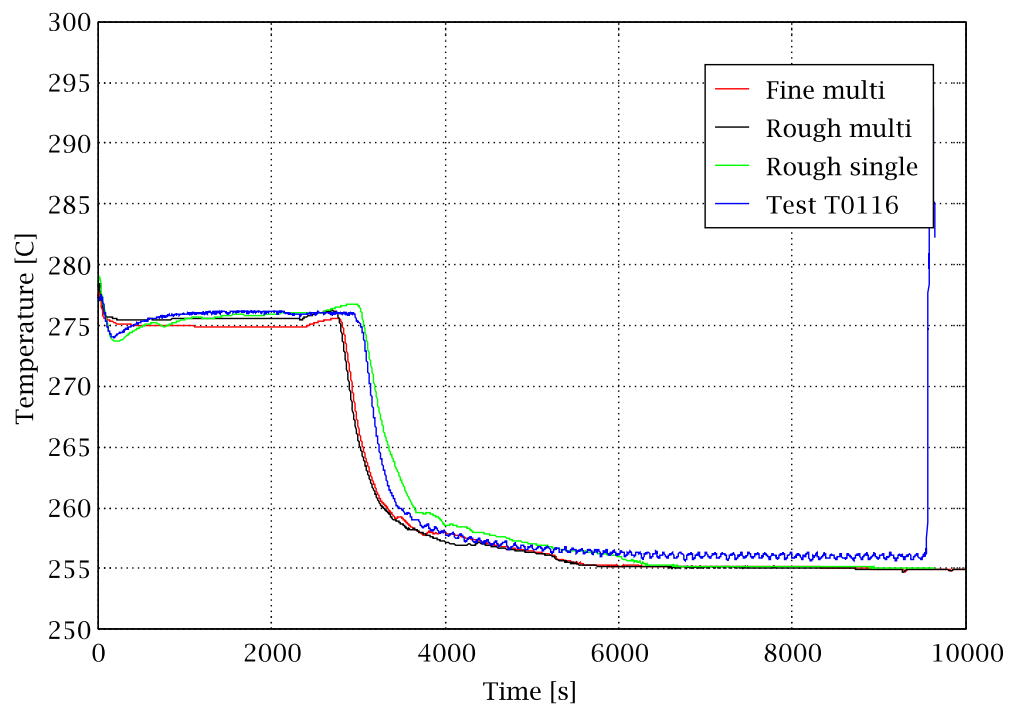
SG 2 Pressure



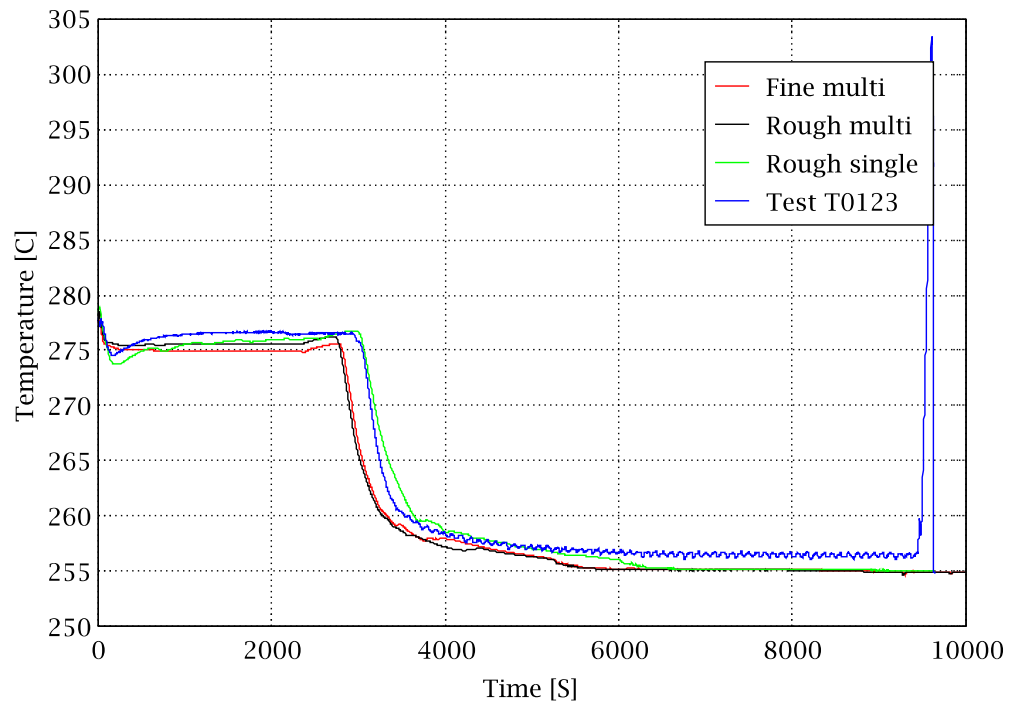
Outlet Temperature of Core Channel A



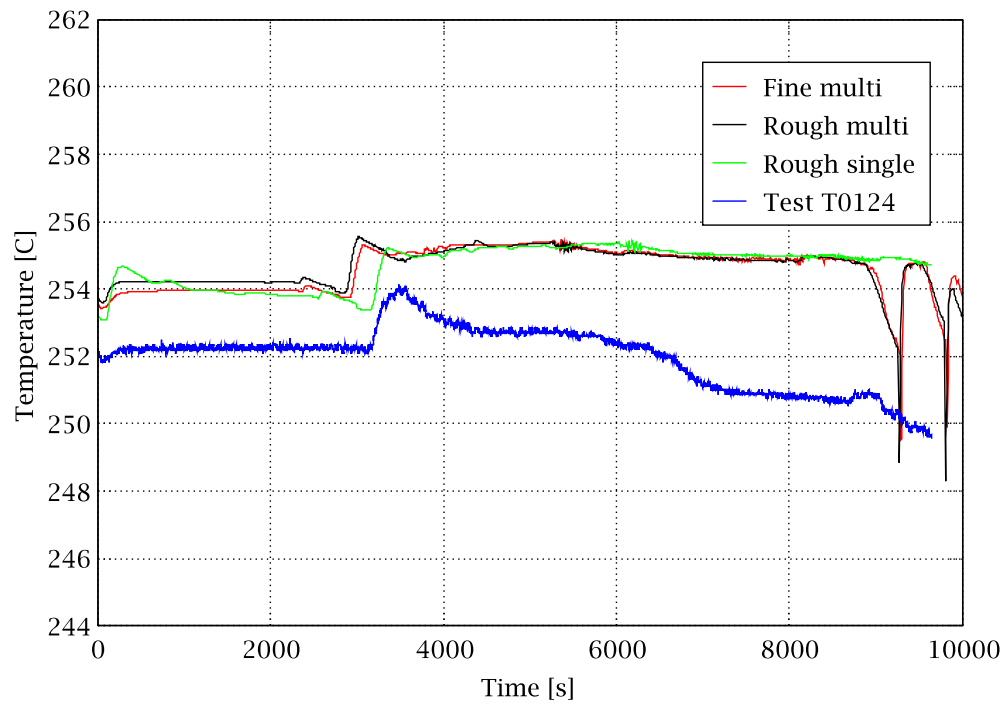
Outer Temperature of Core Channel B



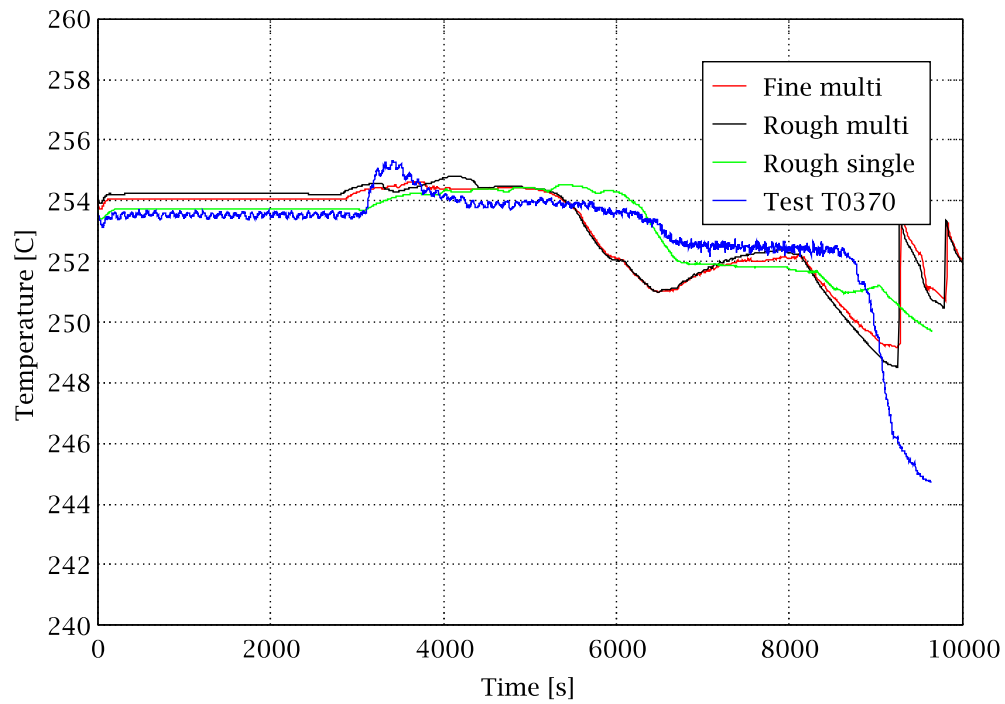
Outlet Temperature of Core Channel C



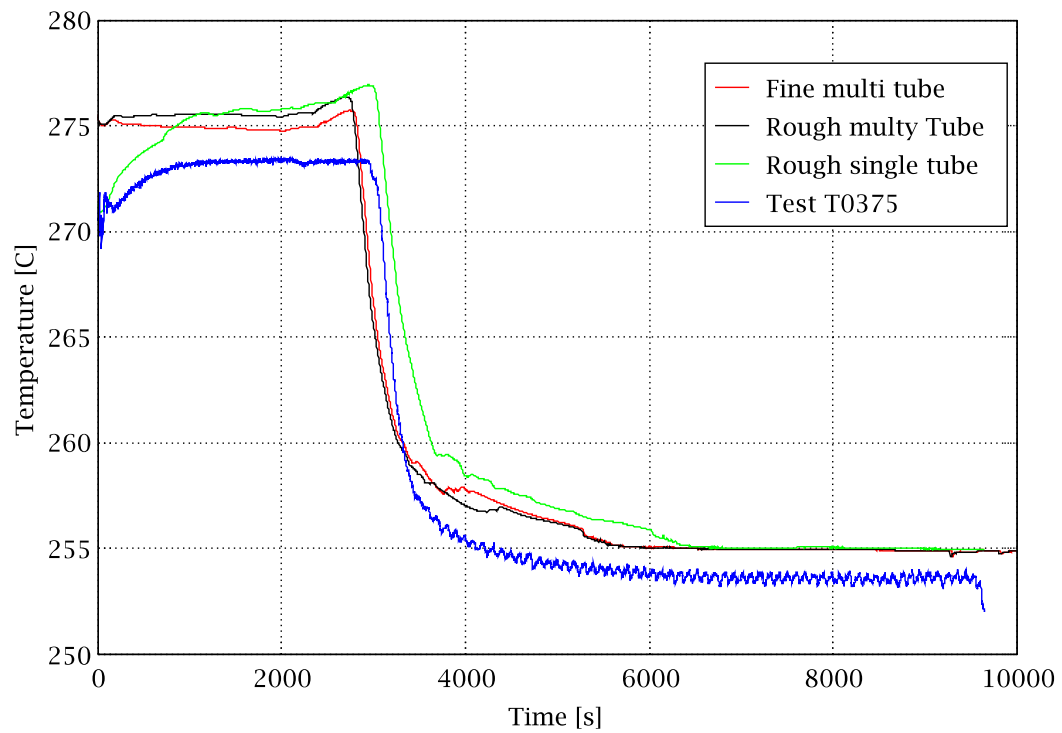
Core Inlet Temperature



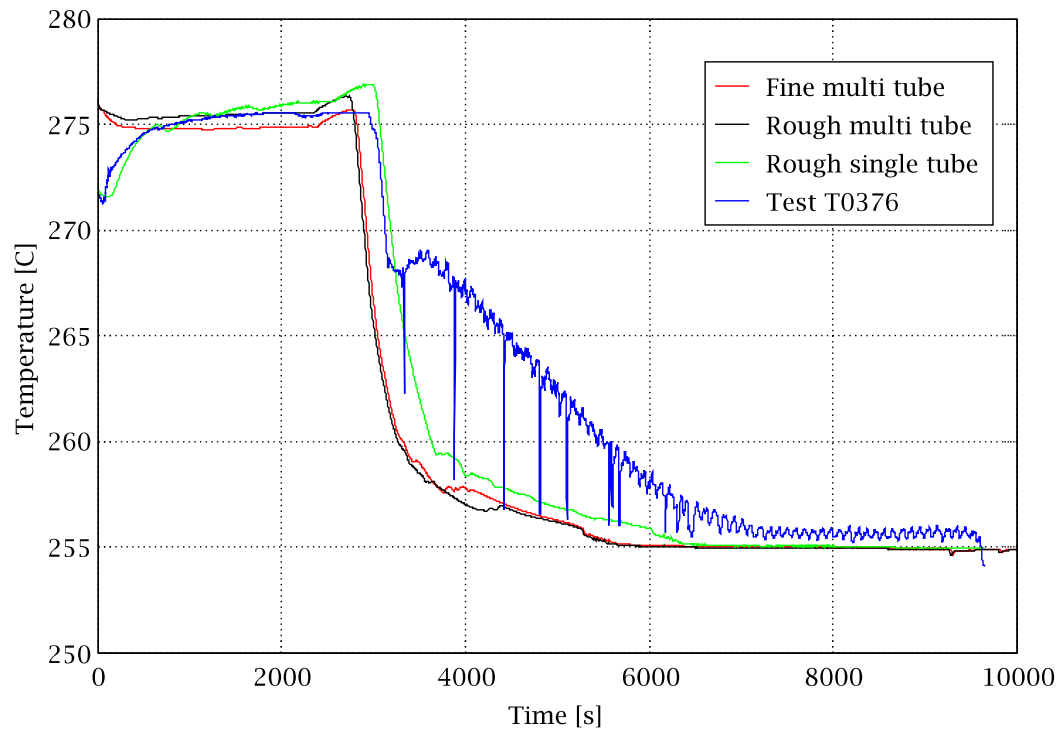
Downcomer Middle Temperature



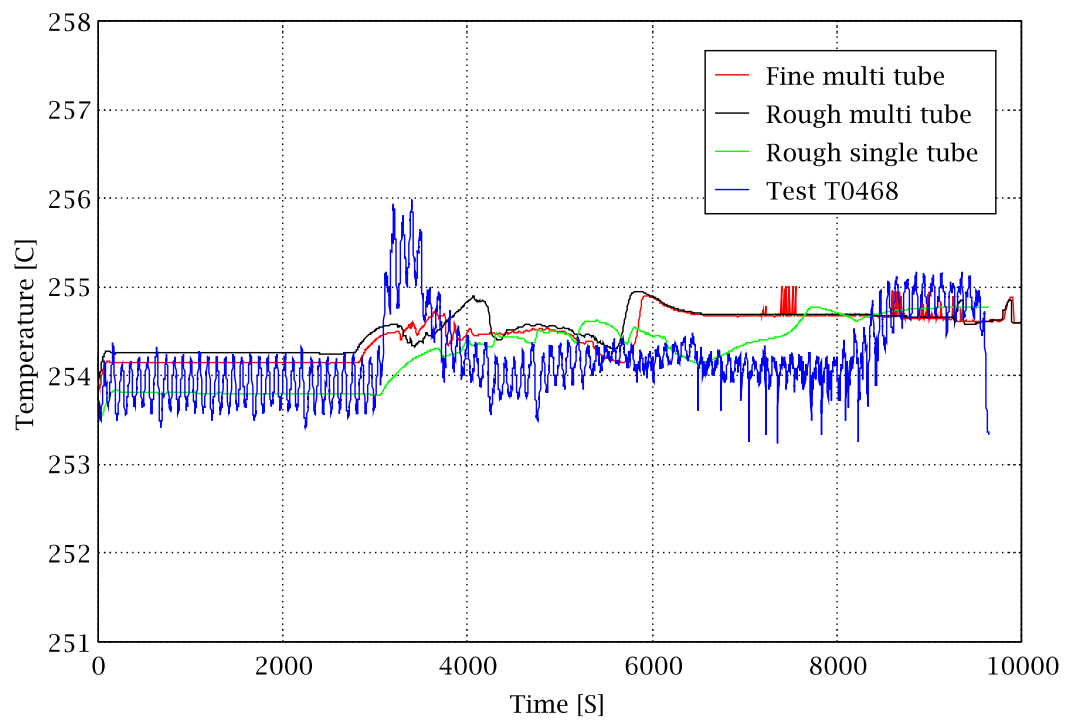
Upper Plenum Bottom Temperature



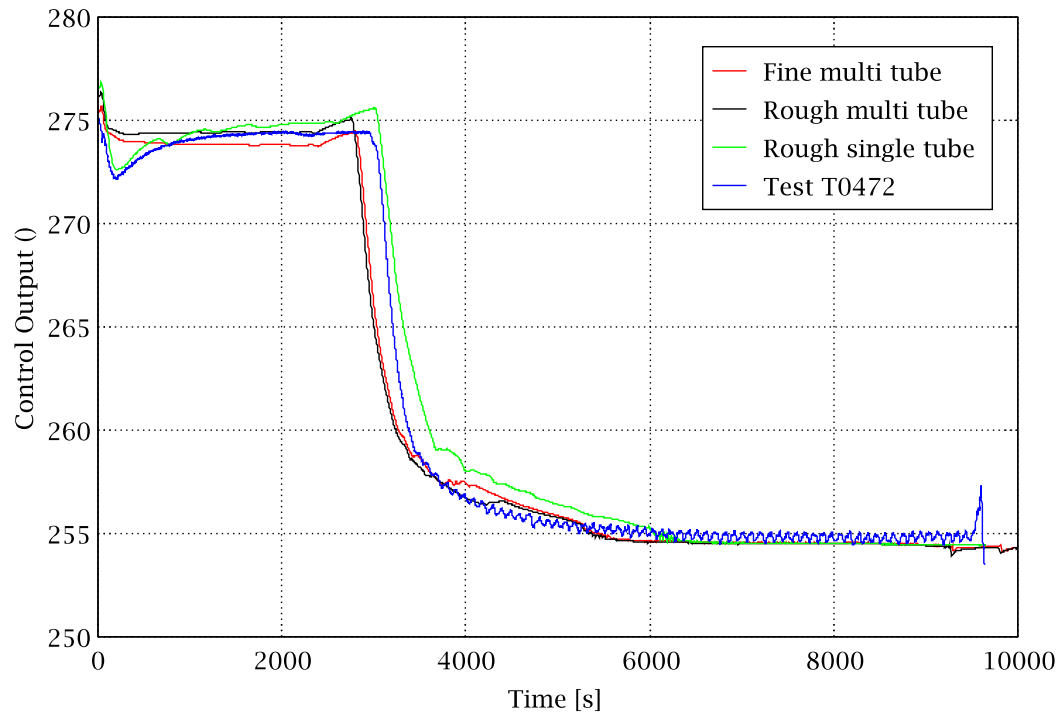
Upper Plenum Top Temperature



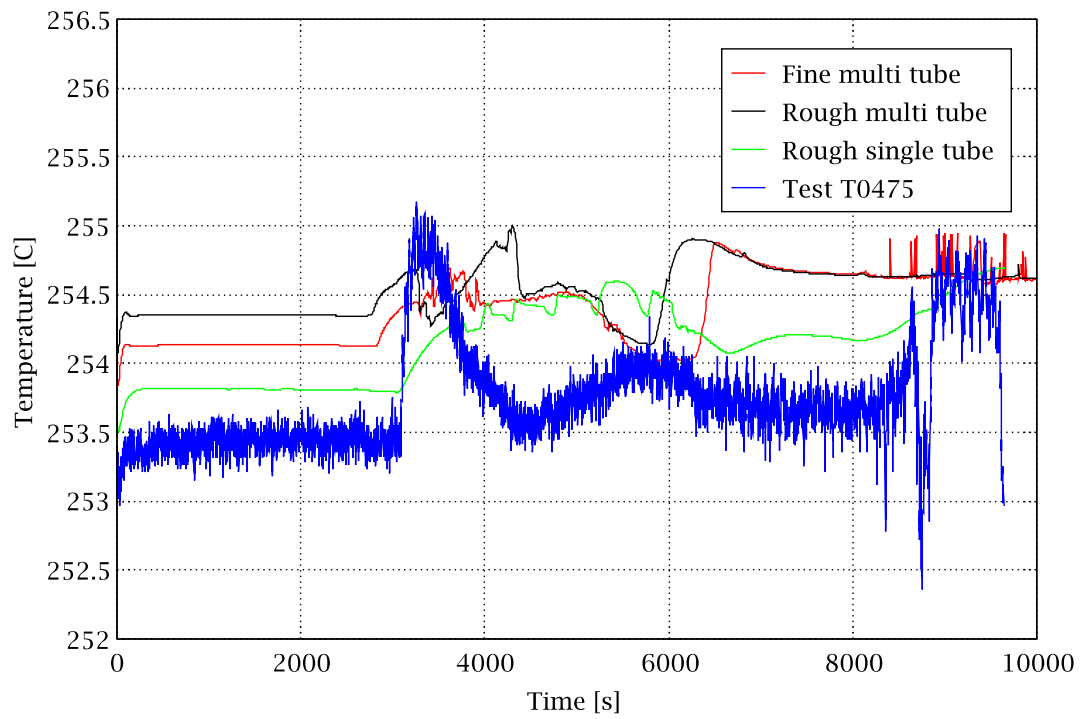
Cold Leg 1 Inlet Temperature



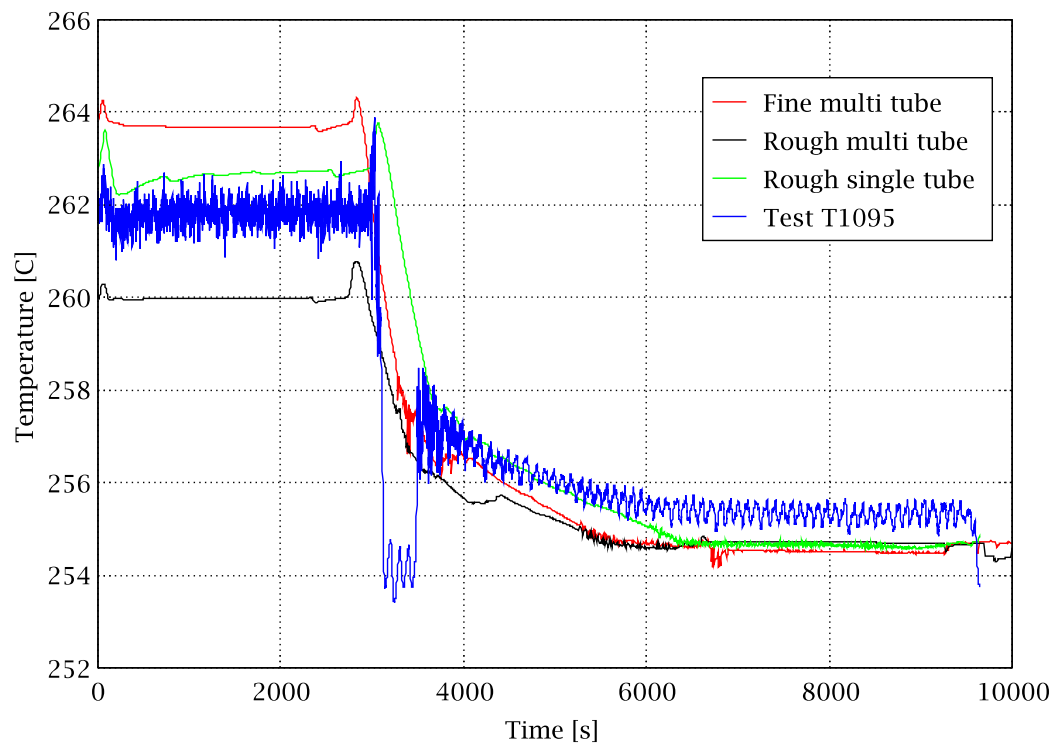
Hot Leg 2 Outlet Temperature



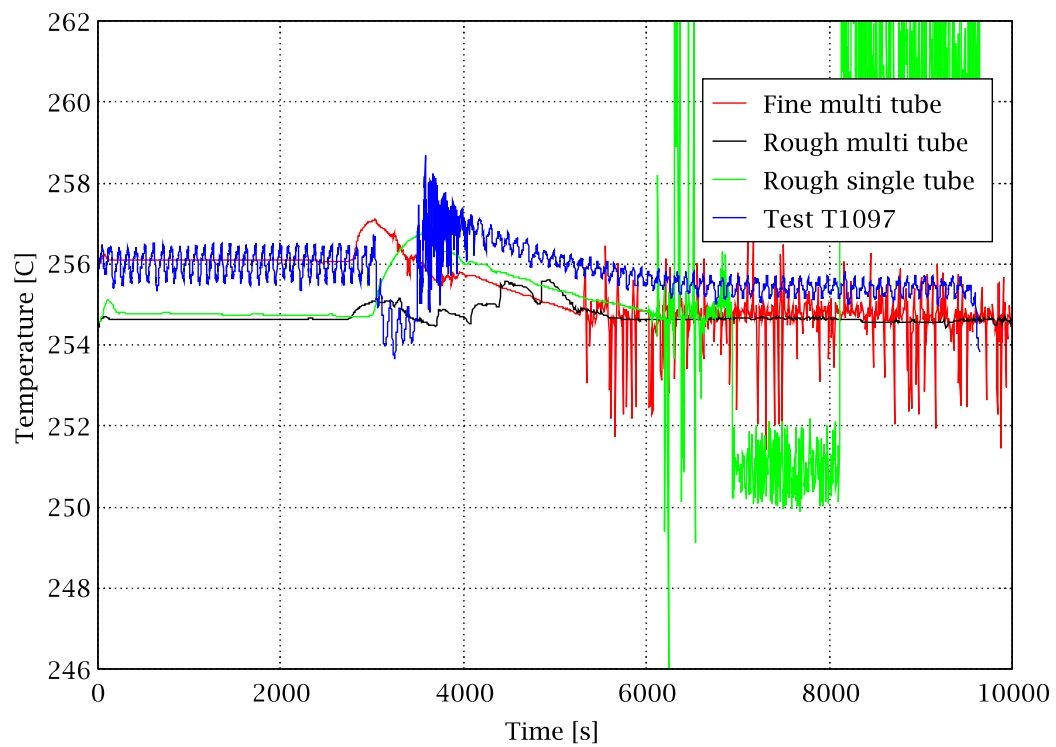
Cold Leg 2 Inlet Temperature



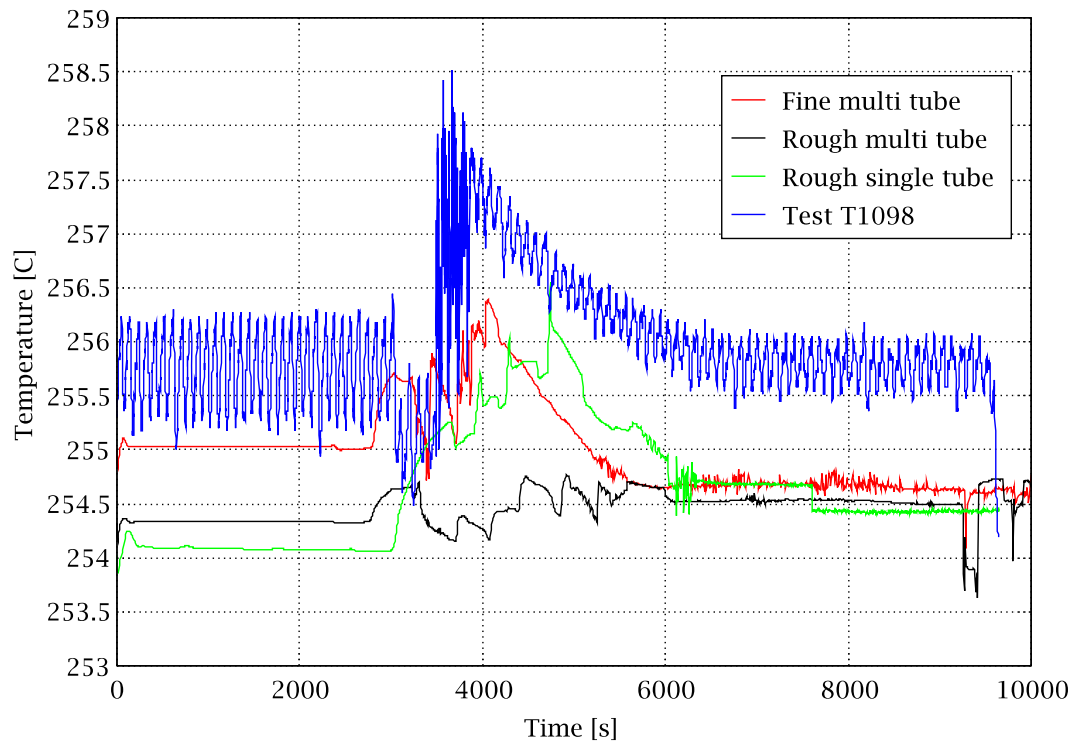
SG 1 Temperature (Tube 10, Hot Side, 0.700 m)



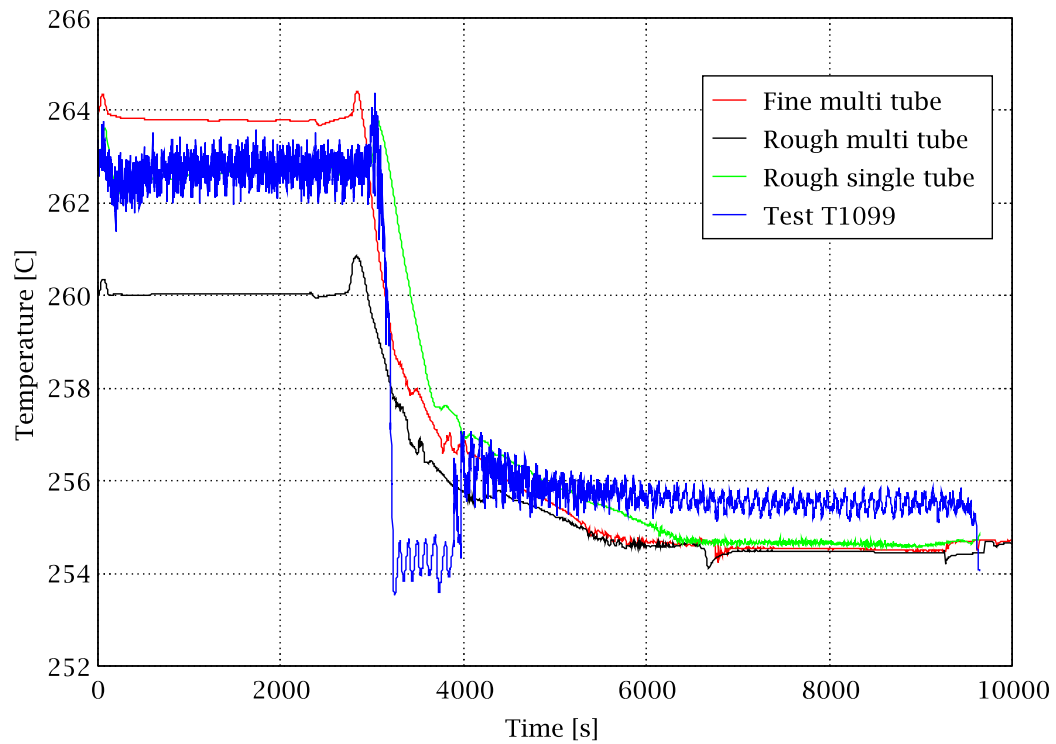
SG 1 Temperature (Tube 10, Top)



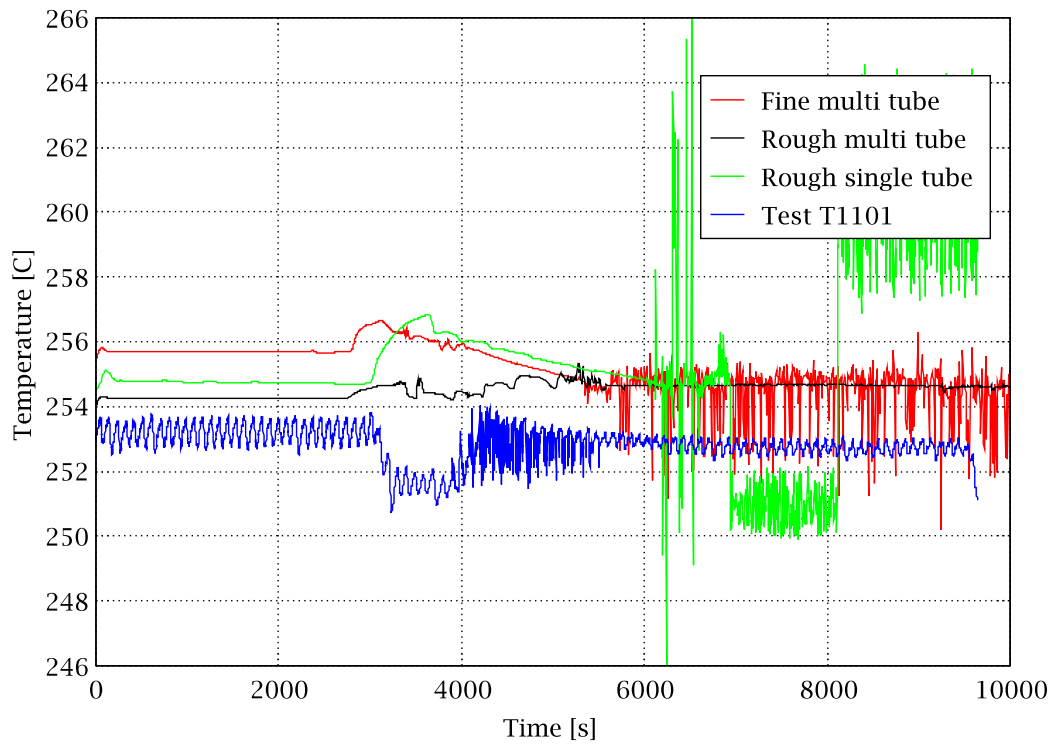
Sg 1 Temperature (Tube 10, Cold Side, 2.000 m)



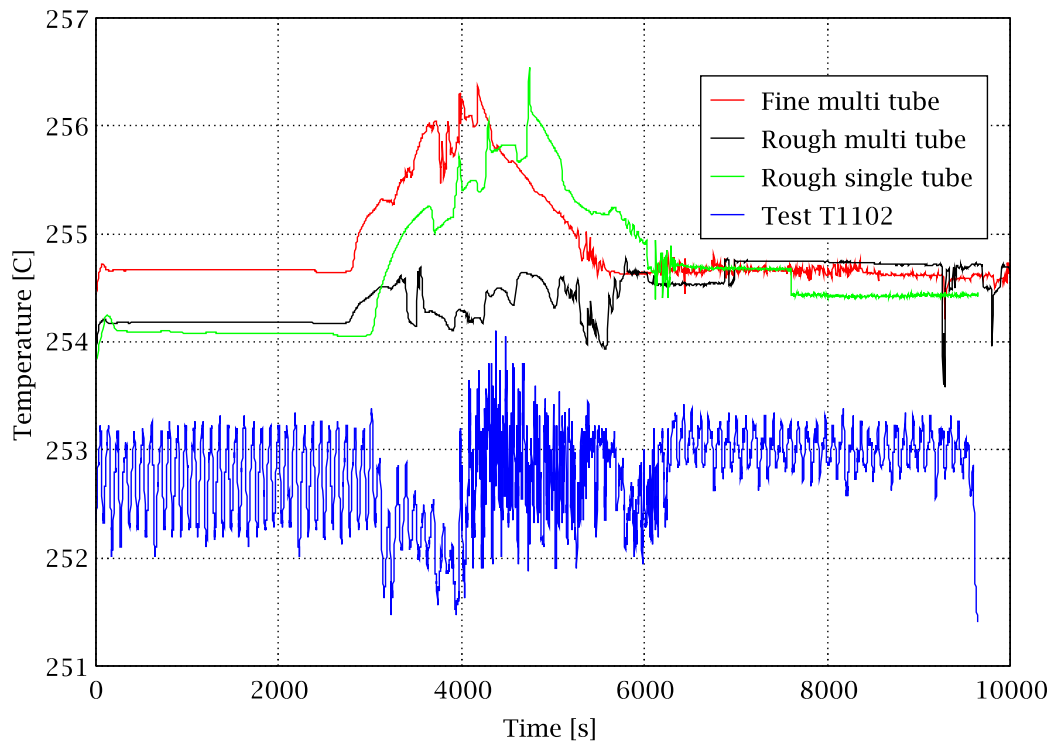
SG 1 Temperature (Tube 28, Hot Side, 0.700 m)



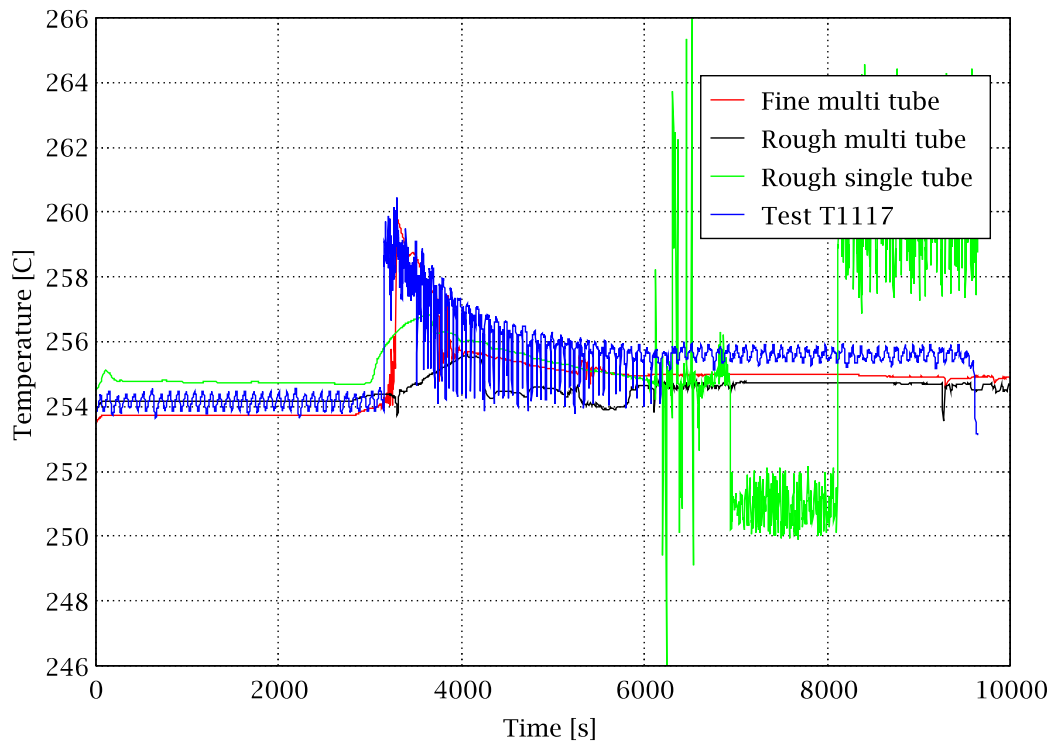
SG 1 Temperature (Tube 28,Top)



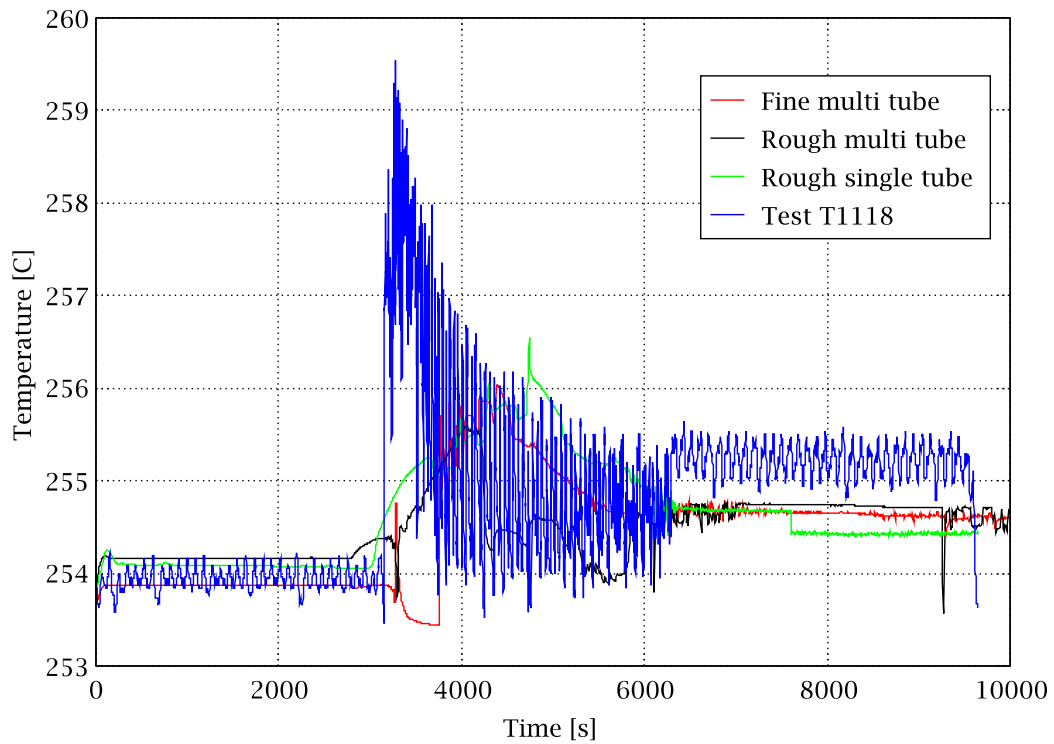
Sg 1 Temperature (Tube 28, Cold Side, 2.000 m)



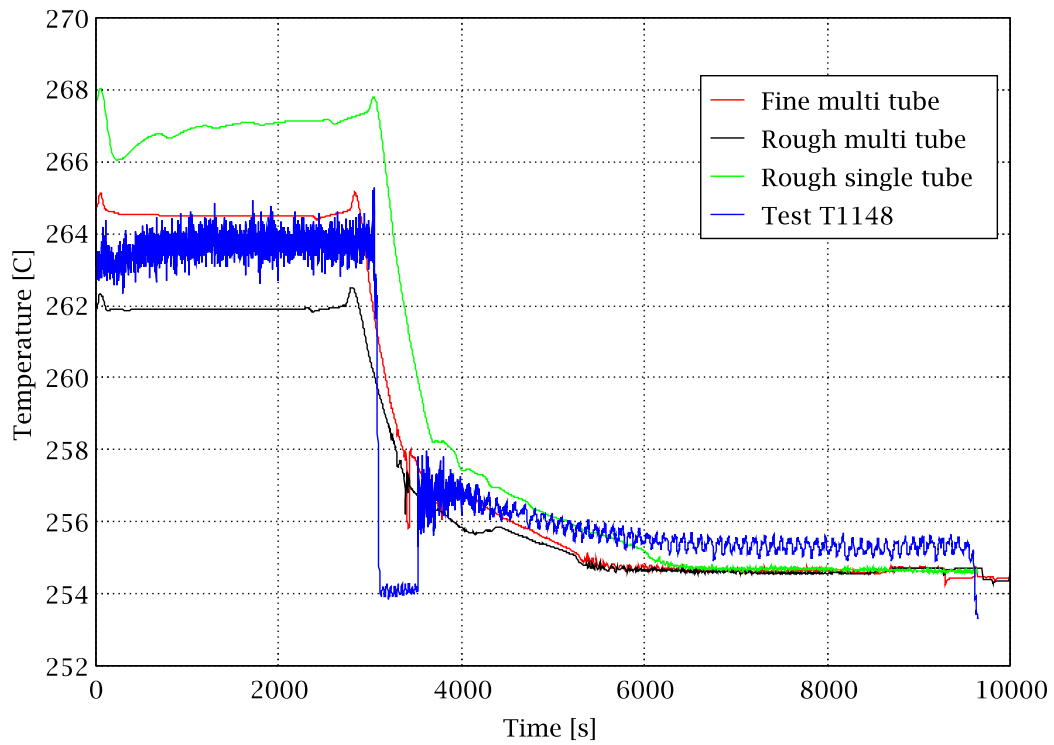
SG 1 Temperature (Tube 50,Top)



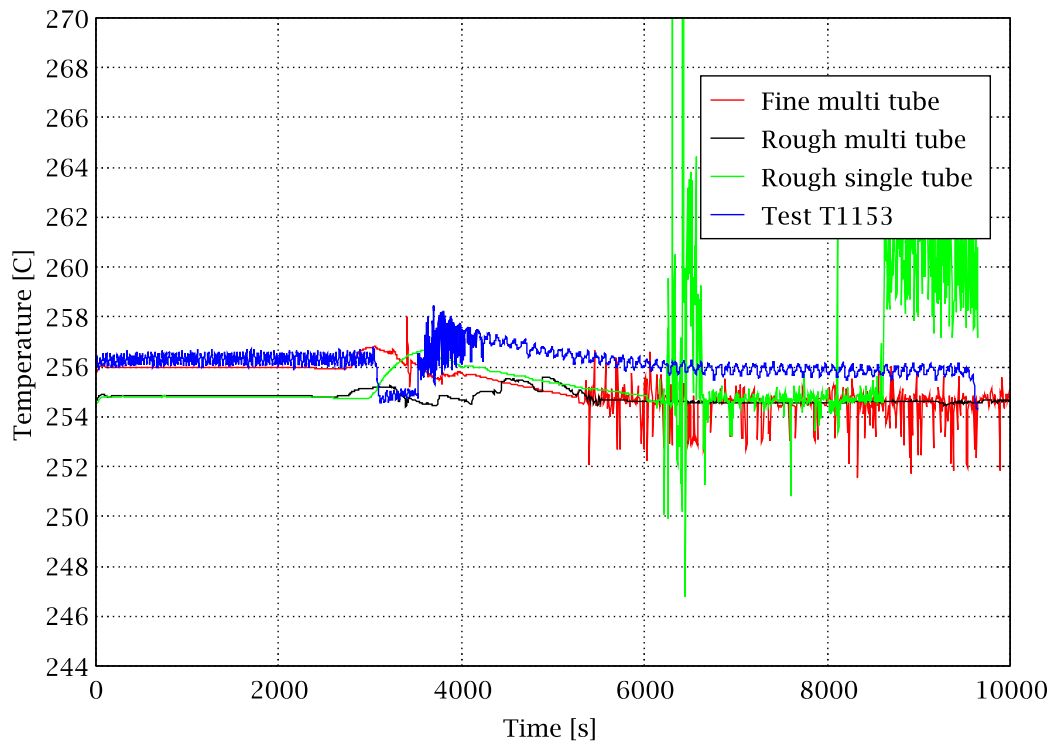
SG 1 Temperature (Tube 50,Cold Side, 2.000 m)



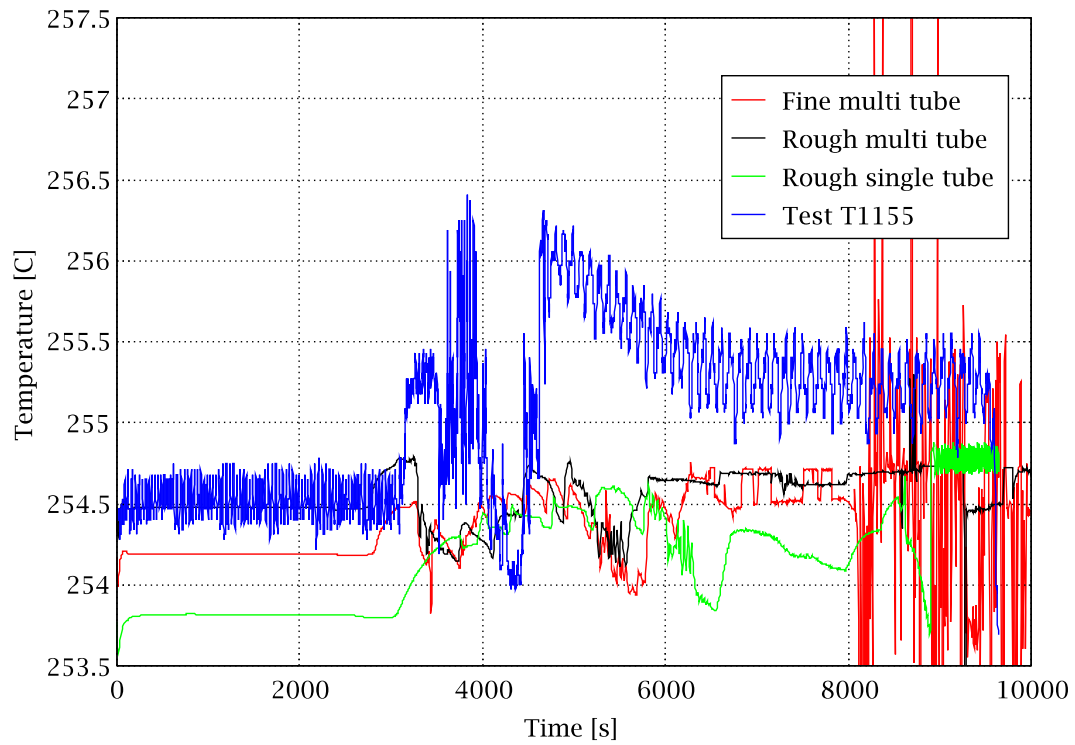
SG 2 Temperature (Tube 10,Hot Side, 0.300 m)



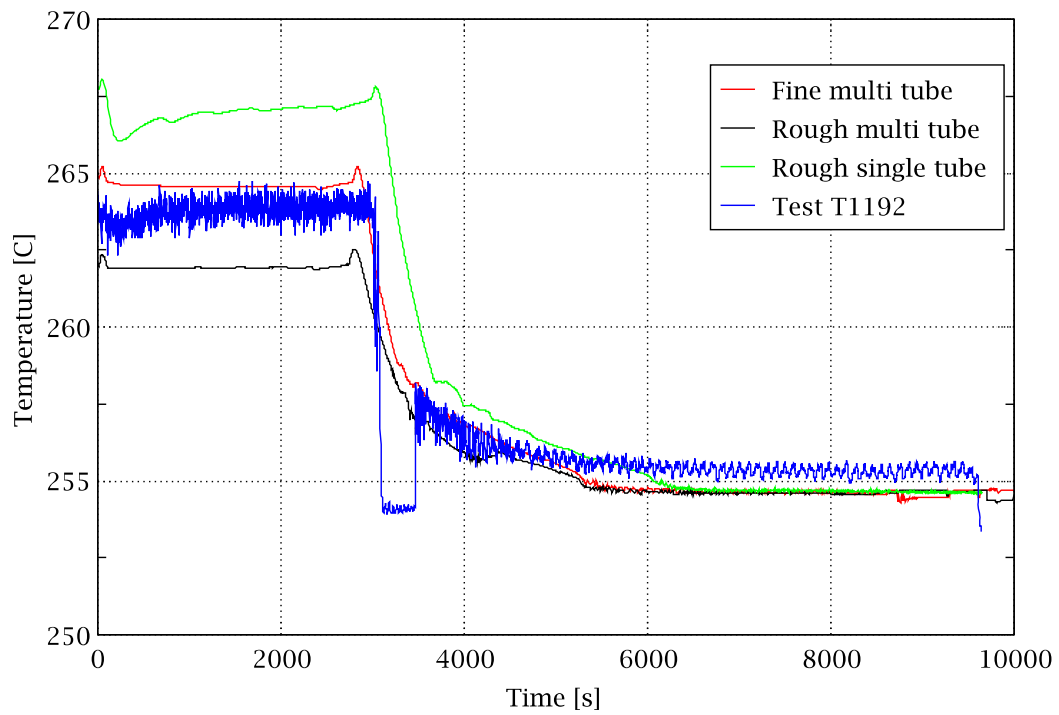
SG 2 Temperature (Tube 10,Top)



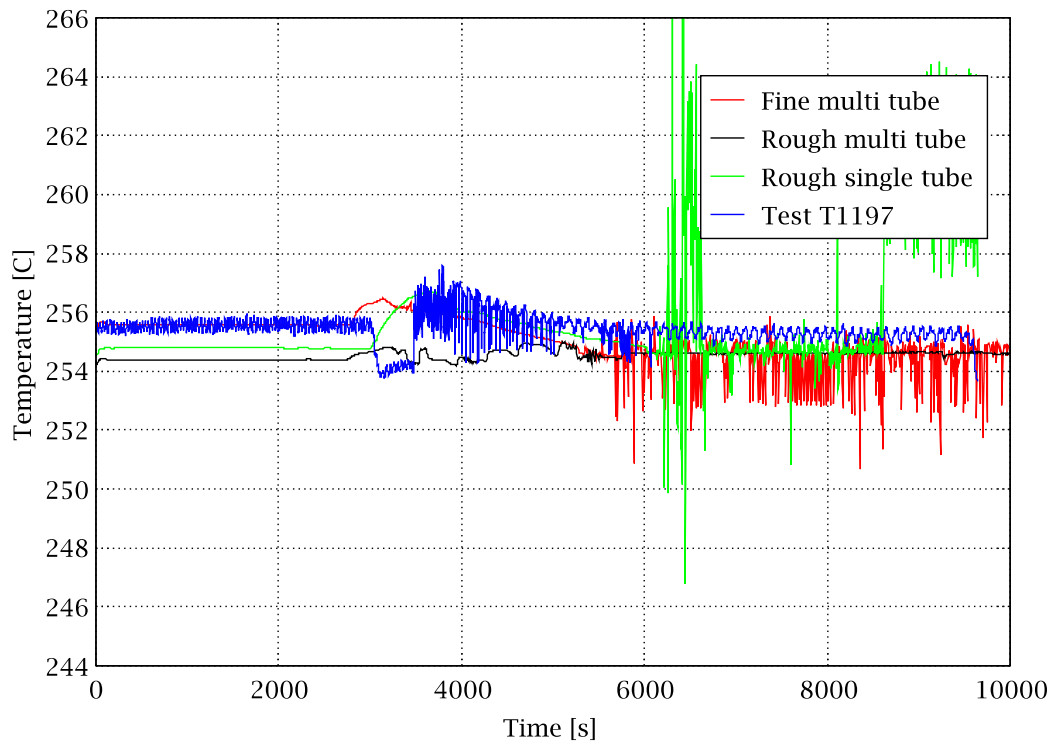
SG 2 Temperature (Tube 10, Cold Side, 0.300 m)



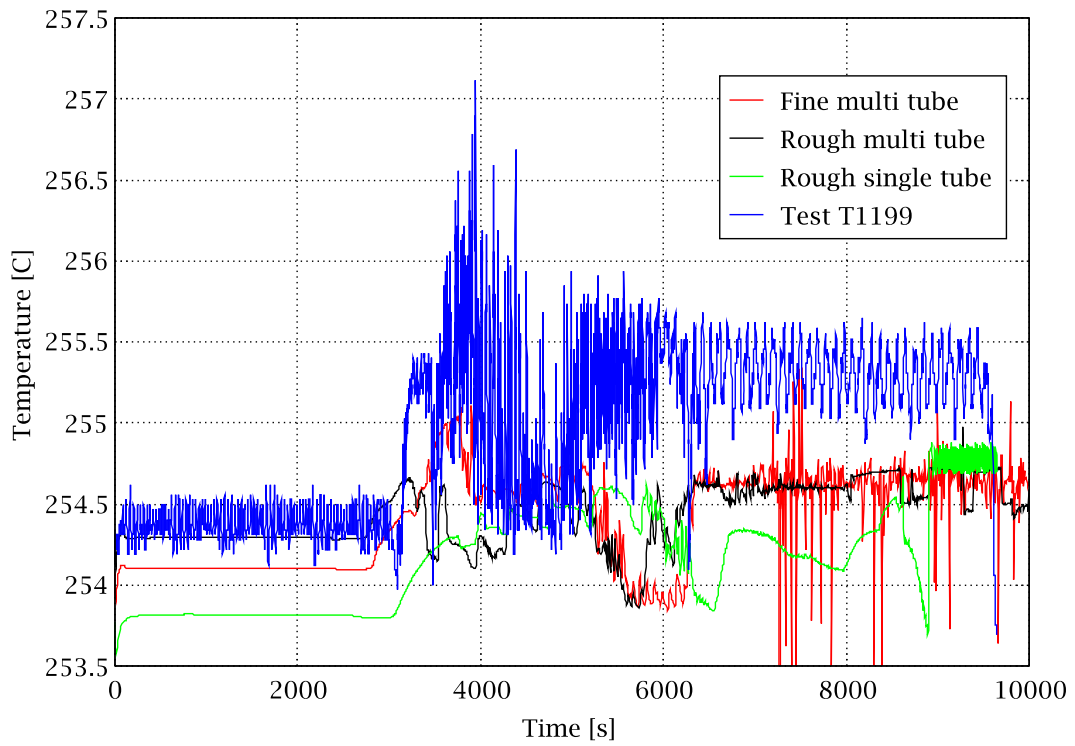
SG 2 Temperature(Tube 32, Hot Side, 0.300 m)



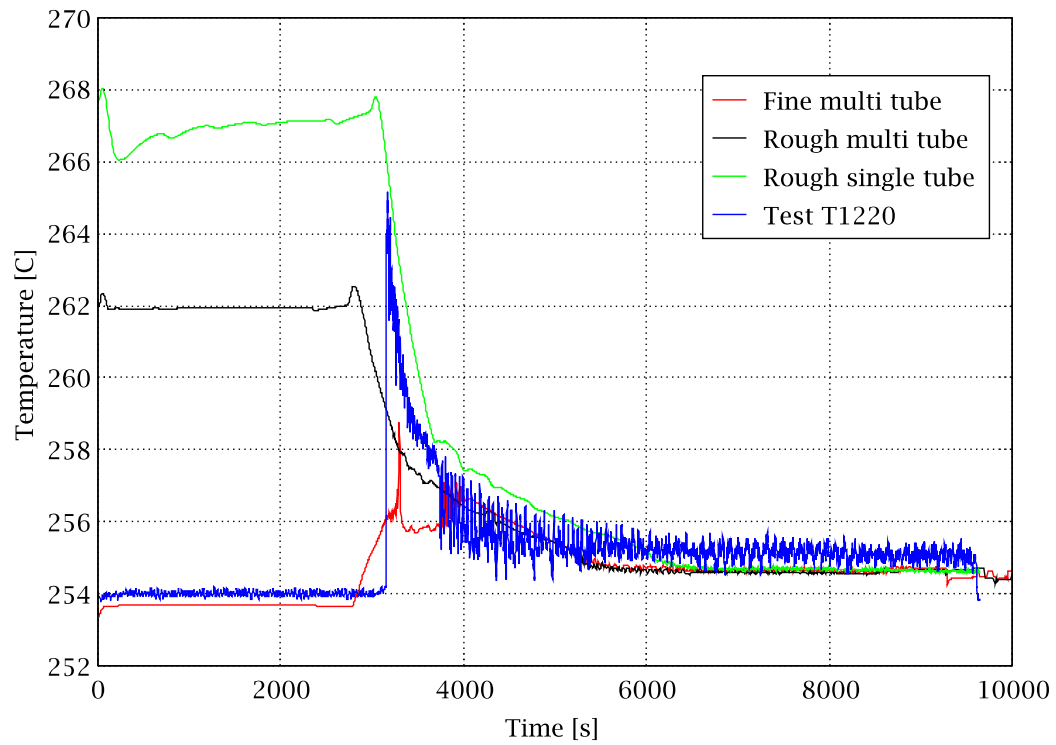
SG 2 Temperature (Tube 32, Top)



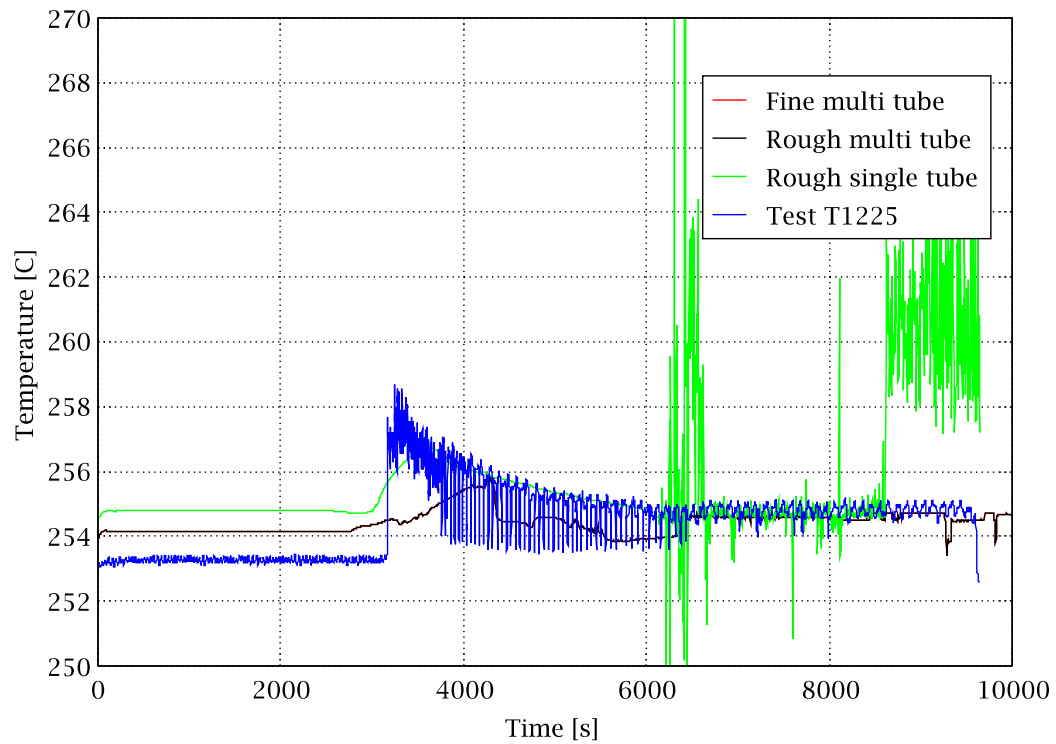
SG 2 Temperature (Tube 32,Cold Side, 0.300 m)



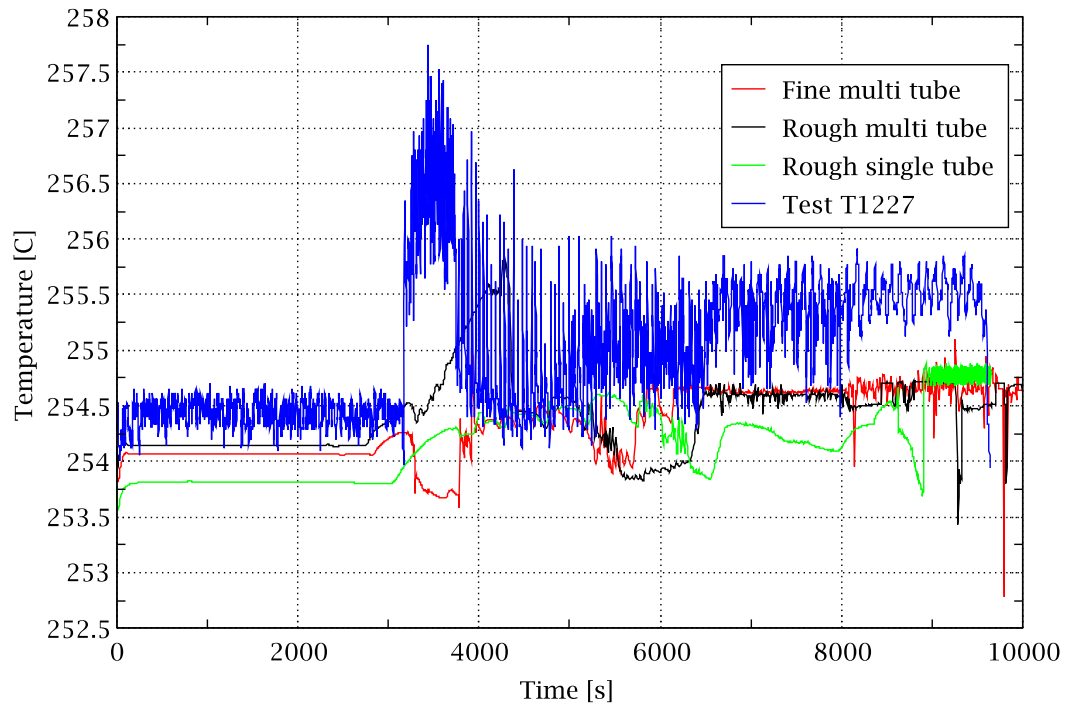
SG 2 Temperature (Tube 50, Hot Side, 0.300 m)



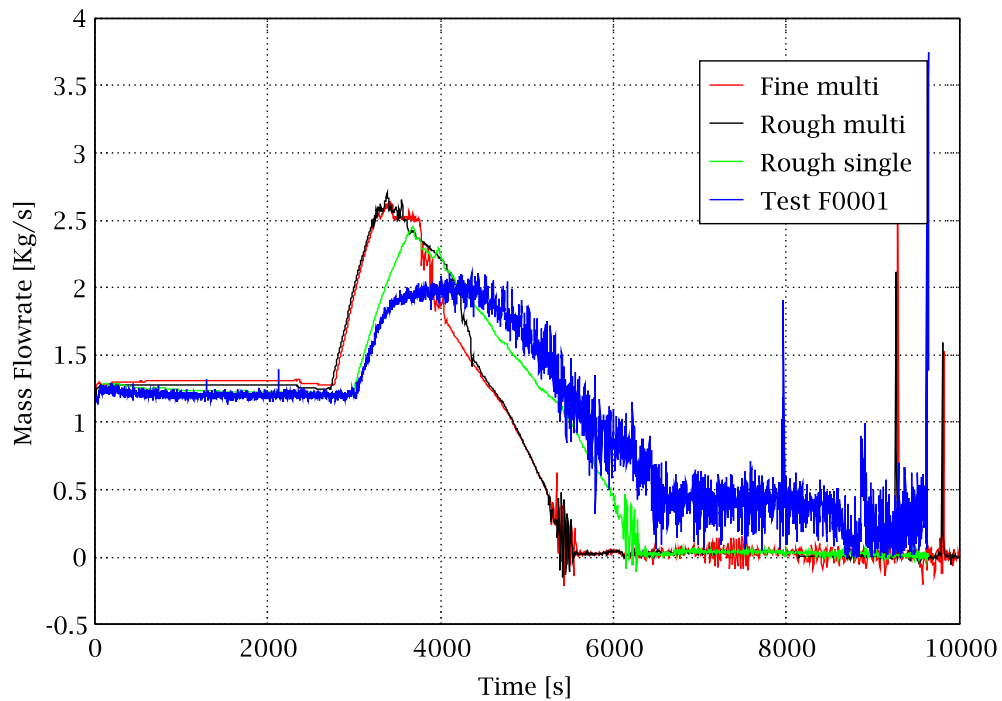
SG 2 Temperature (Tube 50, Top)



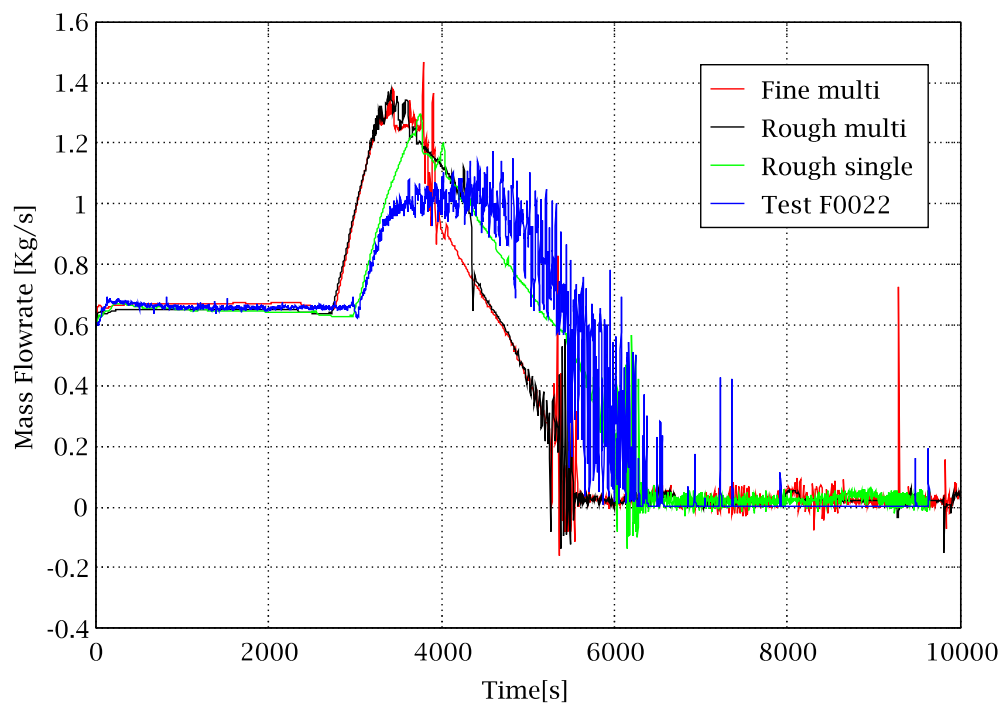
SG 2 Temperature (Tube 50, Cold Side, 0.300 m)



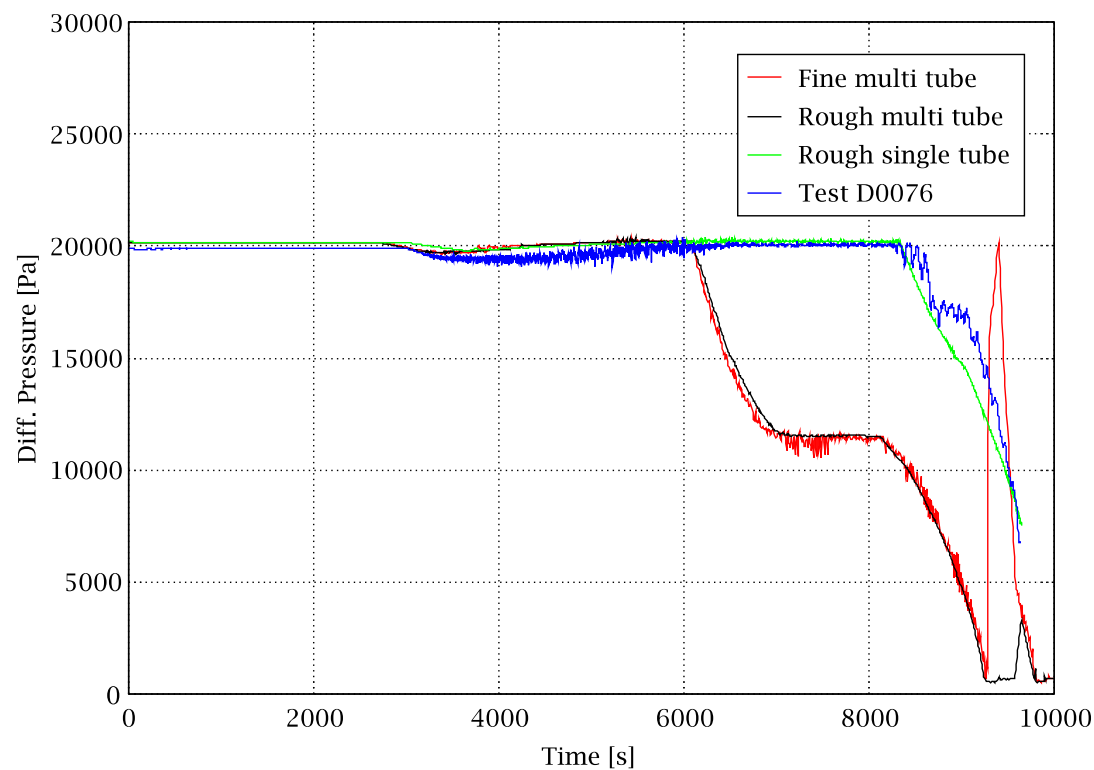
Downcomer Mass Flowrate



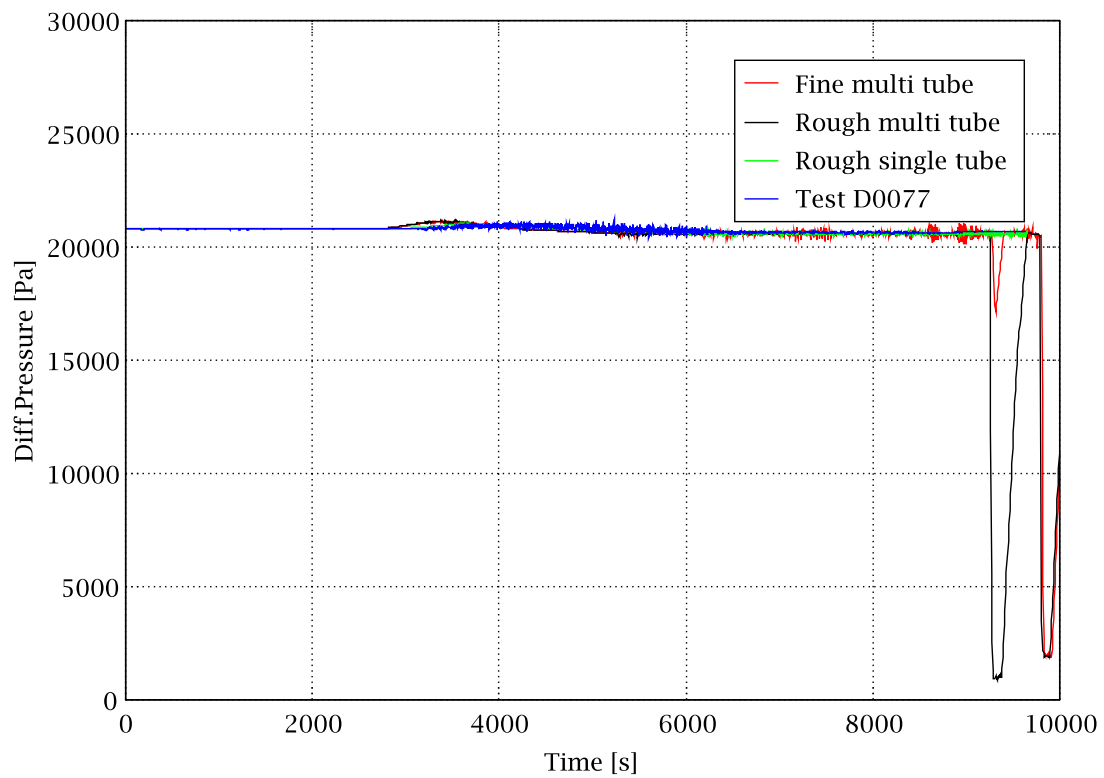
Cold Leg 2 Mass Flowrate



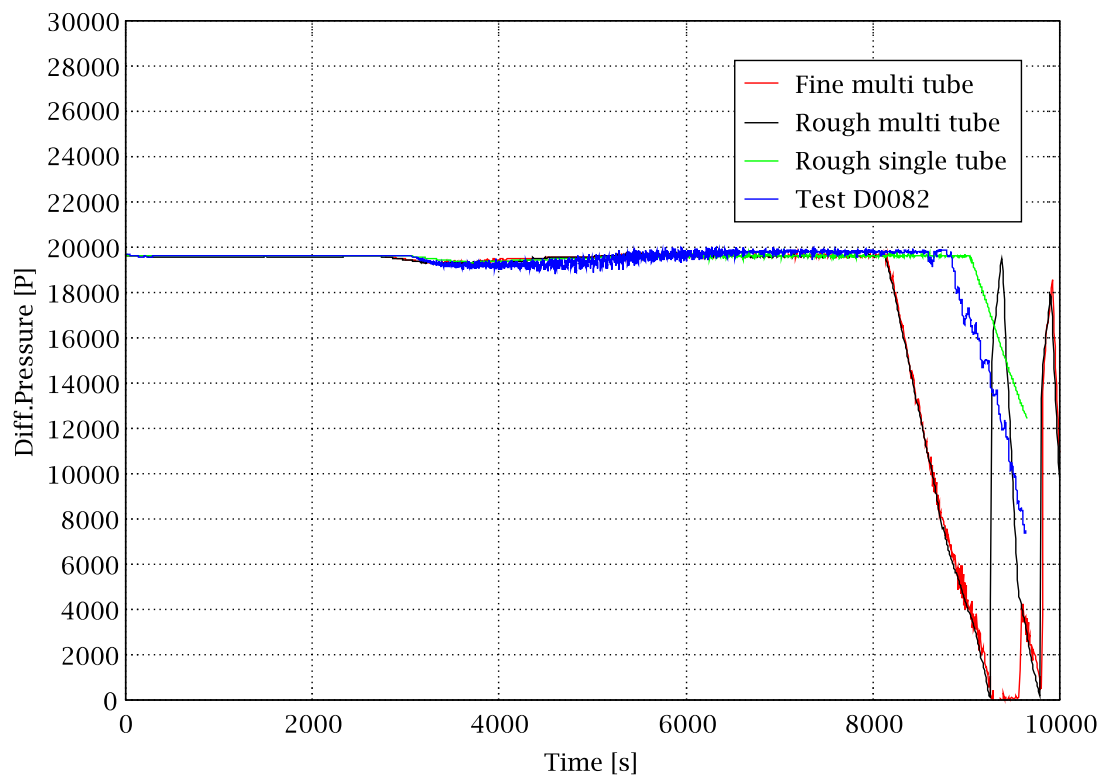
Diff. Pressure in Cold Leg 1 loop Seal (SG Side)



Diff.Pressure in Cold Leg 1 Loop Seal (DC Side)



Diff.Pressure in Cold Leg 2 Loop Seal (SG Side)



Diff.Pressure in Cold Leg 2 Loop Seal (DC Side)

